Alma Mater Studiorum – Università di Bologna

DOTTORATO DI RICERCA IN

CHIMICA

Ciclo XXX

Settore Concorsuale: A3/A1

Settore Scientifico Disciplinare: CHIM 01

Development of innovative chromatography-mass spectrometry analytical methods for the qualitative and quantitative determination of target analytes in complex matrices

Presentata da: Placido Franco

Coordinatore Dottorato	**Supervisore**
Prof. Aldo Roda	**Prof. Aldo Roda**

Esame finale anno 2018

ABSTRACT

The present thesis deals with the development of chromatography-mass spectrometry analytical methods for the analysis of target molecules in complex matrices. These compounds have different applications, ranging from nutraceutical to pharmaceutical or archaeological. Generally, the main aim was to provide accurate quantification of one or several analytes within real samples and then, in order to fulfil the requested standards, several efforts have been put on the development and validation of specific analytical methods, suitable for the system under investigation. The developed methods proved to be able to face the analytical challenges raised by the presence of complex matrices able to interfere with the accuracy of the result and the data interpretation.

During the first year of PhD, my research focused on the analysis of glucosinolates, compounds occurring in the plants of Brassica order. Glucosinolate metabolism leads to compounds called isothiocyanates, known for their anticancer activity. Glucosinolates and isothiocyanates are compounds of strong interest for nutraceutical applications and functional food development, while their analysis is important for the evaluation of the product quality, especially in terms of available amount and stability.

Another important project involved the *in vivo* evaluation of the biodistribution and metabolism of obeticholic acid in a cirrhosis induced rat model. Considering that obeticholic acid has been recently approved for the treatment of cirrhosis, the importance of this study resides in the necessity to assess a safety profile in case of administration to patients with liver diseases, where dangerous accumulation or unexpected metabolites might occur as consequence of the liver impairment.

During my third year of PhD, I worked on the target analysis of different lipid classes in archaeological samples. The determination of specific biomarkers in archaeological finds, indeed, is important because it can address historical questions about past diets, ancient practices, but also vessel production and related use.

INDEX

CHAPTER 1

Glucosinolates and Isothiocyanates

Every day, throughout food consumption, our organism encounters many natural substances having a well-defined biological action, which can be either positive or negative on our health.

The strong awareness that specific edible substances can be very helpful for preventing the rising of many diseases has led the scientific research to focus on the study of the molecules responsible for the health benefit foods.

The capability to combine normal foods with health promoting compounds has brought many food companies to invest huge amount of money in the development of the so-called "functional foods", defined as aliments characterized by normal nutritional value and enriched with biologically active molecules. Following this lead, a great number of new functional foods has been introduced in the market, which is a very important step forward in the sector of the prevention.

This chapter deals with a class of natural molecules, the glucosinolates (GLSs), and specific class of related metabolites, the isothiocyanates (ITCs). These molecules, found mainly in the plants of the Brassica order, are recognized to have a strong chemo preventive activity and are considered the main responsible for the health protective effects of some vegetables, like broccoli, rocket salad and cauliflower.

1.1   Introduction

1.1.1 Structure and properties of glucosinolates

Glucosinolates (GLSs) are natural compounds constituted by a (Z) β-tioglucoside, N-hydroxysulphate group where the sulphur atom is linked to a lateral chain R (Figure 1).
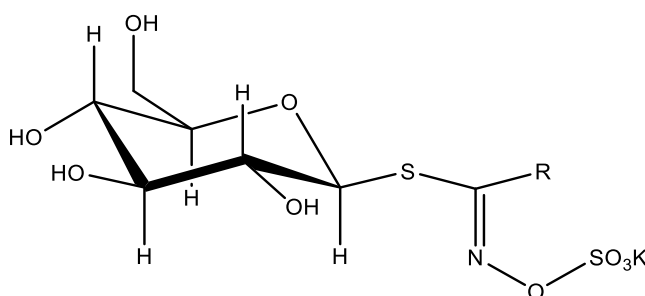
Figure 1. General structure of GLSs

Glucosinolates are hygroscopic molecules presenting partition coefficients (logP) between -1 and -3, they have good thermal stability (the pure solid form is does not degrade up to 110° C, while in matrix they are even more stable) and they naturally occur as completely water-soluble anions and partially soluble in methanol. So far, about 120 GLSs from more than 16 plant families have been identified. Among these, the most important and representative are *Brasicaceae*, *Capparaceae* and *Caricaceae* because of the high variety and amount of GLSs that they produce [1]. These vegetable families include vegetable like broccoli, rocket salad, cauliflower, mustard and turnips, whose organoleptic properties are strongly influenced by GLSs, stored as potassium salts inside the plant vacuoles.

The family of GLSs has a great molecular variety due to the different lateral chain that may occur. These chains can be linear or branched and they often present double bonds, carbonylic, hydroxyl and thio-groups at different oxidation states. Anyway, the most studied GLSs, by virtue of their biological activity, are those with aliphatic, ω-methylthioalchilic, aromatic or heterocyclic lateral chains.

Most plants produce a limited number of GLSs and their distribution, such as the qualitative and quantitative composition, in seeds, leaves, stems and roots is very variable. In the leaves, meanly, the GLSs amount is about the 1% of the dry weight, while in certain seeds the percentage can reach 10% [2]. The content can be influenced by other factors, such as the plant age, the

geographical origin, the soil fertility and composition, and the presence of particular bacteria and microorganisms.

The biosynthesis of GLSs starts from glucose and some aminoacids [3]: aliphatic derivatives have as plausible precursors methionine, alanine, leucine, isoleucine and valine, while the aromatic ones are preceded by tryptophan, phenylalanine and tyrosine. The crucial steps in the synthesis are: lateral chain elongation (regulated by specific genes), glucone synthesis and structural modifications to the lateral chain. The first step in the synthesis is always a homologation of the aminoacid lateral chain by N-hydroxylation followed by decarboxylation, which lead to the formation of an aldoxime. This is oxidised to thiohydroxamic acid, which is then glycosylated at the sulphur atom to produce a desulphoglucosinolate. This one is finally sulphated by the desulphoglucosinolate sulphotranferase (PAPS) to produce the final GLS. The entire synthesis is simplified in Figure 2.
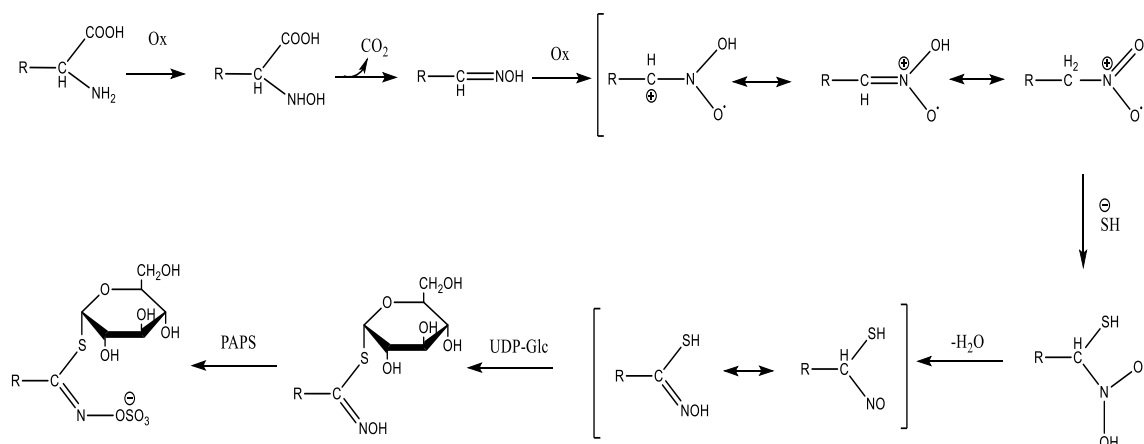
Figure 2. Biosynthesis of GLSs

The modifications to the lateral chain occur only after the GLS formation and they mainly involve oxidation of the methionine sulphur, desaturation and double bond hydroxylation. However, the exact mechanism by which these amendments are made has not been fully elucidated yet.

1.1.2 Metabolism of GLSs

Glucosinolate metabolism takes place when they encounter a specific type of hydrolytic enzymes, the myrosinases (MYRs) [4]. Myrosinases are vegetable endogenous thioglucohydrolase enzymes able to cleave the glucose group off from a GLS with the consequent production of a

thiohydroxamate O-sulfonate intermediate. This immediately evolves to a series of hydrolysis products, as reported in Figure 3 [5].

Figure 3. Metabolism of GLSs

In normal conditions, GLSs and MYR are kept in different cellular compartments. They come into contact only during mechanical damage of the plant, for example during leaf chewing or by tissue damage caused by bruising or freeze–thawing during cultivation, harvest, shipping or handling [6], and it is then that, even in presence of minimum amount of water, the hydrolysis reaction takes place.

The formation of a specific product after the hydrolysis depends on several factors: starting GLS, reaction conditions (pH, temperature, etc.), type of MYR and, eventually, presence of modifier proteins associated to MYR [5]. Indeed, there are different subclasses of MYR, type A-MYR (MYR A), type B-MYR (MYR B) and type C-MYR (MYR C). Normally, MYRs A act alone, while MYRs B and MYRs C are present as complexes with modifier proteins. These proteins can be of two different types: *Epithiospecifier Proteins* (ESPs) and *Epithiospecifier Modifier Proteins* (ESMs1).

1.1.3 Isothiocyanates

Isothiocyanates (ITCs) are a family of metabolites characterized by the presence of the –NCS functional group. Some of the most studied ITCs are reported in Figure 4.

Figure 4. Isothiocyanates best characterized

Even though their general occurrence, ITCs are not present as such in the plants, but they are stored as GLSs, their metabolic precursors. Among all GLS metabolites, ITCs are the most studied and the most interesting due to their numerous health benefit properties. Their antibacterial [7], antifungal [8] and, above all, chemo preventive [9] and antioxidant [10] activities, in fact, have been extensively reported.

Isothiocyanates present both a direct and indirect antioxidant activity. The direct one is mainly based on their capability to quench reactive radicals such as the hydroperoxides or other reactive oxygen species (ROS) [11]. This effect is mainly observed for ITCs having the sulphur atom on the lateral chain at low oxidation state. An important example is the erucin (ERN), the main metabolite of glucoerucin (GER), the main GLS of rocket salad.

The indirect antioxidant activity is based on the induction of cytoprotective enzymes, like the NADPH quinone oxidoreductase 1 (NQO1) [12], which activate immune defences against the oxidant activity of many free radicals by promoting the synthesis of glutathione, enhancing xenobiotic elimination and inhibiting cytokine-mediated inflammation [13]. The most studied ITC for this indirect antioxidant activity is sulforaphane (SFN), the main metabolite of glucoraphanin (GRA), a much-diffused GLS among many *Brassicaceae*, like broccoli or cauliflower. In addition, SFN has been reported to inhibit the activity of phase 1 enzymes such as members of the cytochrome P450 (CYP) enzyme family [14], inflammatory processes [15] and histone deacetylase activity [16]. Furthermore, SFN alters cell proliferation and stimulates apoptosis [17].

On the other hand, not all GLSs appear to act equally and negative effects of some ITCs have been reported as well [18]. For example, the metabolites originated from neoglucobrassicin and epiprogoitrin have been reported to be, respectively, mutagen and goitrogenic. It is worth to highlight that GLS composition differ among the different *Brassica* vegetables on the basis of genetic, botanical, environmental and postharvest factors. In addition, the different stages in plant maturation play also a role in affecting the GLS pattern and content.

Taken together, consumption of GLSs cannot be considered to be protective in general, as many factors can affect the presence of a favourable or unfavourable pattern. Consequently, the analysis and understanding of biological effects is required, from which dietary recommendations for the prevention of cancer can be deduced.

1.1.4 Influence of industrial processing on the GLS content

Considering the high nutritional value possessed by GLSs, many functional products and nutraceuticals have been developed by enriching normal foodstuff with this class of molecules [19]. The main practical problem in the food production is related to the physical and thermal treatments of the raw materials used for this purpose [20]. Indeed, as these processes can influence the final GLS concentration, the best option is to reduce as much as possible the number of preparative/storage processes.

The critical variables are: temperature, which is able to degrade GLSs and/or inactivate MYRs, the use of water for washing up, as it could solubilize the GLSs or hydrolyze them, and the loss of iron ions, ascorbic acid and other enzymatic cofactors.

Another aspect that needs to be carefully considered is the presence of MYRs themselves. It is important to keep them in their active form, in order to allow the ITC formation, but it is also necessary to prevent their action before the consumption, as in this case the food would lose its beneficial properties. Isothiocyanates, indeed, are very reactive molecules and they quickly reduce their concentration once produced. So far, formulations containing both GLSs and MYRs revealed to be poorly effective, as substrate hydrolysis is very fast and the produced ITCs, because of their short half-life, are not efficiently absorbed. Better results were obtained by supplying these two components separately, for example using Arabic gum or maltodextrin capsules, in order slow the hydrolysis reaction down.

An alternative approach is based on the use of GLSs without any MYR component, as intestinal microflora, although less efficient, possesses hydrolytic activity suitable for the GLS conversion into ITCs. Such a strategy is very useful for foods needing cooking before consumption, as in this case the loss of MYR activity would not represent an issue. This approach is supported by the findings reporting that, in absence of active MYR, high amounts of GLSs were recovered in the lower intestinal tract where they are hydrolyzed by the microflora in order to extract glucose [21]. Indeed, it has been demonstrated that high crucifer intake is associated to a different microbiome,

confirming that frequent consumption of GLS containing foodstuff is able to induce the production of bacteria with better hydrolytic properties [22].

1.1.5 Analytical methods for GLS and ITC determination

Considering the importance of the system GLS/ITC, the qualitative and quantitative analysis of these classes of molecules has great importance in the food market, in order to assess the value of the product.

One of the methods traditionally used for total GLS quantification is based on the determination of the glucose moles obtained after MYR catalyzed hydrolysis and after removal of the endogenous contribute [23]. Another method is based on the gravimetric titration of the sulphate ion (using barium chloride) obtained after MYR hydrolysis; the total GLS amount is then indirectly obtained from the determination of the residual barium in solution by X-ray emission spectroscopy [24].

The first method for the analysis of single GLSs was based on GC-FID after derivatization using TMS [25]. Unfortunately, GC methods have the drawback to be not suitable for thermally unstable GLS, such as the indoles, therefore HPLC soon became the most widely used instrumentation for GLS analysis. Nowadays the reference method for this purpose is the ISO 9167-1 procedure, which is based on the *on column* enzymatic desulphation of the GLSs into desulphoglucosinolates (DGLSs) and subsequent HPLC-UV analysis on a C18 column [26]. Although this method is the reference one, many drawbacks can be pointed out: the derivatization procedure is very long in order to be quantitative for all the GLSs (up to 24 hours), the UV detection is not very sensitive and selective, and the quantification is performed using the calibration curve of the desulphosinigrin (desulphobenzylglucosinolate is used as internal standard) and applying specific correction factors for each analyte. Due to all these limitations, nowadays the trend is to shift toward the use of mass spectrometry as detection technique. Indeed, many HPLC-MS/MS methods have been developed in order to analyze many GLSs and discover new ones in different matrices, such as rocket salad [27], broccoli [28], rape [29], cauliflower [30] and also functional foods [31].

As regards GLS breakdown products, ITCs and nitriles can be analyzed by GC, while HPLC with UV detection may be used for analysis of oxazolidinethiones and indoles. For confirmation and structural elucidation, both techniques can be coupled to mass spectrometry, which has proved to be a valuable tool in the structure identification of GLSs and related derivatives [32]. An elegant and sensitive method for the total ITC determination is based on the quantitative reaction with

1,2-benzenedithiole to form the 1,3-benzenedithiol-2-thione, which possesses a very high molar extinction coefficient and that is successively determined via spectroscopy [33].

Despite the high number of analytical methods available, several efforts have been made in the development of innovative procedures allowing the simultaneous determination of different classes of compounds in more complex matrices, like plasma or urine, suitable for *in vivo* pharmacokinetic and metabolism studies.

1.2   Aim and rationale

Glucosinolates and, above all, ITCs have been object of many studies by virtue of their chemo-preventive, anti-inflammatory and bactericide properties. Thanks to these, and considering the fast rising of the nutraceutical field, many functional foods enriched with this kind of molecules are available on the market or under development. Consequently, their low-cost synthesis or extraction and purification from natural sources is a theme of great actuality, especially within food companies.

These compounds are not considered proper drugs and consequently they are not subjected to the long and demanding approval process requesting *in vivo* and *in vitro* studies of toxicity, pharmacodynamics and pharmacokinetics. However, it is still of great importance to accurately monitor their presence, stability and concentration not only in the final product, but in starting materials as well, in order to qualify the nutritional value of the product and to understand the effectivity of these molecules in a non-natural matrix.

The only reference method available for GLS analysis is the ISO-9167-1, which requests the enzymatic conversion of GLSs into DGLSs prior their quantification by HPLC-UV. This method results to be time demanding, relatively expensive, poorly sensitive and many pre-analytical steps are requested. Many HPLC-MS methods are available to overcome these limitations, but none of them has been fully validated for the GLS analysis in functional foods. Additionally, all these methods target only the GLSs, while for ITC analysis a second analysis is always requested, making the comprehensive profiling of both classes longer. The possibility to achieve quantitative information of both of them in the same analysis represents an important tool in the design of these products and the study of GLS stability and biotransformation.

On these basis, the aim of this research project was to develop and validate, in accord to the international guidelines [34], an HPLC-ES-MS/MS for the simultaneous analysis of specific GLSs and the derivate ITCs in different vegetable matrices and functional GLS enriched bakery products. The target compounds of this study were GRA, GER and the relative ITCs: SFN and ERN (Figure 5), as they were the main nutraceuticals used for the functional food production and the most abundant in the starting materials. With this aim, extraction procedures were optimized in order to effectively recover the bioactive molecules from more complex matrices, such as bakery and food products.
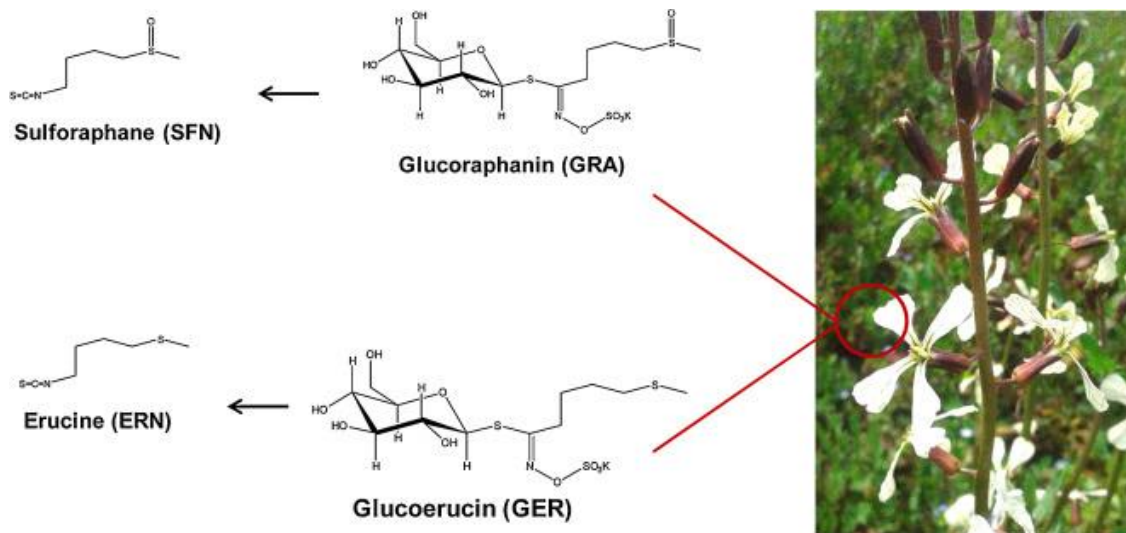
Figure 5. Main GLSs in *E. Sativa* (rocket salad) seeds and related ITCs

The final aim was to develop a direct, robust, fast and reliable method potentially exploitable in the food industry for the simultaneous evaluation of the availability of GLSs and related active metabolites during the entire chain of production, from the starting materials to the final product.

1.3 Materials and methods

1.3.1 Chemicals

Glucosinolates GRA and GER were extracted and purified starting, respectively, from *Brassica Oleracea* [35] and *Eruca Sativa* [36] seeds. Briefly, seeds were pulverized, and the oil removed using hexane. The residue was treated with refluxing ethanol at 70 °C in order to rapidly deactivate MYR. The mixture was then homogenized, centrifuged and the supernatant subjected to ionic exchange chromatography, in order to obtain fractions rich in GLS. The GLS purity was improved by gel-filtration performed using an XK 16/60 column packed with Sephadex G10 chromatography media (Amersham Biosciences), connected to an FPLC System (Pharmacia). Fractions containing pure GLSs were pooled and freeze-dried. The purity of GLSs assessed by HPLC resulted to be 99% (peak area based) and 95% on weight basis.

Isothiocyanate SFN and ERN standards were purchased from Santa Cruz Biotechnology (Dallas, Texas).

Methanol (MeOH) and acetonitrile (ACN) of HPLC-grade (Lichrosolv®) were purchased from Merck (Darmstadt, Germany). Formic acid (98% purity) and ethanol (99.8%purity) were purchased from Fluka (Buchs, Switzerland). Water of HPLC-MS grade (Millipore) was produced using the depurative system Milli-Q Synthesis A 10 (Molsheim, France). Other solvents were all of analytical grade.

Stock standard solutions of GRA and GER were prepared in water/MeOH 50:50 (v/v) at concentration of 5 mg/mL, while SFN and ERN standard stock solutions were prepared in acetonitrile at concentration of 5 mg/mL. These stock solutions were aliquoted and stored at −20 °C to minimize potential analyte degradation. Working standard solutions (WSs) containing both GLSs and ITCs were freshly made by appropriate dilution of the stock solutions in acetonitrile in the range 0.5–200 μg/mL and stored at +4 °C to be used at most for a week. Calibration solutions in the range 0.05–20 μg/mL were freshly prepared before the analysis by 1:10 dilution of the WSs using a mixture of H_2O-ACN (95:5). Quality control samples (QCs) containing the four analytes were obtained in a mixture of H_2O-ACN (95:5) at concentrations 1.7μg/mL, 6.7μg/mL e 16.7μg/mL. These samples were used for the method validation or injected randomly during the analysis in order to control the normal behaviour of the analytical system.

1.3.2   Instrumentation

The chromatographic apparatus consisted of a Waters Alliance 2690 Chromatograph (Milford, MA, USA) with 120 position autosampler and thermostat coupled with a mass spectrometer triple quadrupole and electrospray interface (QUATTRO LC, Waters). The column was a WATERS X-select CSHTM C18 5.0 μm (2.1 mm × 150 mm).

1.3.3   HPLC-ESI-MS/MS conditions

Chromatographic separation was achieved using a reversed phase C18 column. The mobile phase was constituted by HPLC grade water with 0.5% formic acid (A component) and ACN with 0.5% formic acid (B component). Different LC gradients were evaluated during the method optimization. The best separation was obtained with the following gradient of the B component: 3 min 0%, 7 min at 5%, 4 min at 24%, 4 min at 50%, 7 min at 80%, 10 min at 5% (total run time 35 min) at 0.15 mL/min flow rate. Each variation in the eluent composition was linear, except for the last step in which the composition changed instantaneously. The column was maintained at 30 °C and the injected sample volume was 5 μL. In these conditions, the mean retention times were: GRA 6.6 ± 0.2 min, SFN 16.9 ± 0.2 min, GER 18.3 ± 0.1 min and ERN 26.5 ± 0.2 min. The total ion chromatogram (TIC) with all the analytes is reported in Figure 6.

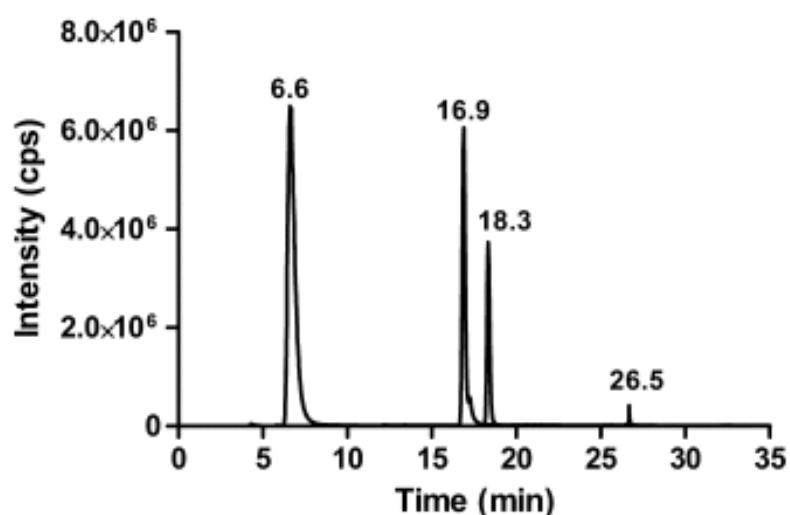**Figure 6.** Total ion current chromatogram reporting the HPLC separation on a C18 column of GRA (6.6 min), SFN (16.9 min), GER (18.3 min) and ERN (26.5 min)

The column effluent was introduced into the ESI source, operating in negative ion mode for GLS (GRA and GER) and positive ion mode for ITC (SFN and ERN), connected to a triple quadrupole mass spectrometer operating in the multiple reaction monitoring (MRM). In Table 1 the MS/MS

experimental conditions have been reported, tuned by direct analyte infusion (20 µg/mL of each analyte; 2 mL/h infusion rate) and afterwards by on column injection of each individual compound and a mixture of all of them. Two signals in extracted ion chromatogram (EIC) were monitored for each compound. The most intense was used for the quantification, the second one for the compound identity confirmation. For GRA and GER the quantification transitions were, respectively, 436.1 > 436.1 and 420.1 > 420.1, corresponding to the deprotonated molecules, while for the confirmation the fragmentation reactions used were, respectively, 436.1 > 97.1 and 420.1 > 97.1, in which the fragment at *m/z* 97.1 corresponded to the bisulphate group. For SFN the quantification transition was 178.2 > 114.2 consisting in the loss of the CH_3SO group, while the qualification reaction was 178.2 > 72.2 corresponding to ion $SCN-CH_3^+$; for ERN, the transition 162.2 > 103.2, corresponding from the loss of the SCN group, was used for the quantification, and the transition 162.2 > 162.2 for the confirmation.

Table 1. MS ionization and detection parameters of GRA, GER, SFN and ERN

	GRA	GER	SFN	ERN
Ionization mode	Negative	Negative	Positive	Positive
Capillary voltage (KV)	-2.3	-2.3	+2.3	+2.3
Cone voltage (V)	+35	+35	-15	-15
Source temperature (°C)	130	130	130	130
Desolvation temperature (°C)	200	200	200	200
Collision gas	Argon	Argon	Argon	Argon
Quantification reaction	436.1 > 436.1	420.1 > 420.1	178.2 > 114.2	162.2 > 103.2
Confirmation reaction	436.1 > 97.1	420.1 > 97.1	178.2 > 72.2	162.2 > 162.2

1.3.4 Method validation

Method validation was performed according to ICH guidelines, determining selectivity, limit of detection (LOD), limit of quantification (LOQ), calibration range, precision, accuracy and matrix effect.

1.3.4.1 Selectivity

The selectivity indicates the capability of a method to discriminate the analytes in respect to other components in the matrix. Selectivity was evaluated comparing the chromatograms obtained from

standard solutions, sample solutions and spiked sample solutions. This procedure was necessary for selectivity evaluation, as no blank sample (analyte free) was available.

1.3.4.2 Calibration range

The calibration range is related to the amount of analyte present in the sample. Ideally, a calibration range must be comprised between, respectively, the 80% and 120% of the minimum and maximum analyte concentrations in the real samples and should exhibit linearity between instrumental response and concentration over the selected range. In this case, quantification was performed by construction of seven-point calibration curves in the calibration range 0.05-20 µg/mL, according to the specific compound to be determined. Specifically, for GRA, GER and SFN the calibration range was 0.05–20 µg/mL, while for ERN was 0.5–20 µg/mL.

1.3.4.3 Precision and accuracy

The precision and the accuracy define, respectively, the reproducibility of an analytical determination (how good is the accord between a series of repeated analysis), and the goodness of such determination (how close is the obtained result to the "real value").

The precision is defined as variation coefficient (*CV%*):

$$CV\% = \frac{DS_{mean}}{[std]_{mean}}$$

The accuracy is defined as *bias%*:

$$bias\% = 100 \cdot \frac{[std]_{mean} - [std]_{theorical}}{[std]_{theorical}}$$

According to the international guidelines, both precision and accuracy must be determined, at least, in triplicate and on three different concentration levels within the calibration range.

1.3.4.4 Limit of detection and quantification

The LOD defines the minimum analyte concentration that can be reasonably distinguished from the background noise. The LOQ, on the other hand, is defined as the minimum analyte concentration that can be measured with satisfying precision and accuracy. Although at least three methods for the LOD/LOQ determination are accepted, the most used, above all for

analytical methods exhibiting baseline, is based on the signal to noise ratio (*S/N*). Specifically, LOD and LOQ are defined as the minimum concentrations giving, respectively, a *S/N* of 3 and 10.

1.3.4.5 Matrix effect

The matrix effect (*ME*) is defined as the increase or decrease in the instrumental response referred to an analyte as consequence of the presence of other components in the real sample. Matrix effect was evaluated for all analytes as ratio between the absolute matrix effect and the peak area of standard sample in mobile phase. Absolute matrix effect was calculated as difference between the peak area of the standard sample in matrix and the peak area of standard sample in mobile phase. The endogenous contribute for each analyte was subtracted from the peak area of standard sample in matrix. Matrix effect was expressed as percentage (*EM%*), so that values close to 0% indicated absence of *ME*, while higher or lower values indicated, respectively, positive or negative *ME*.

1.3.5 Samples and experimental procedures

1.3.5.1 Material characterization

An *E. sativa* ecotype (Nemat) selected as potential source of GER and GRA was used to produce a pressure defatted oilseed meal (DSM) as a food-safe organic material for the GLS enrichment of bakery products, to realize functional foods for the nutraceutical target. The addition of minimum amounts of broccoli flour as additional source of GRA and for the definition of the product taste was possible as well. The new functional bakery products have been developed basing also on recent toxicological studies showing how GLSs and ITCs, at doses lower than 100 μmol/day, lack of toxicity and reveal no evidence of systematic, clinically significant adverse events [37]. *E. Sativa* seeds were defatted by an endless screw press in a temperature and pressure-controlled procedure [38]. The *E. sativa* DSM was characterized for moisture, nitrogen, residual oil and GLS content. In particular, the moisture content was determined by evaluating the difference between its weight before and after oven-drying at 105 °C for 12 h; nitrogen content was determined by the Kjeldhal method [39], using a Tecator digestion system and an automatic Büchi distillation unit (B 324); residual oil was extracted with a Soxhlet apparatus and characterized for its fatty acid composition by the UNI EN ISO 5508 method [40]. Myrosinase activity was also determined by the pH-stat technique [41]. The assays were carried out in triplicate by loading 300 mg of DSM in 15

mL of 1% NaCl into the reaction cell at 37 °C. The reaction was started by adding 0.5 mL of 0.5 M sinigrin solution, after 8–10 minutes of conditioning, maintaining the starting pH constant. One enzyme unit (U) corresponded to 1 μmol/g DSM of sinigrin transformed in 1 minute. An *E. sativa* meal extracted overnight at room temperature with *n*-hexane (1:10 w/v) in a rotary shaker, has been used as reference for maximum MYR activity. Two different defatting procedures were tested: a low temperature-pressure extraction (40–65 °C temperature range), and a high temperature-pressure extraction (initial temperatures higher than 100 °C). Recipes and final food products were produced in the R&D and QA of Colussi-Group (Milan, Italy) by adding 1% of DSM to a standard cracker mixed with wheat flour baked at 200 °C in industrial plant. The addition of active MYR in the cooling phase of production by using mustard meal was also explored. Further information on the recipes is commercially confidential and their property is of Colussi-Group.

1.3.5.2 Extraction of GLSs and ITCs

Analytes from DSM were extracted by following the ISO 9167-1 method with some minor modifications [42]. Briefly, 300-500 mg of DSM were pulverized to a fine powder, incubated in thermal bath at 90 °C for 10 minutes in 4 mL EtOH 70% and then subjected to sonication bath for 30 minutes. Extracts obtained were centrifuged for 30 minutes at a speed of 39800 rpm at a temperature of 4 °C and then filtered. The remaining flour was washed with 4 mL EtOH and filtered. The extracts were combined for the determination of the final volume.

For an effective extraction from the bakery products, a combined procedure of sonication and microwave extraction was carried out. Four grams of crackers finely pulverized in 25 mL of 70% ethanol were sonicated 30 min in a Sonica Sweep System (Soltec) bathroom at 40 kHz. They were then extracted in Teflon vessels with the MARS system (CEM Corporation) setting 400 W as maximum power, heating ramp at 80 °C in 3 min and extraction at 80 °C for 10 min. The extracts were centrifuged 30 min at 25.900 rpm at a temperature of 4 °C (Beckman J2-MC centrifuge, rotor j14) and filtered (qualitative paper Whatman # 4, Sigma Aldrich) in a 50 mL graduated cylinder. The residue was re-extracted and the second extract was centrifuged, filtered and combined to the first for the determination of the final volume.

1.3.5.3 Glucosinolate analysis by ISO 9167-1 method

Glucosinolate content was evaluated by HPLC-UV analysis of DGLSs using de ISO 9167-1 method [26]. Briefly, the extracts obtained according to the procedure reported above were subjected to

enzymatic desulfation by introducing 1 mL of extract containing the GLSs into microcolumns (8 mm internal diameter from BIORAD) filled with 0.5-1.0 mL DEAE Sephadex A-25 resin (Pharmacia), previously conditioned at pH 4.0 or pH 5.6 with 20 mM acetate buffer, depending on the material that has to be analyzed. After sample loading, the resin is washed with the same buffer to remove non-charged molecules, while the GLSs, anionic compounds, are immediately bound at the top of the column. A suitable quantity of purified sulfatase (about 0.10 mL, 0.28 U/mL) is then loaded into the column; as a result of sulfatase action, the sulphate group of the GLSs is removed and the DGLSs are eluted with water (3 mL) after about 12-24 hours. The analysis of DGLSs was performed using a Hewlett-Packard chromatograph 1100 equipped with a diode array detector and ChromSep HPLC column SS (250 mm × 3.0 mm) and a ChromSep guard column Intersil 5 ODS-3 (Varian). The column was eluted at a flow rate of 0.8 mL/min with aqueous acetonitrile (solvent A: water; solvent B: acetonitrile 25%in water) at 30 °C following the program: 1 min 99% A; 22 min of linear gradient up to 88% B; 5 min of linear gradient up to 100% B; 3 min of linear gradient up to 100% A. The DGLSs were detected monitoring their absorbance at 229 nm.

1.4 Results and discussion

1.4.1 Chromatographic and MS condition optimization

Preliminary experiments using standard solutions of the analytes were performed in order to select the optimal separation conditions. The column chosen was a WATERS X-select CSH TM C18 5.0 μm (2.1 mm × 150 mm), as, to date, no other stationary phases giving better chromatographic results have been reported; besides, the small internal diameter ensured the possibility of using low flow rates with a reduction of mobile phase volume. Mobile phase composition was chosen in order to improve the chromatographic separation and the detection sensitivity. An "ion pairing reagent" was used to enhance the ionization process occurring at the ES interface and to improve the chromatographic interactions between analytes and stationary phase. At this regard different amounts of trifluoroacetic acid, acetic acid and formic acid into mobile phase were studied. Best results, in terms of peak shape, sensitivity and noise suppression, were obtained using phases acidified with 0.5% formic acid. The choice of acetonitrile as organic component instead of methanol or methanol/acetonitrile mixtures was made in order to reduce elution time without any loss of resolution power or ionization efficiency. Different flow rates, in the range 0.10–0.15 mL/min, were tested as well in order to reach the best compromise in terms of peak symmetry, resolution and time of analysis. It was observed that the increase of flow rate caused a reduction of the peak width and analysis time, without significantly affecting resolution and selectivity. So, a flow rate of 0.15 mL/min was considered optimal for our purposes. As regards the temperature influence, different column temperatures were tested in the range 20–60 °C. In this range, a slight reduction of retention times and peak symmetry were observed with temperature increase and, for this reason, the column temperature was set at 30 °C. In the best conditions, the chromatographic run time was 35 min, in order to obtain a versatile method that can be successfully applied to different complex matrices containing GRA, GER, SFN and ERN but also a wider range of GLSs. For example, analyzing a real sample of broccoli extract, this method allowed the separation of more than seven GLSs (Figure 7). Glucosinolates are natural molecules all characterized by the presence of the sulphate group, whose high acidity makes them occur as negatively charged molecules and therefore easily detectable in ES negative ion mode. Isothiocyanates, on the other hand, have no acidic groups and they respond only in positive ionization mode. For this reason, an MRM program constituted of two different detection windows, one operating in negative and the other in positive mode, was set making possible the

simultaneous analysis of GLSs and ITCs. Moreover, MRM detection mode ensured high sensitivity and specificity, reducing the interferences and increasing the signal to noise ratio.
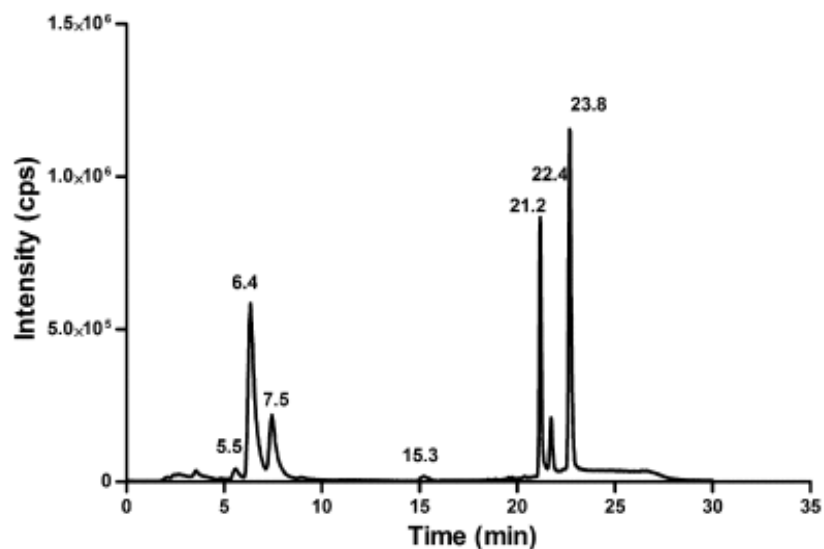
Figure 7. Chromatogram obtained from broccoli extract. Based on literature data and *m/z* values, GLS identified are: glucoiberin (5.5 min), glucoraphanin (6.4 min), epiprogoitrin (7.5 min), gluconapin (15.3 min), glucobrassicin (21.2 min), 4-metoxyglucobrassicin (22.4 min) and neoglucobrassicin (23.8 min)

1.4.2 Method validation

The developed method for the analysis of GRA, GER, SFN and ERN fulfils all the standard requirements of the ICH Guidelines [34] including the sample clean-up and pre-analytical treatment.

1.4.2.1 Selectivity

Selectivity was established by injection of single standards and of mixtures of them, in order to determinate their retention time. The comparison between standard solutions and samples fortified with known amounts of analyte, using MRM and EIC modes, showed absence of any interference in the matrices.

1.4.2.2 Calibration curves

Seven-point calibration curves ranging from 0.05 to 20 μg/mL for GRA, GER, SFN and from 0.5 to 20 μg/mL for ERN, based on peak areas and without internal standard, were used for the quantification, as described in Section 2.4. As no significant matrix effect was observed (Matrix

Effect < 10%), as described in Section 1.4.2.5, calibration curves were obtained in mobile phase, allowing a more accurate quantification than methods using matrix-matched standard curves. Correlation coefficients for all analytes were ≥0.998, meaning a good linearity in the calibration ranges and making possible not to use any internal standard.

1.4.2.3 Precision and accuracy

Precision (SD%) and Accuracy (Bias%) values, determined in intra-day and inter-day assays, as described in Section 1.3.4.3, were less than 10% for all GLSs and ITCs studied. These results indicate that the method fulfils the ICH criteria, being sufficiently precise and accurate, and although its use is recommended, internal standard is not necessary.

1.4.2.4 Limit of detection and quantification

Limit of detection and quantification were determined as described in Section 1.3.4.4. Limit of detection values were 10 ng/mL (GRA), 1 ng/mL (GER), 1 ng/mL (SFN) and 200 ng/mL (ERN). Limit of quantification values were 20 ng/mL (GRA), 2 ng/mL (GER), 2 ng/mL (SFN) and 400 ng/mL (ERN).

1.4.2.5 Matrix effect

Matrix effect percentage values close to 0% showed absence of matrix effect, values higher and lower than 0% indicated, respectively, ionic increase (positive matrix effect) or ionic suppression (negative matrix effect). Matrix effect was evaluated analyzing in triplicate three different concentration levels, using the same QCs reported in Section 1.3.1. Diluting 1:10 (v/v) cracker or vegetable extracts, matrix effect observed was less than 10% at all concentrations levels for all the analytes.

1.4.3 Mass spectrometry analysis of GLSs and ITCs

Glucosinolates are naturally negatively charged molecules by virtue of the presence of the sulphate group, consequently they are easily detected in negative ionization mode. Different attempts were made in order to analyze them in positive ionization mode, but none of them proved to be effective. Isothiocyanates, on the other hand, have no acidic groups and the positive ionization mode revealed to be the best choice for their analysis.

The optimization of MS conditions has been carried out throughout the tuning of the electrospray ionization parameters: capillary and cone voltages, collision energy and source temperature. The

proper tuning of these parameters allowed us to gain high current intensities for a sensitive detection of the compounds.

1.4.3.1 Mass spectrometry characterization of GLSs

Electrospray ionization in negative mode of GLSs affords [M - H]⁻ ions which have been used for the quantification of these analytes. Besides, the use of tandem mass spectrometry with low collision energies in MRM acquisition mode ensures cleaner spectra compared to single ion recording (SIM), without significant loss in sensitivity of the deprotonated molecule. The increase in collision energy, on the other hand, yielded extensive fragmentation, providing structural information and allowing to select secondary transitions for a further confirmation of the selected compound. On these basis, direct infusion was performed for each single standard and the most intense ion produced in the electrospray source was selected and furtherly subjected to tandem mass spectrometry characterization at different collision energies, with the aim to select the best conditions required for the analysis.

In Figure 8, GRA tandem MS spectrum of the precursor ion [M - H]⁻ (*m/z* 436.1) and the assumed fragmentation mechanism are reported.
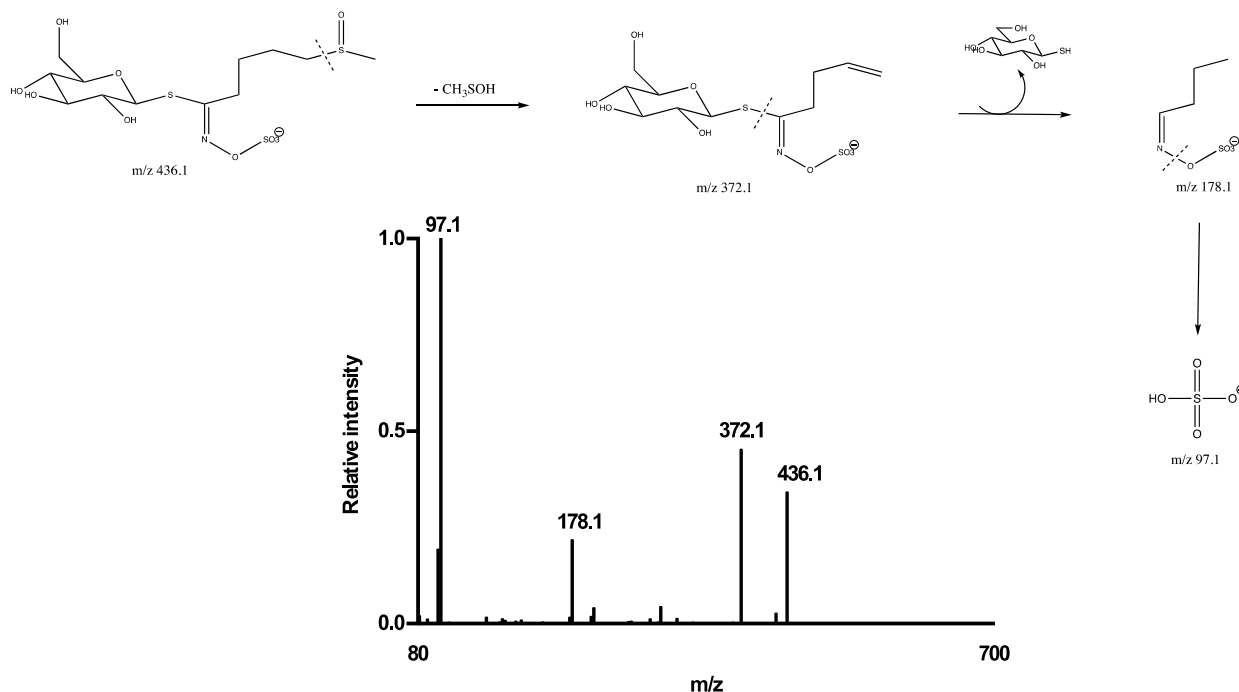
Figure 8. Tandem MS spectrum of the GRA precursor ion [M - H]⁻ (*m/z* 436.1)

In the GRA tandem MS spectrum, the base peak at *m/z* 436.1 corresponds to the [M - H]⁻ ion, but other three main fragments can be observed at *m/z* 372.1 (obtained from the loss of the neutral fragment CH_3SOH), *m/z* 178.1 (due to the successive loss of the thioglucose moiety) and *m/z* 97.1 (corresponding to HSO_4^- ion) [27]. Consequently, in the MRM program, the transition 436.1 > 436.1 at low collision energy was selected for the quantification, while the transition 436.1 > 97.1 at higher collision energy for the confirmation.

In Figure 9, GER tandem MS spectrum of the precursor ion [M - H]⁻ (*m/z* 420.1) and the assumed fragments are reported.
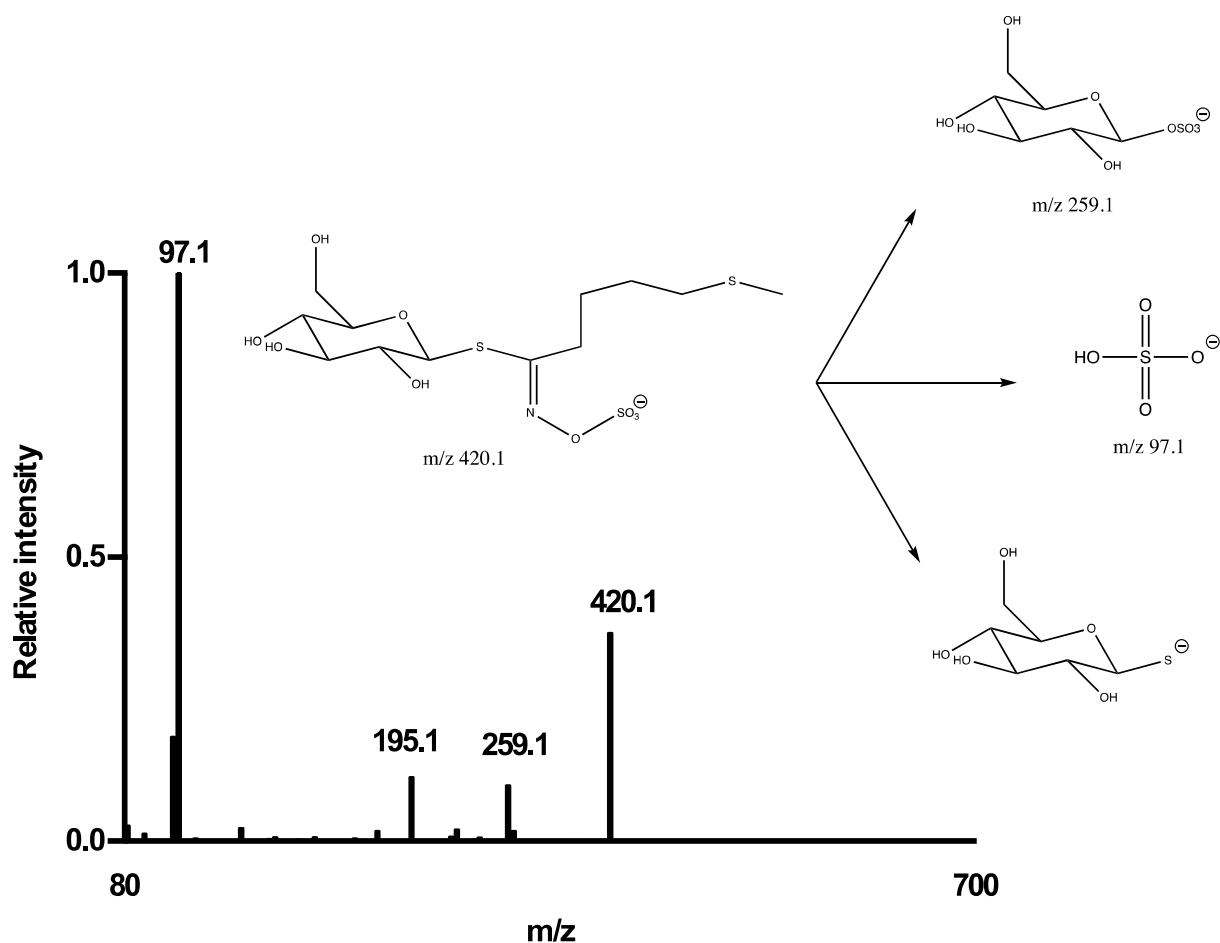
Figure 9. Tandem MS spectrum of the GER precursor ion [M - H]⁻ (*m/z* 420.1)

Compared to GRA, GER shows a more limited fragmentation. The [M - H]⁻ (*m/z* 420.1), besides the bisulphate ion (*m/z* 97.1), affords only peaks at *m/z* 259.1 and 195.1, whose hypothesized structures are showed in Figure 9 [27]. Consequently, in the MRM program, the transition 420.1 > 420.1 at low collision energy was selected for the quantification, while the transition 420.1 > 97.1 at higher collision energy for the confirmation.

1.4.3.2 Mass spectrometry characterization of ITCs

Electrospray ionization in positive mode was selected as the best option for ITC detection. Similarly to GLSs, the MRM acquisition mode was selected in order to improve the sensitivity of the method. Consequently, in order to determine the best transitions for the quantification and the confirmation, the most intense ion produced in the electrospray source was selected and subjected to tandem mass spectrometry analysis at different collision energies to properly tune the analysis conditions.

Sulforaphane shows the MS/MS spectrum of the precursor ion [M + H]$^+$ reported in Figure 10.
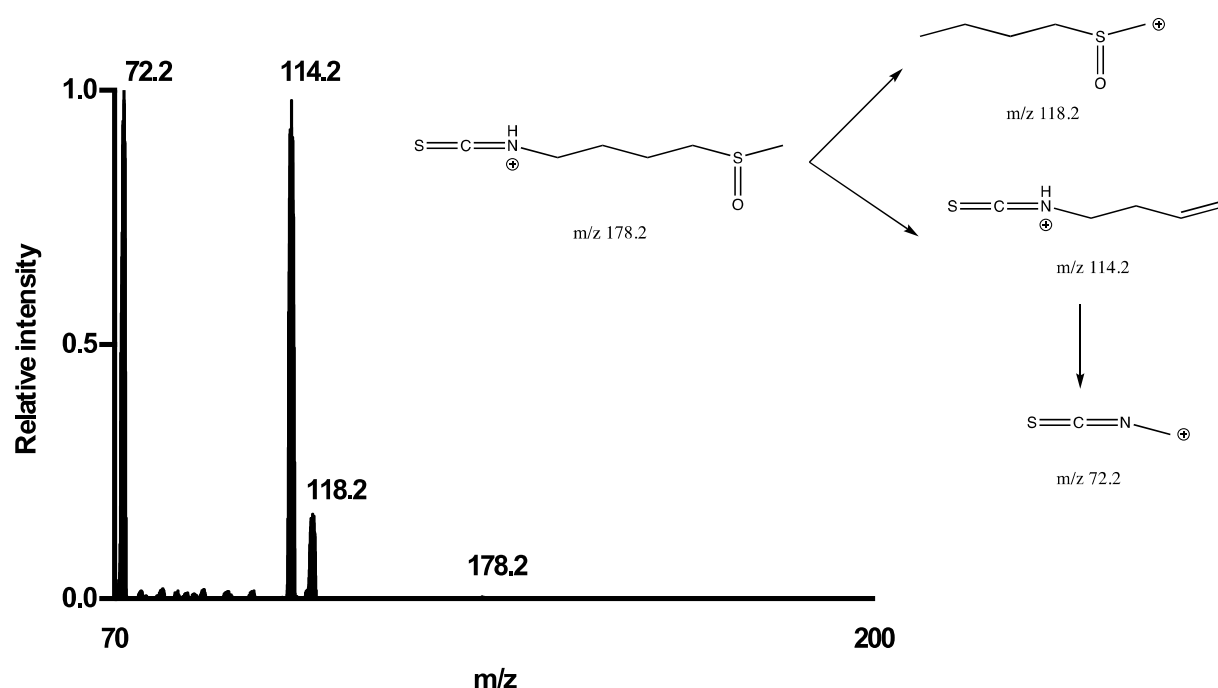
Figure 10. Tandem MS spectrum of the SFN precursor ion [M + H]$^+$ (*m/z* 178.2)

The tandem MS spectrum obtained after isolation of the [M + H]$^+$ ion of SFN (*m/z* 178.2) shows three main fragments. The ion having *m/z* 118.2 corresponds to the loss of the SCN group, while signals at *m/z* 114.2 and 72.2, are related first to the loss of the CH$_3$SO group and to the successive cleavage of a CH$_2$CH$_2$CH$_2$ moiety. In this case, the collision energy used to induce the fragmentation was high enough to lead to a very low intensity of the protonated molecule [M + H]$^+$ in favor of the other fragments, definitely more intense. Consequently, in the MRM program, the transitions 178.2 > 114.2 and 178.2 > 72.2 were selected, respectively, for the quantification and the confirmation.

Erucin shows the MS/MS spectrum of the precursor ion [M + H]$^+$ reported in Figure 11.
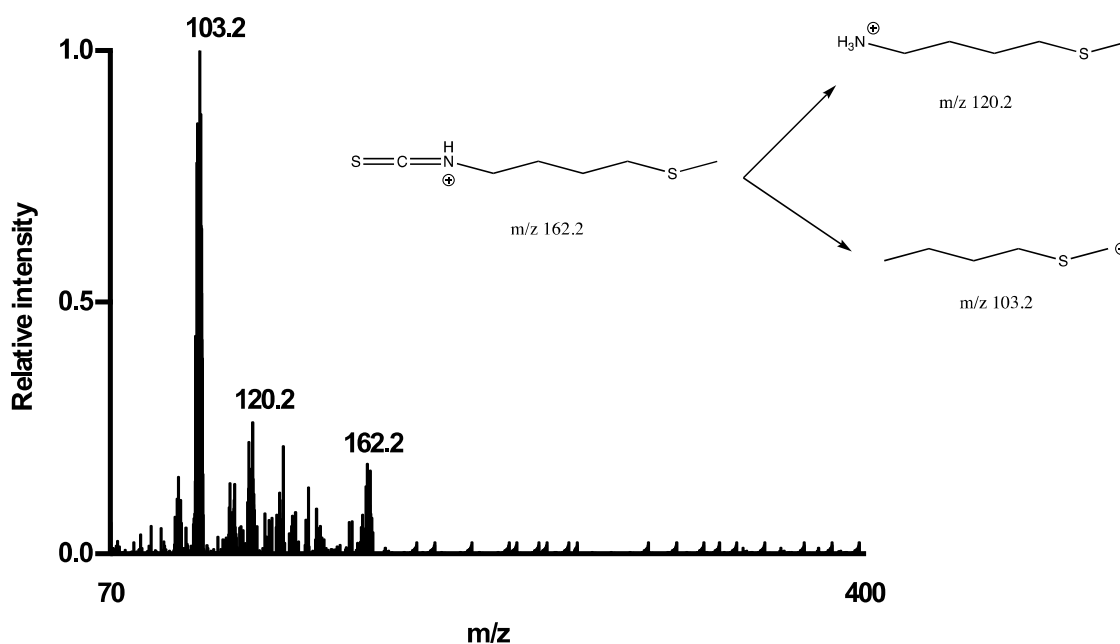
Figure 11. Tandem MS spectrum of the ERN precursor ion $[M + H]^+$ (*m/z* 162.2)

In this spectrum, the two most intense fragments of the precursor ion $[M + H]^+$ (*m/z* 162.2) were tentatively identified as reported in Figure 11. In the end, the transitions 162.2 > 103.2 and 162.2 > 162.2 were selected, respectively, for the quantification and the confirmation.

1.4.4 Design of GLS enriched bakery products

E. sativa DSM was derived from a pressing pilot extraction plant [38]. It showed a moisture of 7.4%, 31% proteins, and a 20.5% residual oil content with 37% erucic acid. Food-grade products containing rapeseed oil are regulated to a maximum of 2% [43] and 5% [44] erucic acid in the USA and in the EU, respectively. Defatted seed meals produced starting from *E. Sativa* by this way can be considered safe for food enrichment up to a maximum concentration of 25%. The GLS content was evaluated both by HPLC analysis of DGLSs and by HPLC–ES-MS/MS as described above. For vegetable samples, it has been demonstrated a very good agreement with the described HPLC–ESI-MS/MS method (Table 2), with the advantage of a reduction in the analysis time from two days to 35 min. The maximum activity of MYR was 24 ± 3 U for *E. sativa* DSM defatted by Hexane. The DSM produced for food enrichment showed a residual activity (11 ± 2 U) for the low temperature pressure extracted DSM, and no residual enzymatic activity for the high temperature pressure extracted DSM. The peculiarity of the produced DSMs is the high content in GLSs and the presence of only GLSs actually considered safe as food additive, with beneficial effects as widely

described in the literature [37,45]. Glucosinolates, indeed, cannot be considered to be protective in general. Depending on the species and growth phase, plants may harbor a favorable or unfavorable pattern of GLSs. It is noteworthy to highlight two GLSs present in broccoli: epiprogoitrin and neoglucobrassicin. The first one is known to be a goitrogenic while the second is a potential mutagenic [18]. Both DSMs were able to maintain a good concentration in GLSs even after pressure oil extraction and heat treatments. In addition, this method proved to be suitable for the separation and analysis of different and more complex matrices such as broccoli in which several GLSs are present, as described above (Figure 7).

Table 2. Values of GLS content in E. Sativa DSM expressed as mean ± standard deviation of three replicates

		HPLC-ES-MS/MS (μmol/g)	ISO 9167-1 (μmol/g)
(MYR+) DSM	GRA	0.44 ± 0.01	0.60 ± 0.10
	GER	89.8 ± 2.2	92.2 ± 7.4
	Total GLSs	90.2 ± 2.2	92.8 ± 7.4
(MYR-) DSM	GRA	0.47 ± 0.01	1.7 ± 0.8
	GER	74.6 ± 2.0	72.0 ± 3.0
	Total GLSs	75.1 ± 2.0	73.7 ± 3.0

1.4.5 Quality control and improving of GLS enriched bakery products

The DSM with no MYR activity (MYR−) has been chosen to proceed with the development of the enriched bakery products. Indeed, as shown in Figure 12, the final bakery products made of DSM with MYR- afforded definitively higher amounts of GLSs than the recipe with MYR+. This demonstrates that during the preparation and baking of the product, degradation of GLSs to form ITCs occurs. Unfortunately, ITCs were not detected during the analysis, likely because the conditions experienced during the preparation were unfavorable to allow the persistence of these compounds until the analysis.
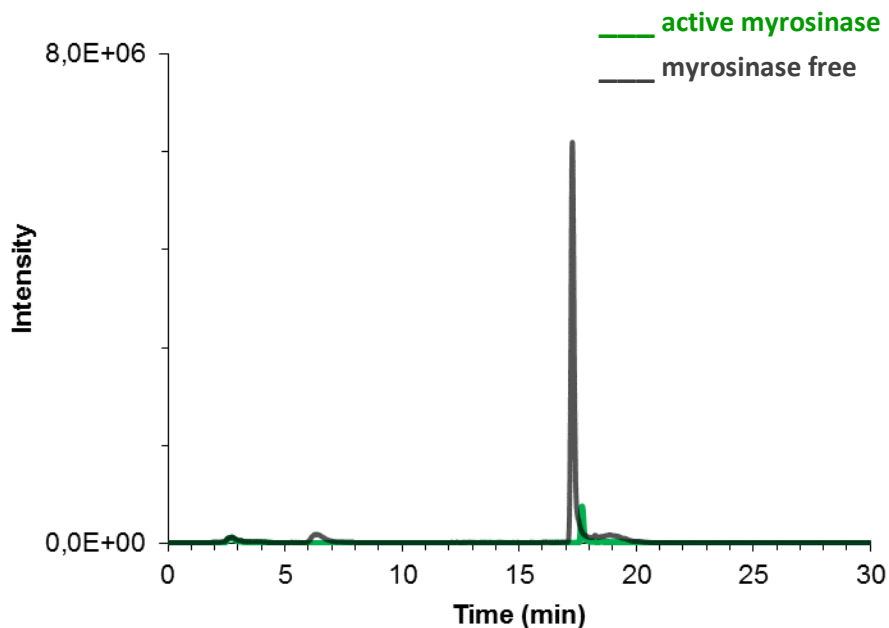
Figure 12. HPLC-ESI-MS/MS analysis of functional bakery products enriched with *E. sativa* DSM with active MYR (green) and MYR free (grey)

The selected DSM would be theoretically able to ensure an intake of GLSs up to 75 μmol/100 g of product, adding only 1% of *E. sativa* DSM to standard industrial recipes of crackers after baking at 180 °C. The extraction of GLSs from bakery products, which proved to be a more complex matrix than vegetables, was very challenging and constituted one of the critical steps in the method optimization. Indeed, the typical extraction of GLSs with heated solvents, as reported in the ISO 9167-1 protocol, was not sufficient for efficiently extracting GLSs from bakery products (Fig. 13).
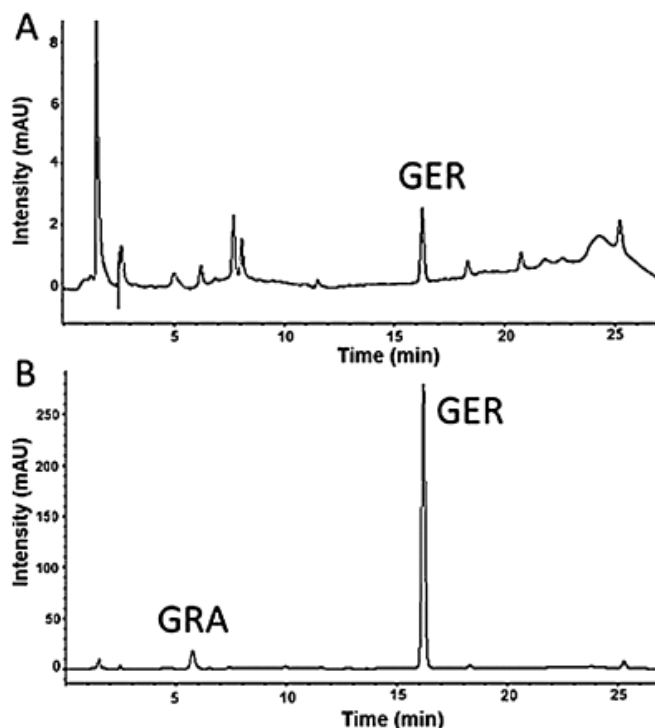
Figure 13. HPLC analysis of DGLSs of *E. sativa* DSM enriched crackers. (A) GLS extraction as described in ISO 9167-1, (B) GLS optimized extraction via a sonication step followed by microwave assisted extraction

The extraction strategy was optimized combining known methods for the extraction of GLSs, particularly GER from *E. sativa* seeds [46]. Specifically, a combined pre-sonication and microwave assisted extraction (MAE) allowed a recovery of 95.9% of total GLSs, as reported in Table 3.

Table 3. Recovery (%) of total GLSs from enriched bakery products under different extraction procedures, as evaluated by HPLC–UV analysis of DGLSs

GLS extraction	Total GLSs (μg/100 g)	Recovery (%)
ISO 9167-1	10.0 ± 0.3	14 ± 1
MAE, 70% ethanol	29.0 ± 0.9	52 ± 4
Pre-sonication, MAE, 70% ethanol	71± 4	96 ± 11

The GLS content was evaluated both by HPLC–UV analysis of DGLSs and by HPLC–ES-MS/MS and, also for a complex matrix as a bakery product, it has been demonstrated a very good agreement of data for both target GLSs (Table 4).

Table 4. GLS content in *E. Sativa* DSM enriched cracker, determined both by HPLC-ESI-MS/MS and HPLC-UV

	HPLC-ESI-MS/MS of intact GLSs	HPLC-UV of DGLSs
GRA (μmol/100 g)	3.0 ± 0.1	1.3 ± 1.0
GER (μmol/100 g)	68 ± 3	70 ± 3
Total GLS (μmol/100 g)	71± 3	71 ± 4
Recovery (%)	94 ± 6	96 ± 11

It is interesting to note that this result was achieved in HPLC–ES-MS/MS without any pre-cleaning of samples. This is very important because it allows to bring down a significant cost deriving from the pre-analytical procedure, especially if considered within an industrial point of view where the quality control needs to be performed as cost-effectively as possible. Furthermore, still from an industrial point of view, only 5% of the total GLS has been lost in the process of mixing and cooking, thus confirming the potential use of *Brassicaceae* meals in nutraceutical products. Probably a minimal content of GER was oxidized to the GRA in the whole industrial process. The recipe for the production of crackers enriched with *E. sativa* DSM was defined with the aim of maximizing the yield of intact GLSs in the dough characterized from the absence of activity of the enzyme (MYR− DSM). Such a conceived product may exert its beneficial effects only after the slow hydrolysis of GLSs to ITCs by intestinal microbiome. The addition of active enzyme (MRY+ DSM) to the dough may be possible in the cooling phase of production using mustard seed meal. In this case, it is reasonable that no GLS degradation occurred, being the enzyme added to a completely dried product. On the basis of this last concept, the developed HPLC-ESI-MS/MS method was evaluated also for the simultaneous determination of ITCs and GLSs during a simulated chewing process using artificial saliva (Figure 14).
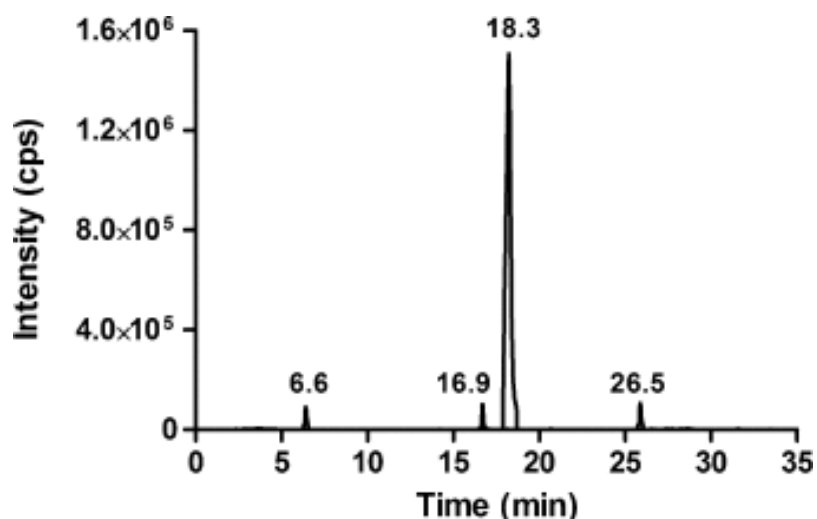
Figure 14. HPLC-ESI-MS/MS analysis of functional bakery products enriched with *E. sativa* DSM with active MYR subjected to a simulated chewing process with artificial saliva

This experiment was performed in order to verify the effectiveness of using a bakery product with active MYR in producing the bioactive compounds during the consumption of the product. Results, as reported in Table 5, shows that small amounts of ITCs might be formed in the chewing process already, opening a new lead for the exploitation of this strategy for a slow and controlled release of ITCs, independent from the action of the microbiome.

Table 5. GLS and ITC amounts obtained from chewing simulated extraction from crackers

GRA (µg/100 g)	GER (µg/100 g)	SFN (µg/100 g)	ERN (µg/100 g)
1.2 ± 0.1	16.5 ± 1.0	0.1 ± 0.0	18.2 ± 1.1

1.5   Conclusions

E. Sativa contains a wide range of compounds with nutraceutical and organoleptic properties and is used, since ancient times, in traditional medicine. Recently *E. sativa* has appeared to be an interesting industrial non-food crop, due to its wide climatic and agronomical adaptation and to the good yield of oil with high erucic acid content, which makes it a promising alternative for energy and biolubricant chain. *E. sativa* DSM represents a co-product of the biodiesel chain, particularly rich in high added value compounds such as GLSs, whose valorization makes the entire chain environmentally and economically sustainable.

In this context, an HPLC–ESI-MS/MS method for the simultaneous determination of GLSs and ITCs has been developed and validated according to ICH guidelines. The method showed to be robust and selective, precise and accurate, and permits the quantification of the GLSs and ITCs during all various stages of the industrial process from biomass evaluation to GLS-based functional food production. This method was compared with the ISO 9167-1 reference method for GLS analysis and the results were in good agreement, with the great advantages of much shorter analysis time and the total absence of any pre-analytical derivatization steps, which are required in the reference method. Concerning ITC characterization, the most widely HPLC method involves their cyclocondensation with 1,2-benzenedithiole to give1,3-benzodithiole-2-thione which shows a high molar extinction coefficient at a relatively long wavelength (ε = 23,000 $M^{-1}cm^{-1}$ at 365 nm), thus enabling ITC determination in HPLC–UV coupled to a previous solid phase extraction of 1,3-benzodithiole-2-thione via a reversed phase cartridge from samples with ITC content as low as 1 pM [33]. The method of derivatization always implies an increase in working times and, in this case, the use of reagents toxic to the environment (German Water hazard class 3 for 1,2-benzenedithiole) and probably to humans. The new HPLC–ESI-MS/MS method could replace not only the ISO 9167-1 protocol currently used, but also all the HPLC–UV methods used for the qualitative and quantitative determination of ITCs [47]. The new method is a potent tool for potential application in industrial health food production, facilitating the design and optimization of new containing GLS/ITC functional foods starting from the evaluation of the best biomasses to the final product. The thermal stability, enzymatic metabolism and all the other parameters affecting the stability of these molecules can be then easily quantified, allowing a faster and predictive design of new functional foods.

CHAPTER 2

Obeticholic acid in decompensated liver cirrhosis

Bile acids (BAs) are naturally occurring compounds synthetized *in vivo* from cholesterol. The most recognized function of BAs is their ability to dissolve lipophilic molecules and transport them throughout the systemic circulation. This is related to their amphipathic structure which leads to the formation of micelles in association to phospholipids in biliary fluid, where BAs are present at millimolar levels, then beyond their critical micellar concentration (CMC). Recently, the role of BAs as natural agonists of Farnesoid X receptor (FXR) and TGR5 has been reported, opening the lead to new insights in BA physiological functions. Indeed, considering that these two receptors are involved in several hepatic diseases and metabolic disorders, new semisynthetic analogues of endogenous BAs with improved binding potency towards FXR and TGR5 have been synthetized and subjected to clinical studies by different research groups and pharmaceutical companies.

Among these semisynthetic derivatives, Obeticholic acid (OCA) received in 2017 accelerated approval by the FDA for the treatment of Primary Biliary Cirrhosis (PBC) and is currently under advanced investigation for its use toward other hepatic pathologies, such as Non-Alcoholic Steatohepatitis (NASH). Considering the poor data available on OCA metabolism in impaired liver conditions, an *in vivo* assessment of OCA biodistribution in a model of cirrhosis should be mandatory for a total safety profile definition.

This chapter deals with the development and validation of an HPLC-ESI-MS/MS method for the analysis of OCA, its metabolites and endogenous BAs in different biological fluids and organs. This method has been successively applied for the determination of OCA metabolism and biodistribution in an induced liver cirrhosis rat model.

2.1　Introduction

2.1.1 Natural bile acids

Bile acids (BAs) are endogenous acidic steroids synthetized in the liver from cholesterol, representing the main metabolites and the main excretion pathway from the body. Bile acids are involved in a series of physiological functions, such as the dissolution and transport of lipids through the formation of mixed micelles, the stimulation of biliary flow and the complexation of cations, such as Fe^{2+} and Ca^{2+}, in order to promote their intestinal absorption [48].

Starting from cholesterol, the primary BAs, cholic acid (CA) and chenodeoxycholic (CDCA), are synthetized in the liver via cytochrome P450-mediated oxidation in a multi-step process [49]. Then, primary BAs are converted to the secondary BAs in the intestine by action of the intestinal microflora. Specifically, deoxycholic acid (DCA) and litocholic acid (LCA) are synthetized, respectively, from CA and CDCA through a 7α-dehydroxylation reaction. Another secondary BA, ursodeoxycholic acid (UDCA) is produced in the intestine by the action of bacteria able to cause the epimerization of the hydroxyl group in position 7 of CDCA from α to β position [49]. Both primary and secondary BAs are subjected in the liver to phase II metabolism by the conjugation reaction with glycine, taurine, glucuronic acid and sulphuric acid (Figure 15). Bile acids, despite the high number occurring within different species, share a common structure composed of a steroid backbone with four rings (conventionally labelled as A, B, C and D), a five-carbon sidechain terminating in a carboxylic acid, and different hydroxyl groups, whose orientation and position is variable and specific to each BA [49]. Bile acids present the typical chair conformation, which is due to the cis junction between the A and B rings; in some vertebrates, this junction is in trans position and for this reason they are called Allo-BAs. In the chair conformation, it is possible to define a concave side and a convex side. Hydroxyl groups and carboxylic groups are oriented toward the concave side, making it hydrophilic, while methyl groups are oriented toward the convex side, which is then hydrophobic. Hydroxyl groups, according to the specific BA and the species, can be either β (normally indicated with a solid line) or α (indicated with a dashed one) oriented. For example, human BAs present hydroxyl groups in positions 3α, 7α/β and 12α, while in murine species the hydroxyl group can be found in position 6β, but never in 12.
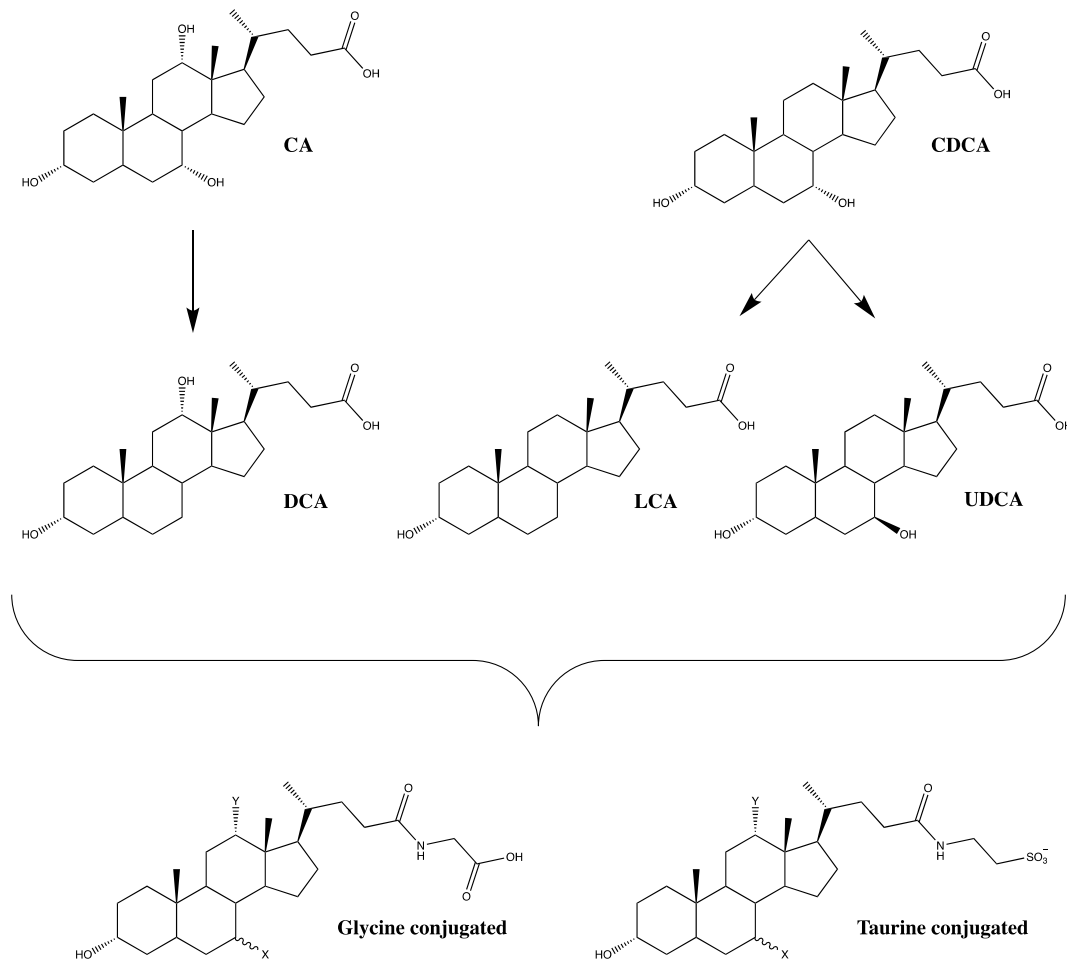
Figure 15. Principal BAs in human

Bile acid synthesis follows two different metabolic pathways [50]: the classic neutral (mainly in the hepatocytes) and the alternative acidic one, which takes place in the liver and macrophages (Figure 16). The first pathway is the most important and it leads to the production of CA and CDCA, while the second one has a minor role and produces only CDCA. In the main route, the first step is the reaction catalyzed by the cholesterol 7α-hydroxylase (CYP7A1), consisting on the addition of the 7α-hydroxyl group to the cholesterol moiety. This reaction is very important because is the rate determining step of the entire biosynthesis process and is then involved in the regulation of BA levels in the body.
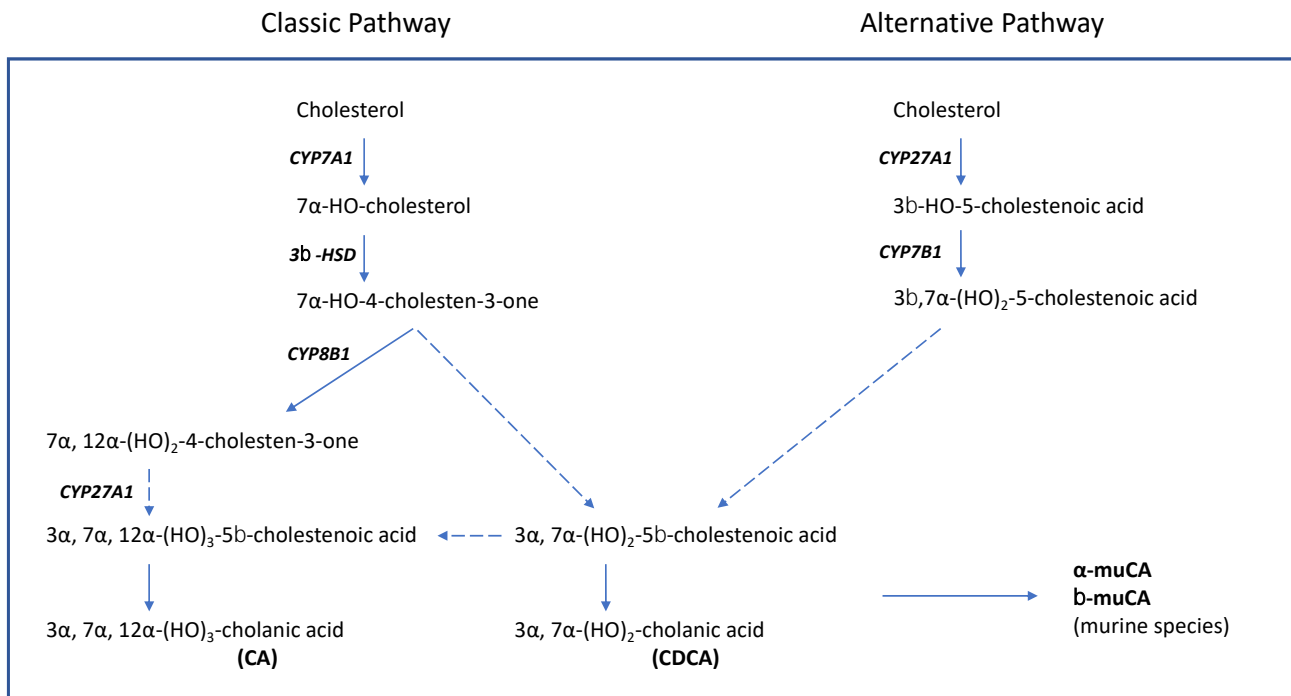
Figure 16. Biosynthesis of BAs

2.1.2 Enterohepatic circulation of BAs

Following the consumption of lipids by diet, the duodenum cells secrete cholecystokinin in the circle. The subsequent binding of this hormone to the smooth muscle cells of the gallbladder wall promotes contraction. This results in the pulsatile secretion of bile (containing high concentrations of BAs) in the duodenum [51].

Under physiological conditions, the body BA pool is constant and is about 3-5 g; this homeostasis is made possible by two processes: BA reabsorption at intestinal level and their *de novo* synthesis from cholesterol. Up to 95% of the secreted BAs are reabsorbed at the intestinal level, not together with the products of lipid digestion, but through a defined enterohepatic circulation process [51].

The enterohepatic circulation is an extremely efficient recovery system, which seems to occur at least twice per meal, involving the liver, biliary tree, duodenum, colon and portal circle by which the reabsorbed molecules return to the liver. This recirculation is made necessary by the fact that the ability of hepatocytes to produce BAs is limited and insufficient to satisfy intestinal physiological needs if they were lost in high quantities.

Most BAs are reabsorbed in the distal ileum, the lowest part of the small intestine, by means of a sodium-dependent transporter present in the enterocytes, called Apical sodium-dependent Bile

Acid Transporter (ASBT) [52], which carries out a transport of two sodium ions and a molecule of BA.

Once inside the enterocyte, BAs are transported by the intervention of the Ileal Bile Acid-Binding Protein (IBABP) through the cytosol to the basolateral membrane, which is crossed thanks to the action of the Organic Solute Transporter alpha and beta (OSTα/OSTβ) [53]. Through the portal circle, carried by albumin, they finally reach the liver, where their uptake from the circle is very efficient, so that from 50 to 90% are removed at the first step. Conjugated BAs are largely extracted by an active sodium-dependent transport mechanism, using the Na^+-dependent taurocholate co-transport polypeptide (NTCP) [54]. However, sodium-independent transport may also take place by proteins from the family of Organic Anion Transporting Polypeptides (OATP), mainly OATP1B1 and OATP1B3 isoforms.

In the enterohepatic circulation, the limiting passage is represented by the secretion of BAs in the biliary canal, largely due to the Bile Salt export pump (BSEP) [54] in an ATP-dependent process. This pump transports anionic BAs, which are the majority. Dianionic bile acids, like the conjugates with glucuronic and sulphuric acids, are secreted by different transporters such as MRP2 and BCRP. The unconjugated BAs are too lipophilic for being secreted as such, therefore they require conjugation with glycine and taurine, in order to increase the hydrophilicity. Indeed, in humans, before being secreted in bile, free BAs are conjugated almost entirely (up to 98%) with the amino acids glycine or taurine, to give respectively glycoconiugated and tauroconiugated BAs [55]. In particular, about 75% of CA and CDCA are conjugated with glycine, giving glycocholic acid (GCA) and glycochenodeoxycholic acid (GCDCA), while the remaining 25% with taurine to give taurocholic acid (TCA) and taurochenodeoxycholic acid (TCDCA). The conjugation process also has the effect to reduce the toxicity of the starting compounds.

Once secreted into bile, BAs reach the ileum and then, if not reabsorbed, they enter the colon where a series of reactions accomplished by intestinal microflora lead to some structural modifications [56]. In particular:

- Deconjugation of the conjugated BA lateral chain to produce free BAs plus glycine or taurine. This reaction is catalyzed by bacterial Bile Salt Hydrolase (BSH).
- 7α-dehydroxylation reaction on primary BAs to produce secondary BAs. This reaction is catalyzed by the enzyme 7α-hydrolase and takes place only on unconjugated BAs, then preliminary deconjugation is a mandatory requisite.

- Oxidation and epimerization reactions on hydroxyl groups involve bacterial Hydroxysterol Dehydrogenase enzymes and, although it can occur at all positions, the most important is the reaction at position 7. The most prominent example is the conversion of CDCA to UDCA.

Part of the secondary BAs produced in the colon are passively reabsorbed, while the unabsorbed fraction is lost through feces. It is important to underline that the formation of more lipophilic compounds in the colon area, although might appear uncommon, occur in order to enhance the reabsorption of BAs throughout the colonic mucosa and maintain constant the physiological BA pool. The reabsorbed secondary BAs, in analogy to their primary precursors, are taken up by the liver, conjugated and secreted into bile, being furtherly involved in the enterohepatic circulation.

2.1.3 Receptorial activity of BAs

Bile acids have been known for several physiological functions:

- They are physiological surfactants able to promote the dissolution and the transport of lipids derived from diet. Indeed, thanks to the formation of micelles, BAs tend to include idrophobic substances with consequent formation of lipid emulsions with increased dispersion in the water mean.

- At pancreatic level, they stimulate the secretion of digestive enzymes and cholecystokinin

- They have a powerful antimicrobial activity in the intestine, especially DCA

- They are able to regulate the biliary flow by osmotic mechanism

Despite all these function, the presence of such a complex metabolism and fine regulation of their physiological concentrations have not been always clear and fully understood. The breakthrough point in the comprehension of BA physiological role was the discovery of their activity as endogenous ligands for two receptors: the Farnesoid X receptor (FXR) [57] and G protein-coupled receptor TGR5 [58].

The FXR is a nuclear receptor, mainly expressed in the liver and small intestine, which is involved in the regulation of BA synthesis by a negative feedback mechanism. At intestinal level, the activation of this receptor increases the expression of IBABP and basolateral OSTα/β. Additionally, it increases the expression of fibroblast growth factor 15/19 (FGF15/19), which reaches the liver and suppresses the formation of BAs from cholesterol by inhibition of CYP7A1, limiting step of the entire biosynthesis, conjugation and transport of BAs [57]. At the same time, FXR regulates the processes of conjugation in the liver and, through the induction of the canalicular bile acid transport protein (ABCB11) and phospholipidfloppase (ABCB4), is able to limit and control BA

cytotoxicity in the intestinal tract [59]. Totally, FXR plays a major role in the cross-talk between liver and gut, limiting both BA synthesis and their toxic effects on hepatocytes or enterocytes. On these basis, FXR proved to be a very important target in clinical practice, considering its relevance in several liver and biliary tract diseases, such as cholestasis, gallbladder stones, hepatic inflammation, inflammatory bowel disease, cirrhosis and non-alcoholic steatohepatitis [59].

The membrane receptor TGR5, on the other hand, is widely distributed, including endocrine glands, adipocytes, muscles, immune organs, spinal cord, and the enteric nervous system. The effect of TGR5 activation depends on the tissue where it is expressed and the signaling cascade that it induces. Generally, its activation plays a role in the control of glucagone-like peptide 1 (GLP-1) secretion, which regulates pancreatic functions and sugar levels in blood [58]. Therefore, its role in regulation of basal metabolism and energy expenditure is well known and, consequently, is now recognized as a potential target for the treatment of metabolic disorders, such as type 2 diabetes and obesity [60].

2.1.4 Semisynthetic analogues of BAs

It has been showed that, among all endogenous BAs, CDCA and CA are the most potent ligands towards FXR and TGR5, respectively [61].

On these basis, in recent years several efforts have been focused on the synthesis of semisynthetic analogues of CA and CDCA, with the goal to discover new lead candidates characterized by a more potent and selective activity towards FXR and TGR5 [62, 63]. This is due to the increasing awareness that both FXR and TGR5 are involved in several gastrointestinal and hepatic diseases and consecutively, the demand for new drugs able to target these receptors is increasing. The two receptors present small differences in the structure of the binding site, therefore it is possible to develop BA analogues with specific selectivity toward only one target or either able to ligate both, opening new leads for the simultaneous treatment of cholestatic liver diseases and metabolic disorders.

It has been reported that small amendments in the structure of natural BAs can deeply modify the biological properties and for this reason the structure-activity relationship for what concerns the selective interactions with FXR and TGR5 have been studied in detail [62, 64].

A prominent example is given by three semisynthetic analogues which are property of Intercept Pharmateuticals: INT-747, INT-777 and INT-767; the first two compounds are, respectively, activators of FXR and TGR5, while the third shows affinity for both. While INT-777 and INT-767 are

still in advanced clinical phase, INT-747 (also known as obethicolic acid or OCA) has been recently granted with the FDA approval for the treatment of primary biliary cirrhosis (PBC) and is currently sold under the commercial name of Ocaliva®.

2.1.5 Obeticholic acid in the treatment of PBC

Primary biliary cirrhosis, also referred as primary biliary cholangitis, is a chronic autoimmune hepatic disease whose main features are the inflammation and the continue destruction of the hepatic biliary ducts [65]. These events lead to cholestasis, parenchymal injury due to BA excess, and eventually end-stage liver disease. The etiology of PBC has not been fully elucidated yet and no clear cause agents have been identified so far [66]. Recurring symptoms, observed in over 20% of patients with diagnosed disease are fatigue and pruritus [67]. Historically, the endogenous UDCA has been used as the only approved therapy for PBC, but only 40% of the treated patients has shown positive response to this compound [68]. Many other agents have been tested for the treatment of this degenerative disease, including colchicine [69], fibrates [70], and methotrexate [71]. However, these other therapies have not showed any effectiveness, thus a critical need for new pharmacotherapies to treat PBC and prolong survival from this disease is one of the most demanding issues nowadays.

Obeticholic acid is a semisynthetic BA analogue obtained from CDCA through the addition of a 6α-ethyl group. This structural modification confers two main advantages in respect to its endogenous analogue: a 100-fold higher binding affinity toward FXR and higher resistance against the 7α-dehydroxylation by intestinal bacteria, allowing an increased persistence within the enterohepatic circulation [62]. This compound is rapidly absorbed and efficiently conjugated to glycine and taurine and then undergo enterohepatic recirculation, similarly to CDCA. Pharmacokinetic profiles are also broadly similar, with the exception of the 7-dehydroxylation step being restricted to CDCA [72], as the steric hindrance provided by the ethyl group in position 6α impairs this kind of reaction. OCA is a first-in-class agonist that selectively binds to the FXR, accomplishing the suppression of the hepatic BA production and increasing bile flow, thus leading to a reduced exposure of the liver to toxic levels of BAs [73]. These actions should clinically translate into decreased parenchymal liver injury caused by BAs, resulting in improved biochemical enzyme profiles and decreased disease progression of PBC. Thus, the novelty introduced by OCA is based on its capability to bind FXR with high selectivity and potency (EC50 0.09 μM vs 8.6 μM of CDCA), which is totally different mechanism in respect to UDCA (no activity

toward FXR), whose therapeutic efficacy was only based on the displacement of more detergent BAs in the human pool. OCA has been successfully evaluated in clinical studies in PBC patients [74]. In addition, OCA enhances insulin sensitivity in patients with NAFLD and type 2 diabetes [75] and reduces liver fibrosis in NASH patients [76]. OCA has recently been granted accelerated approval by the U.S. Food and Drug Administration for the treatment of PBC and is commercially available as OCALIVA® (Intercept Pharmaceuticals, Inc.).

The encouraging results from Phase II and III studies represent a significant milestone in PBC; however, longer term efficacy of OCA and the general applicability to the entire PBC population is still to be confirmed in prospective follow-up studies. This is of particular importance given the limited number of patients enrolled in this kind of clinical trials, which is a symptom of the relative infrequency of PBC globally [77].

2.2 Aim and rationale

The liver has a network of nuclear receptor-regulated pathways that coordinate the synthesis, hepatic uptake and transport of BAs, modulating their concentrations in the liver. The most relevant nuclear receptor is FXR, which is agonistically controlled by BAs and which regulates a variety of target genes involved in controlling BAs, lipids, glucose, inflammation, and fibrosis.

FXR activation inhibits BA synthesis and protects against the toxic hepatic accumulation of BAs by regulating most of the BA hepatic transport proteins and promoting detoxification from the liver through phase I and phase II metabolism. These mechanisms make FXR agonists a target for treating cholestatic liver diseases, as PBC, PSC and NASH.

OCA is a 6α-ethyl derivative of CDCA, the natural FXR agonist in humans. OCA is a first-in-class selective FXR agonist, originally described for its anti-cholestatic and hepatoprotective properties. OCA has been successfully applied in the treatment of PBC and has received accelerated approval from FDA. Additionally, it is under clinical evaluation for the treatment of other hepatic diseases, such as NAFLD and NASH.

In healthy rats, OCA is metabolized in a similar manner to the structurally related CDCA but is more metabolically stable in terms of intestinal bacterial 7α-dehydroxylation. Unfortunately, poor data are available on OCA metabolic profile and biodistribution in conditions of severe liver impairment. Indeed, the increased plasma concentration of BAs in liver disease is due to deficient liver uptake, impaired metabolism, defective bile secretion, dysbiosis in the gut microbiota, and a portosystemic shunt between the portal vascular system and systemic circulation. It is thus important to evaluate whether, due to its high lipophilicity, OCA occurs at high hepatic and serum levels in end-stage liver disease. Besides, it is essential to assess OCA metabolic profile in conditions of hepatic failure to determine if any uncommon and potentially toxic metabolites are formed to facilitate its excretion.

Given that OCA is used to treat PBC, and considering the above safety issue, this chapter deals with the metabolism and biodistribution of OCA and endogenous BAs after a single oral dose (30 mg/kg) in rats with CCl$_4$-induced decompensated cirrhosis. With this aim, an HPLC-ES-MS/MS method was developed and validated to quantify endogenous BAs, OCA and its main metabolites in rat plasma, liver, stools, small intestine content, colon content, urine and kidney samples. The targeted endogenous BAs were only free BAs and their relative taurine conjugates, as glycine conjugates do not occur in rat. As regards OCA metabolism, a series of possible metabolites were

assumed on the basis of the typical metabolic pathways involving BAs. The method was tailored in order to cope with different analytical challenges, such as:

- Sensitivity issues related to the presence of very low concentrations in biological samples.

- Selectivity issues related to the necessity to discriminate structurally similar compounds (isomers, epimers, etc...).

- Suitable and efficient clean-up procedures from the very complex biological matrices investigated.

- Identification of unknown or uncommon hepatic metabolites potentially occurring in case of liver impairment conditions.

The metabolism and biliary secretion of OCA in a bile fistula model in cirrhotic rats in the three hours following intravenous infusion of OCA has been reported as well. This kind of experiment allowed the evaluation of BA net hepatic uptake, biotransformation, and secretion during cirrhosis progression.

2.3 Materials and methods

2.3.1 Chemicals

Endogenous BA analytical standards (CA, CDCA, DCA, LCA, UDCA, and their taurine conjugates) were purchased from Sigma-Aldrich (Saint Louis, USA). Standards of OCA, its taurine conjugate (T-OCA) and glycine conjugate (G-OCA) were kindly provided by prof. Roberto Pellicciari (University of Perugia, Italy). Isopropanol (iPrOH), MeOH and ACN (HPLC-grade, Lichrosolv®) were purchased from Merck (Darmstadt, Germany). Acetic acid (98% purity) and ammonium hydroxide (98% purity) were purchased from Fluka (Buchs, Switzerland). Water of HPLC-MS grade (Millipore) was produced using the depurative system Milli-Q Synthesis A 10 (Molsheim, France). Other solvents were all of analytical grade.

Stock standard solutions of all the BA standards were prepared in MeOH at concentration of 1 mM. These stock solutions were aliquoted and stored at -20 °C to minimize potential solvent evaporation. Mixed WSs containing all compounds were made by appropriate dilution of the stock solutions in MeOH in the range 0.1–100 μM and stored at 4 °C. Calibration solutions in the range 0.01–10 μM were prepared before the analysis by 1:10 dilution of the WSs in mobile phase, which was a mixture of H2O-MeOH-ACN (35:15:50). The QCs containing all the analytes were obtained at concentrations 0.2 μM, 1.0 μM and 5.0 μM. These samples were used for the method validation or injected randomly during the analysis in order to control the normal behavior of the analytical system.

1.3.2 Instrumentation

The chromatographic apparatus consisted of a Waters Alliance 2690 Chromatograph (Milford, MA, USA) with 120 position autosampler and thermostat coupled with a mass spectrometer triple quadrupole and electrospray interface (QUATTRO LC, Waters). The column was a WATERS X-select CSHTM Phenyl-Hexyl 5.0 μm (2.1 mm × 150 mm).

1.3.3 HPLC-ESI-MS/MS conditions

Chromatographic separation was achieved using a reversed phase Phenyl-Hexyl column. The mobile phase was constituted by HPLC grade water with 15 mM ammonium acetate at pH 8.00 (A component) and ACN-MeOH (75:25) (B component). Different LC gradients were evaluated during

the method optimization. The best separation was obtained with the following gradient of the B component: 10 min 35%, 11 min at 45%, 4 min at 90%, 10 min at 35%, (total run time 35 min) at 0.15 mL/min flow rate. Each variation in the eluent composition was instantaneous. The column was maintained at 45 °C and the injected sample volume was 5 μL. The TIC with all the analytes is reported in Figure 17.
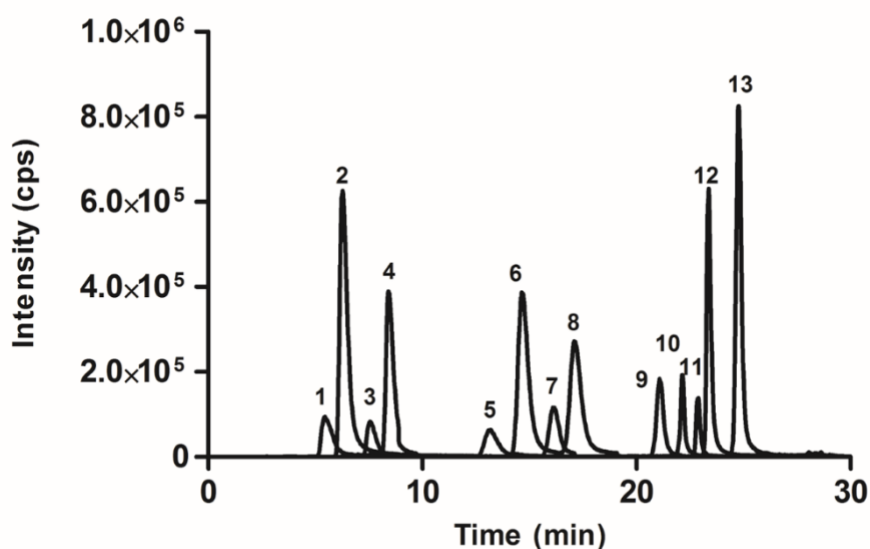
Figure 17. Total ion current chromatogram reporting the HPLC separation on a Phenyl-Hexyl column of endogenous BAs, OCA, T-OCA and G-OCA. The elution order is: TUDCA (1), UDCA (2), TCA (3), CA (4), TCDCA (5), CDCA (6), TDCA (7), DCA (8), G-OCA (9), TLCA (10), T-OCA (11), LCA (12), OCA (13)

The column effluent was introduced into the ESI source, operating in negative ion, connected to a triple quadrupole mass spectrometer operating in MRM mode. The experimental MS conditions were properly tuned by direct infusion of each compound (1 μM of each analyte; 2 mL/h infusion rate). Capiilary voltage was set at -2.7 KV, cone at 60 V (unconjugated BAs) or 90 V (conjugated BAs), source and desolvation temperature were respectively set at 130 °C and 200 °C, while the collision gas was argon. The two most abundant signals in extracted ion chromatogram (EIC) were monitored for each compound. The most intense was used for the quantification, the second one for the compound confirmation. Specifically, for unconjugated BAs, only the transition [M - H]$^-$ > [M - H]$^-$ was used, while for conjugated BAs the transition [M - H]$^-$ > [M - H]$^-$ was used for the quantification and the transitions [M - H]$^-$ > taurine fragment (*m/z* 124.4) or [M - H]$^-$ > glycine fragment (*m/z* 74.3) were used for the confirmation. In Table 6 were reported the retention times and the MS/MS transitions used for the identification and quantification of each compound.

Table 6. Retention times and MS/MS transitions for all the analyzed BAs

BA	Retention time (min)	Transition ($m_1/z_1 > m_2/z_2$)
CA	8.3	407.4 > 407.4
CDCA	14.3	391.4 > 391.4
DCA	17.8	391.4 > 391.4
UDCA	6.2	391.4 > 391.4
LCA	23.3	375.4 > 375.4
TCA	7.4	514.4 > 514.4 (quantification) 514.4 > 124.4 (confirmation)
TCDCA	13.1	498.4 > 498.4 (quantification) 498.4 > 124.4 (confirmation)
TDCA	17.8	498.4 > 498.4 (quantification) 498.4 > 124.4 (confirmation)
TUDCA	5.3	498.4 > 498.4 (quantification) 498.4 > 124.4 (confirmation)
TLCA	22.1	482.4 > 482.4 (quantification) 482.4 > 124.4 (confirmation)
OCA	24.7	419.4 > 419.4
T-OCA	22.8	526.4 > 526.4 (quantification) 526.4 > 124.4 (confirmation)
G-OCA	20.9	476.4 > 476.4 (quantification) 476.4 > 74.3 (confirmation)

2.3.4 Sample preparation

2.3.4.1 Bile samples

Rat bile samples were thawed and diluted 1:100 or 1:10 (v/v) with mobile phase. The final solution was filtered, transferred to an autosampler vial and 5 µL were injected into the HPLC-ESI-MS/MS system.

2.3.4.2 Plasma and urine samples

Plasma (100 µL) or urine (200 µL) samples were diluted 1:6 (v/v) with 0.1 M NaOH and heated to 64°C for 30 minutes. This solution was subjected to solid phase extraction (SPE) procedure using C18 cartridges. The SPE cartridge was conditioned with 5 mL of MeOH and 5 mL of water prior to sample loading. Plasma samples were loaded into the conditioned cartridge and then washed with 10 mL of water. The cartridge was then eluted with 5 mL of MeOH. The eluate was dried under vacuum and then reconstituted with 100 µL of the mobile phase, filtered, transferred to an autosampler vial and 5 µL were injected into the HPLC-ES-MS/MS instrument.

2.3.4.3 Liver and kidney samples

Aliquots weighing approximately 0.5 g were taken from different points of the sample. These aliquots were weighted and 2 mL of phosphate buffer (0.005 M, pH 7.2) was added. The mixture was homogenized using a potter, which was then washed with 3 mL of MeOH. The mixture was subjected to sonication bath for 5 minutes, heated to 37 °C for 20 minutes, and centrifuged at 2100 rpm for 15 minutes. One milliliter of the supernatant dried under vacuum and the resulting residue then suspended with 2 mL of sodium hydroxide (0.1 N). The resulting solution was sonicated for 10 minutes, heated to 64°C for 30 minutes and SPE clean-up was carried out on C18 extraction cartridges as described above. The eluate was dried under vacuum, reconstituted with 100 µL of the mobile phase, filtered, transferred to an autosampler vial and 5 µL injected into the HPLC-ES-MS system.

2.3.4.4 Feces and intestinal content samples

Feces or intestinal content sample was collected and homogenized using a mixer. Aliquots weighing approximately 1 g were taken from the homogenate. Each aliquot was weighed and 3 mL of iPrOH were added. The mixture was left under stirring overnight and then centrifuged at 2100

rpm for 10 minutes. The supernatant was then diluted 1:10 (v/v) with mobile phase, filtered, transferred to an autosampler vial and 5 μL injected into the HPLC-ES-MS system.

2.3.5 Method validation

Method validation was performed according to ICH guidelines. Selectivity, LOD, LOQ, calibration range, precision, accuracy and matrix effect were evaluated for each analyte in all the studied matrices according to the protocols reported in paragraph 1.3.4. The matrix effect in each biological matrix was calculated at three concentration levels as the ratio of the analyte in mobile phase with respect to the analyte in the real sample fortified at the end of the clean-up. The recovery after SPE was calculated as percentage ratio of each analyte concentration at three concentration levels after and before SPE extraction.

2.3.6 *In vivo* studies

2.3.6.1 CCl$_4$-induced rat model of cirrhosis

All experiments were carried out according to the guidelines set forth by EEC Directive 86/609 on the care and use of experimental animals. The protocol for the induction of cirrhosis was approved by the Institutional Ethics Committee of the University of Bologna (Protocol CES 25. 57/80). All studies involving animals are reported in accordance with the ARRIVE guidelines [78].

Male Winstar-Han rats (Charles River Laboratories, Calco, LC, Italy), weighting 225-250 g, were housed for 3 weeks before the experiments, in order to achieve a complete adaptation in view of the following possibly harmful procedure. The induction of cirrhosis was preceded by one-week phenobarbital administration (0.3 g/L in drinking water), therefore at the beginning of the study (1 month after the animal were housed), their weight was considerably increased. Cirrhosis was induced by carbon tetrachloride (CCl$_4$) inhalation [79]. Phenobarbital administration was continued throughout the study as an enzyme inducer. Animals were housed in a controlled environment (22–24 °C), maintained on a standard 12 hours light/dark cycle and had free access to food and water throughout the study. The rats were placed in a gas chamber (70×25×30 cm) and compressed air, bubbling through a flask containing CCl$_4$, was passed into the gas chamber via a flow meter (1 L/min). Animals were exposed to the gas atmosphere twice a week, starting with 0.5 min of bubbling and 0.5 min in the gas atmosphere. Afterwards, the time was increased to 1

min and then by 1 min until 5 min of air flow and 5 min in gas atmosphere were reached. The mortality rate associated with this induction method was approximately 15%.

Throughout the study, at weekly intervals, the animals were weighted and their conditions were monitored, including body weight changes, external physical appearance, behavioral and physiological changes (e.g., body temperature, hormonal fluctuations, and clinical pathology).

In order to define a cirrhosis score for each animal, histological activity and fibrosis, biochemical, clinical encephalopathy and ascites scores were combined into overall scores. All animals used for this study had overall cirrhosis score between 10 and 30.

2.3.6.2 Biodistribution of OCA and endogenous BAs

Rats with decompensated cirrhosis were divided into 7 groups (3 rats each). Group 8 contained healthy control rats. Eight hours after food withdrawal, OCA suspended in 300 μL saline solution was administered by gavage at a single dose of 30 mg/kg.

Groups 1, 2, 3, 4, 5, and 6 were sacrificed respectively at 1, 2, 4, 8, 24, and 48 h following OCA administration. OCA, its metabolites and endogenous BAs were measured in plasma, liver, kidneys, and the contents of small intestine and colon.

Rats of groups 5 and 6 were kept in metabolic cages for 24 h and 48 h. In these two groups, OCA and its metabolites were also measured in urine and stools for complete mass balance and biodistribution evaluation. The cirrhotic rats of group 7 were placed in metabolic cages for 24 h without OCA administration. Group 8 comprised matched control healthy rats, receiving OCA with the same modalities. Globally, 21 cirrhotic rats and 18 healthy rats were used for the biodistribution study.

At the sacrifice time, after anesthesia (20 mg/kg Zoletil), blood was withdrawn in heparinized tubes, centrifuged and plasma collected as supernatant. Additionally, liver, intestinal contents (small and large intestine), kidneys, stools, and urine were collected. All biological samples were immediately stored at -80 °C before the analysis.

2.3.6.3 Intravenous infusion of OCA in the bile fistula rat model

The study was performed on 12 rats: 3 healthy rats and 9 cirrhotic rats (3 rats/group) at 8, 10, and 13 weeks following CCl$_4$ administration. In anesthetized rats, the bile duct was cannulated and OCA was intravenously infused at a dose of 1 μmol/min/kg over 1 h [80]. Bile was collected every 15 min for 3 h. The concentrations of endogenous BAs, OCA and its metabolites in bile were

measured. The bile flow was gravimetrically calculated and expressed as µL/min/kg, while the secretion rate was calculated from the bile volume and the BA concentration and expressed as µmol/min/kg.

2.3.7 Quantification and statistical analysis

A seven-point calibration curve in the range 0.05-10 µM in mobile phase was used for the quantification of the different analytes within all the different biological matrices, except for plasma. For quantification in plasma, a calibration curve in BA serum free was used, by subjecting the single concentration points to the SPE clean-up described above. Considering that endogenous BAs naturally occur in plasma, this kind of matrix was preliminary subjected to a specific treatment [81] with catalytic carbon in order to get rid of the endogenous contribute and obtaining a blank serum. Linear calibration curves were obtained from the plot of the standard analyte peak area versus analyte concentration using a least-squares regression analysis.

The quantitative data are presented as mean ± standard deviation (SD). A paired t-test was used to assess specific differences between cirrhotic and healthy rats in the different matrices analyzed. The comparisons between healthy and cirrhosis groups in a specific organ/fluid were performed considering the total OCA concentrations or recoveries, intended as the sum of OCA and the quantified metabolites, at the same time-points. The level of statistical significance was set at $p < 0.10$. The choice of this value as cutoff can be considered reasonable when a small number of animals for each group is used and many biochemical data are collected.

2.4 Results and Discussion

2.4.1 Mass spectrometry analysis of BAs

Bile acids and their conjugates with taurine and glycine are acidic compounds and therefore are easily detected in negative ionization mode. The optimization of MS conditions has been carried out throughout the tuning of the electrospray ionization parameters: capillary and cone voltages, collision energy and source temperature. The proper tuning of these parameters allowed us to gain high current intensities for a sensitive detection of the compounds. In negative ionization mode, both free and conjugated BAs afforded the best signal intensities at low collision energies following the transition $[M - H]^- > [M - H]^-$, which was chosen for quantification purposes. For confirmation, possible fragmentation reactions, occurring at higher collision energies, were investigated. As depicted in Figure 18, free BAs did not afford any fragmentation, while taurine and glycine conjugates provided the ions having m/z 124.4 (taurine ion) and 74.3 (glycine ion), respectively. Consequently, the transitions $[M - H]^- > 124.4$ and $[M - H]^- > 74.3$ were selected, respectively, for the identification of taurine and glycine conjugates.
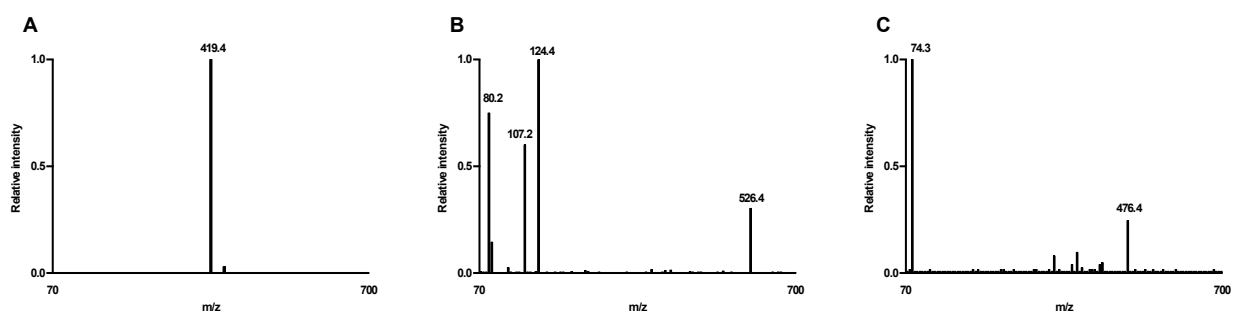
Figure 18. Tandem MS data of OCA (A), T-OCA (B) and G-OCA (c) precursor ions (m/z 419.4, 526.4, 476.4, respectively)

2.4.2 Method validation

Calibration curve parameters for OCA, T-OCA, G-OCA and the endogenous BA quantification, in the range 0.05-10 µg/mL, were obtained from the plot of the analyte standard peak area versus analyte concentration using a linear least-square regression analysis. Determination coefficients (r^2) of the calibration curves were ≥ 0.995 for all analytes, both in mobile phase and plasma, meaning a good linearity over two orders of concentrations.

Limits of detection in mobile phase and plasma ranged from 2 ng/mL to 10 ng/mL, while limits of quantification in mobile phase and plasma from 5 ng/mL to 25 ng/mL for all the investigated analytes.

Variation coefficients and bias% calculated, both intra- and inter-daily, were less than 5% for all analytes at the different concentration levels, indicating that the method possesses satisfying precision and accuracy, and then suitable for the purpose of the study.

The comparison between standard solutions and fortified samples with known amounts of analyte and blank samples showed good selectivity in multiple reaction monitoring (MRM) mode, as no interfering signals, potentially able to affect the identification of the target analytes, were observed.

Matrix effect percentage was evaluated at three concentration levels in all the studied matrices. Matrix effect values higher and lower than 0% indicated, respectively, ionic increase (positive matrix effect) or ionic suppression (negative matrix effect). In all the studied matrices, with the exception of plasma, matrix effect values were negligible, being always below 10% for all the studied analytes. In plasma, matrix effect higher than 20% was observed, leading to the necessity of calibration curves built in BA-free plasma.

The efficiency of solid phase extraction during sample clean-up was calculated by Rec%. Experimental values were close to 100% for all the investigated analytes, indicating the efficacy of this process. The pre-analytical treatment of the different matrices was tailored in order to obtain a sensitive and selective quantification of the investigated BAs. For this reason, different SPE procedures have been tested throughout the screening of different eluents and stationary phases. The main advantages of the pre-analytical protocols that we have developed consist on the low matrix effects and the high recoveries at different concentration levels, and the possibility to concentrate the sample with consequent increase in the sensitivity of the detection. Additionally, with the exception of plasma, the possibility to use calibration curves in mobile phase allowed a fast and accurate quantification in all the analyzed matrices.

2.4.3 Tentative *in vivo* metabolism of OCA

In rat, natural BAs are preferentially conjugated with taurine and not with glycine, although this alternative cannot be excluded in general. Sometimes, it is also possible that hydroxylation of the sterol moiety occurs, in order to promote the secretion into bile. Furthermore, during intestinal transit, the unabsorbed fraction in the small intestine reach the terminal ileum and the colon

where BAs are metabolized by the intestinal bacteria. This involves dehydroxylation, oxidation and epimerization reactions, as these kinds of products have been observed in stools. In the liver and small intestine, conjugation with glucuronic or sulphuric acids at one or more hydroxyl groups occurs, leading to the formation of (di)glucuronides and (di)sulphates, in order to produce more hydrophilic compounds easily excreted through stools or urine. On these basis, it has been assumed that OCA might undergo similar metabolism and then all the possible expected metabolites have been investigated and tentatively identified according to the *m/z* values of the [M - H]⁻ ion or possible fragmentation reactions. Since the standards necessary for their precise identification and quantification were not available, a semiquantitative analysis was performed for these compounds using the calibration curve of the most similar BA analogue. Figure 19 reports the structure of all the assumed OCA metabolites tentatively investigated for the assessment of OCA metabolism.
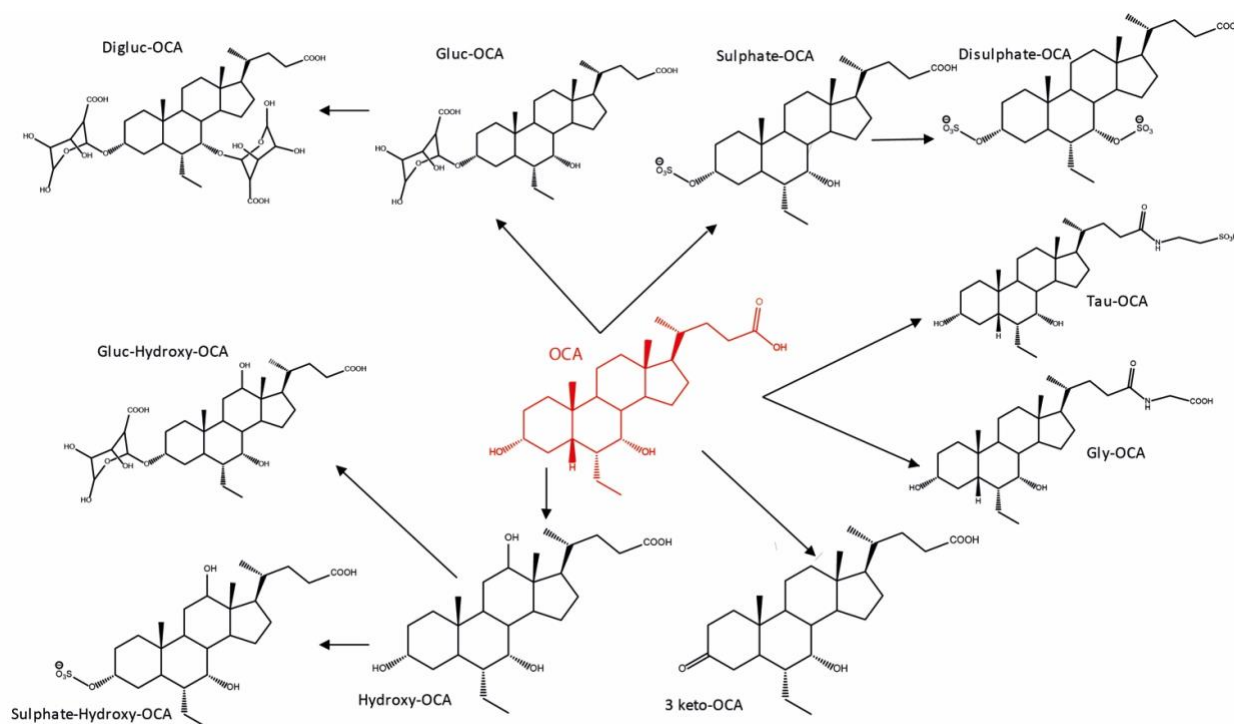

Figure 19. Structures of all the assumed OCA metabolites

2.4.4 Concentrations of OCA, its metabolites and endogenous BAs

2.4.4.1 Plasma

In cirrhosis, OCA and main metabolites concentrations were significantly higher than in controls: mean maximum levels (28.3±6.9 µmol/L) were reached 8 h after OCA administration (0.45 ± 0.07

μmol/L in controls) (p<0.01). In cirrhosis, OCA was initially unconjugated. It then decreased with formation of T-OCA and the monoglucuronide (Glu-OCA), as reported in Figure 20A. After 24 h, total OCA concentration was 5.1 ± 2.9 μmol/L, both free and taurine-conjugated. After 24 h, OCA concentration in controls was significantly lower, 0.27 ± 0.04 μmol/L (p<0.05), and mainly unconjugated (Figure 20B).

Concentrations of endogenous BAs were higher than total OCA, in both cirrhotic and healthy rats. As a general trend, OCA and its metabolites concentrations of were higher in rats with high endogenous BAs.

2.4.4.2 Liver

At 24 h after administration, the mean hepatic total OCA concentration in cirrhotic rats was significantly higher (p<0.10) than in controls (1.21 ± 0.43 vs 0.56 ± 0.11 μmol/g, respectively), as shown in Figure 20C and 20D. The maximum hepatic concentration in cirrhosis was reached after 24 h. However, it was still present after 48 h (0.47 ± 0.17 μmol/g), significantly higher than in controls (0.08 ± 0.02 μmol/g) (p<0.05). OCA was mostly conjugated with glycine (~50%) and to a lower extent with taurine (~30-40%). The maximum concentration of OCA in the liver of cirrhotic rats was about 2 times higher than in controls. However, the total hepatic concentration of endogenous BA was at least 100 times (50-80 μmol/g) higher. In particular, liver concentration of endogenous BAs in cirrhotic rats was about 2 times higher than in healthy rats. This result is in agreement with Fischer [82], who showed that hepatic concentrations of bile acid in cirrhosis are about 1.8 times higher than in healthy subjects.

2.4.4.3 Small intestine content

At 1 h after administration, OCA was not present in the intestinal contents of either cirrhotic or control rats. It then increased progressively, reaching a maximum after 24 h (4.7 ± 2.4 in cirrhosis and 1.8 ± 0.7 μmol/g in controls), without significant differences (p NS) between the groups (Figure 20E and 20F). T-OCA was the predominant form, followed by free OCA, which increased progressively up to 8 h. In the small intestine, the maximum BA concentration was always higher than the OCA concentration in both cirrhotic and healthy rats. Endogenous BAs maintained similar values, while OCA decreased over time.

2.4.4.4 Colon Content

In cirrhosis, OCA concentration in the colon increased over time, reaching a plateau after 24 h and decreasing at 48 h (0.55 ± 0.22 µmol/g and 0.37 ± 0.28 µmol/g, respectively), as shown in Figure 20G. OCA concentration in cirrhotic rats was similar to controls (p NS) after both 24 h and 48 h (0.40 ± 0.10 µmol/g and 0.28 ± 0.06 µmol/g), as reported in Figure 20H. OCA was mostly present in unmodified form, because the unabsorbed conjugated form in the small intestine underwent bacterial deconjugation. Colon bacteria, on the other hand, are responsible for the formation of 3-oxo-OCA, obtained from the oxidation of the hydroxyl group in position 3. Moreover, the endogenous BAs were still higher than OCA in both groups.

2.4.4.5 Kidneys

OCA, its main metabolites and endogenous BAs were present at very low concentrations in kidneys, at less than 0.001% of the administered dose in both cirrhotic and healthy rats (data not shown).
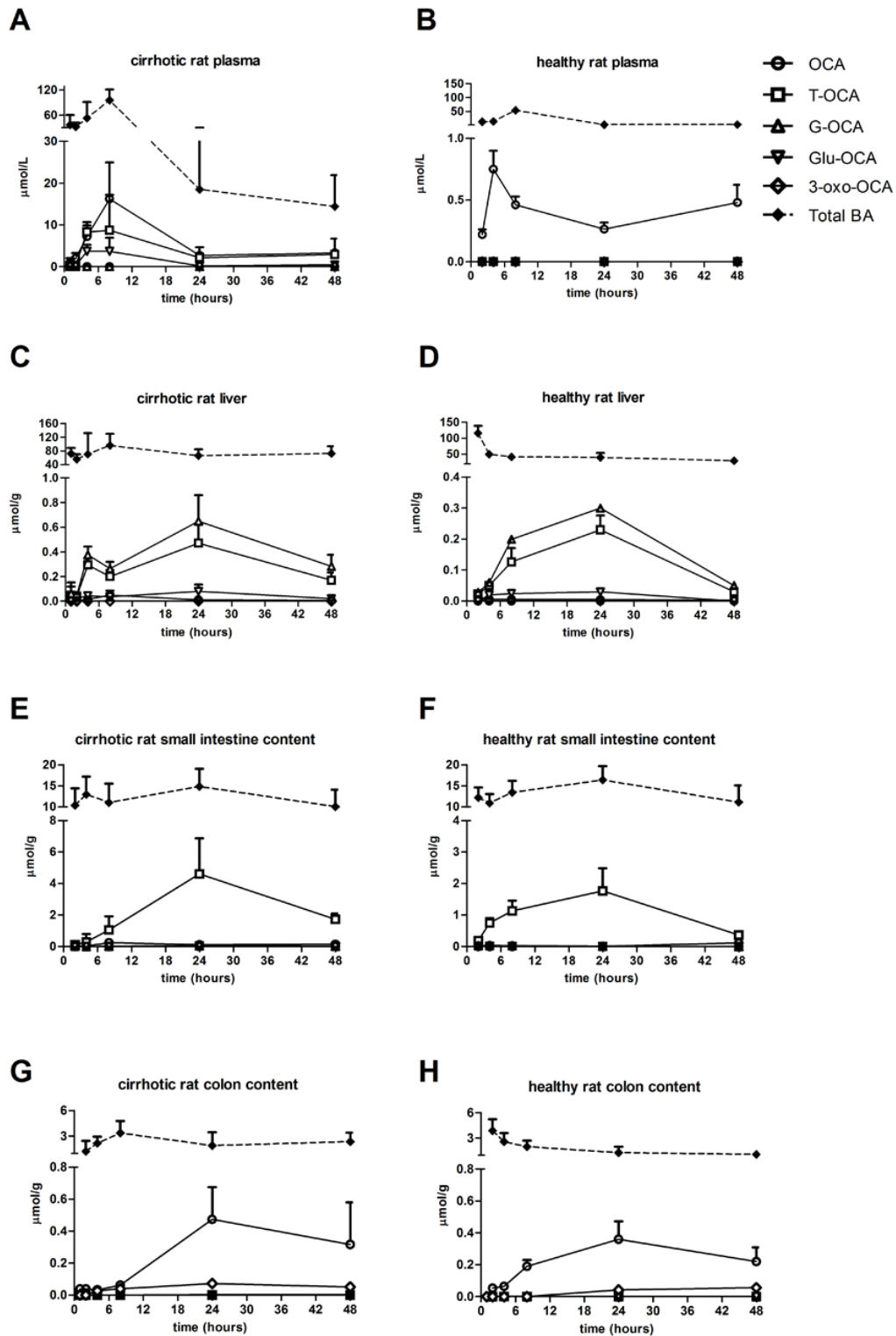
Figure 20: Concentrations (mean ± SD) of OCA, its metabolites, and endogenous BAs in different organs and fluids of cirrhotic and healthy rats, at different time-points after a single oral administration of OCA (30 mg/kg)

2.4.5 Biodistribution of OCA, its metabolites and endogenous BAs in different organs

The biodistribution of OCA and endogenous BAs in different organs was assessed at 24 h and 48 h after OCA administration (Table 7, Table 8, and Figure 21). We selected these time points because they can be reasonably considered the most relevant for a steady-state organs biodistribution.

2.4.5.1 Plasma

OCA and its metabolites reached higher concentrations in cirrhosis than controls. However, this represented only $0.3 \pm 0.2\%$ and $0.3 \pm 0.3\%$ of the recovered dose, at 24 h and 48 h respectively, showing a lack of major compartmentalization in peripheral blood (Figure 21). These values are higher ($p<0.10$) than controls (Table 7) and consistent with the different biodistribution of the endogenous BAs, as commonly observed in cholestasis. The total BA plasma concentration was significantly higher in cirrhotic rats than in controls (Table 8). Total BA concentrations were similar in cirrhosis treated with OCA and in untreated cirrhosis (p NS).

2.4.5.2 Liver

Cirrhotic and healthy rats showed differences in the biodistribution of OCA and its metabolites. At 24 h after administration, there was no significant difference (p NS) in the recovered OCA doses between cirrhotic and healthy rats ($40 \pm 12\%$ and $26 \pm 8\%$, respectively). However, 48 h after administration, significant differences ($p<0.01$) were found ($23 \pm 7\%$ in cirrhotic rats and $4 \pm 2\%$ in controls) (Figure 21). In cirrhotic rats, endogenous BAs were always higher than OCA with no significant difference at 24 h and 48 h after administration (p NS) (Table 8).

2.4.5.3 Intestine

There was no significant difference (p NS) between cirrhotic and controls rats in terms of OCA and metabolites recovery in small intestine and colon 24 h after administration. Here, they represented $48 \pm 14\%$ of the recovered dose in cirrhotic and $71 \pm 20\%$ in control rats (Figure 21). Similarly, 48 h after administration, comparable OCA amounts were recovered in intestinal contents of cirrhotic ($37 \pm 12\%$) and control rats ($24 \pm 6\%$) (p NS).

2.4.5.4 Feces and urine

At 24 h after administration, total excretion of OCA in stools was relatively low in both cirrhotic and control rats (10 ± 3% and 3 ± 1% of the recovered dose, respectively) (Figure 21). This shows that OCA presents a relatively long biological half-life. At 24 h after administration, excretion of OCA in stools was significantly higher in cirrhotic rats than in controls (p<0.05). At 48 h, however, OCA was significantly lower in cirrhotic rats (40 ± 15%) than in controls (72 ± 17%, p<0.10).

OCA urinary excretion was determined in cirrhotic rats only: the recovered dose at 24 h and 48 h after administration was 0.36 ± 0.17% and 0.08 ± 0.02%, respectively. In healthy rats, OCA concentration in urine was under the LOQ.

At both 24 h and 48 h, faecal BAs were similarly present in unconjugated form in control and cirrhotic rats. No significant differences (p NS) in stool excretion were observed between cirrhotic and control rats (Table 8). There were higher urinary concentrations of free and tauro-conjugated BAs in cirrhotic rats than in control rats (p<0.10) (Table 8).

Total OCA recoveries at 24 h and 48 h were 85 ± 12% and 98 ± 15% in cirrhotic rats, and 86 ± 14% and 87 ± 16% in controls (Table 7). This means that OCA was not metabolized into uncommon or unidentified compounds and was almost entirely recovered in the expected organs and fluids.

In addition, 24 h and 48 h after administration of OCA, there were no differences in the distribution of BAs in the various tissues. The main differences were found between cirrhotic and heathy rats, but these differences were not influenced by administration of OCA.
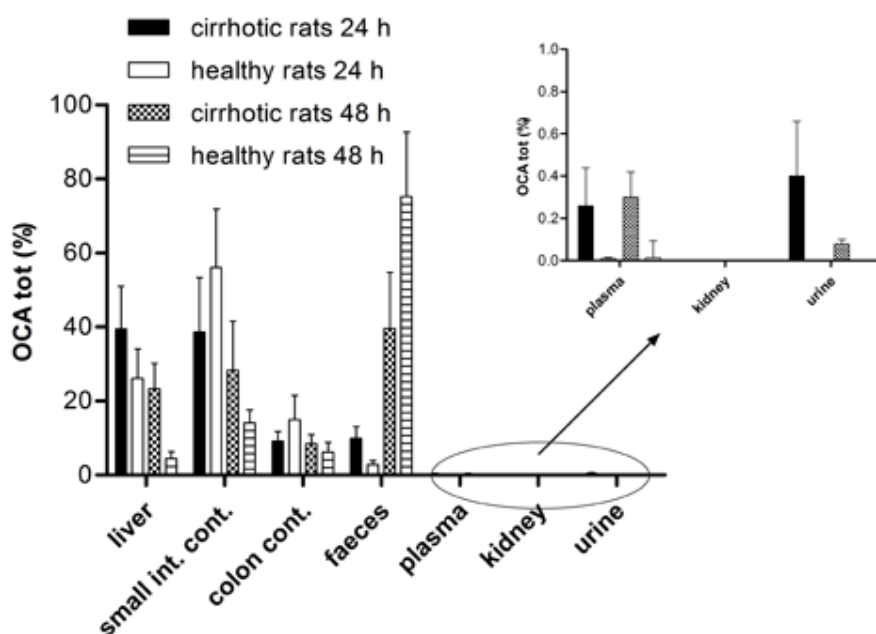

Figure 21. Percentage biodistribution (mean ± SD) of total OCA recovered at 24 h and 48 h after a single oral administration of OCA (30 mg/kg) in decompensated cirrhotic rats and healthy controls

Table 7. Percentage recovery of OCA and its main metabolites in the various organs and fluids 24 h and 48 h after administration (mean values ± SD)

		% RECOVERY AFTER 24 h (MEAN±SD)						
		OCA	T-OCA	G-OCA	Glu-OCA	3-oxo-OCA	Total OCA	P-value
Plasma	Cirrhosis	0.12±0.10	0.10±0.07	n.d.	n.d.	n.d.	0.22±0.15	<0.10
	Healthy	0.01±0.01	n.d.	n.d.	n.d.	n.d.	0.01±0.01	
Liver	Cirrhosis	0.27±0.10	14±6	18±4	1.6±0.2	n.d.	34±9.8	NS
	Healthy	0.20±0.10	9.0±3.8	12±4.3	1.3±0.5	n.d.	22±6.9	
Small int.	Cirrhosis	4.8±3.9	28±7	0.43±0.33	0.10±0.09	n.d.	33±10.8	NS
	Healthy	0.30±0.2	48±16	n.d.	n.d.	n.d.	48±16	
Colon	Cirrhosis	6.8±1.4	0.06±0.03	0.10±0.04	n.d.	1.14±0.81	8.1±2.1	NS
	Healthy	11±5.1	0.13±0.07	0.17±0.05	n.d.	1.6±0.05	13±5.2	
Kidneys	Cirrhosis	n.d.	n.d.	n.d.	n.d.	n.d.	n.d.	n.c.
	Healthy	n.d.	n.d.	n.d.	n.d.	n.d.	n.d.	
Feces	Cirrhosis	8.7±2.6	n.d.	n.d.	n.d.	0.41±0.33	9.1±2.7	<0.10
	Healthy	2.3±1.2	n.d.	n.d.	n.d.	0.13±0.11	2.3±1.2	
Urine	Cirrhosis	0.03±0.03	0.01±0.01	0.01±0.01	0.29±0.21	n.d.	0.34±0.22	<0.10
	Healthy	n.d.	n.d.	n.d.	n.d.	n.d.	n.d.	
		% RECOVERY AFTER 48 h (MEAN±SD)						
		OCA	T-OCA	G-OCA	Glu-OCA	3-oxo-OCA	Total OCA	P-value
Plasma	Cirrhosis	0.12±0.10	0.14±0.10	n.d.	n.d.	n.d.	0.26±0.10	<0.10
	Healthy	0.01±0.01	n.d.	n.d.	n.d.	n.d.	0.01±0.01	
Liver	Cirrhosis	0.25±0.15	8.2±2.6	13±4	1.4±0.07	n.d.	23±6.1	<0.10
	Healthy	0.10±0.10	1.6±0.6	2.2±1.3	n.d.	n.d.	3.9±1.8	
Small int.	Cirrhosis	1.6±1.5	25±11	0.10±0.10	1.1±0.1	n.d.	28±12	<0.10
	Healthy	3.0±1.2	8.9±2.1	n.d.	0.40±0.20	n.d.	12±3.0	
Colon	Cirrhosis	6.8±1.4	0.07±0.01	0.15±0.10	n.d.	1.2±0.9	8.2±2.1	NS
	Healthy	4.0±2.3	0.10±0.05	n.d.	n.d.	1.3±0.9	5.4±1.9	
Kidneys	Cirrhosis	n.d.	n.d.	n.d.	n.d.	n.d.	n.d.	n.c.
	Healthy	n.d.	n.d.	n.d.	n.d.	n.d.	n.d.	
Feces	Cirrhosis	38±17	n.d.	n.d.	n.d.	1.1±1.0	39.1±16	<0.10
	Healthy	62±15	0.70±0.44	n.d.	n.d.	2.7±1.2	65±14	
Urine	Cirrhosis	n.d.	0.04±0.02	0.03±0.02	n.d.	n.d.	0.07±0.02	<0.10
	Healthy	n.d.	n.d.	n.d.	n.d.	n.d.	n.d.	

n.d.= not detected
n.c.= not calculated
NS = not significant

Table 8. Concentration of free, taurine-conjugated, and total endogenous BAs 24 h and 48 h after OCA administration in cirrhotic and control rats, reported as μmol/L or μmol/g (mean values ± SD)

	Free endogenous BAs ± SD						
	cirrhotic rats 24 h	healthy rats 24 h	p-value 24 h	cirrhotic rats 48 h	healthy rats 48 h	p-value 48 h	cirrhotic rats 24 h no OCA
Plasma	12.6±7.1	0.9±0.5	<0.10	8.1±5.2	2.4±0.8	NS	17±15
Liver	4.1±2.8	3.8±1.3	NS	6.1±2.6	3.9±1.8	NS	18±16
Small int.	1.5±1.1	0.4±0.3	NS	1.2±0.4	4.4±1.4	<0.10	4.8±4.1
Colon	1.9±1.1	1.3±0.6	NS	2.4±0.9	1.1±0.3	<0.10	0.55±0.32
Feces	1.3±0.5	1.4±0.3	NS	4.8±2.1	1.5±0.7	<0.10	0.51±0.12
Urine	3.4±1.4	0.17±0.08	<0.10	4.2±1.7	0.8±0.3	<0.10	4.2±3.6
	Taurine conj. endogenous BAs ± SD						
Plasma	5.3±4.2	1.8±1.1	NS	6.2±2.2	0.8±0.3	<0.10	10±5.3
Liver	54±20	36±14	NS	66±27	26±7.6	<0.10	54±20
Small int.	13.3±4.5	16±8.3	NS	8.9±3.3	6.8±2.6	NS	0.50±0.31
Colon	n.d.	n.d.	n.c.	n.d.	n.d.	n.c.	n.d.
Feces	n.d.	n.d.	n.c.	n.d.	n.d.	n.c.	n.d.
Urine	1.8±1.1	0.07±0.03	<0.10	2.0±0.6	2.1±1.5	NS	1.4±1.1
	Total endogenous BAs ± SD						
Plasma	18±9.8	2.7±1.2	<0.10	14±6.1	3.2±0.7	<0.10	27±17
Liver	58±17	40±12	NS	72±25	30±6.5	<0.10	72±30
Small int.	14.8±3.6	16.4±7.2	NS	10.1±2.8	11.2±3.1	NS	5.3±4.1
Colon	1.9±1.1	1.3±0.6	NS	2.4±0.9	1.1±0.3	<0.10	0.55±0.32
Feces	1.3±0.5	1.4±0.3	NS	4.8±2.8	1.5±0.7	NS	0.51±0.12
Urine	5.2±2.5	0.24±0.09	<0.10	6.2±2.2	2.9±1.5	<0.10	5.6±4.1

n.d.= not detected
n.c.= not calculated
NS = not significant

2.4.5.5 OCA and endogenous BA composition

In both cirrhotic and control rats, T-OCA was the main OCA metabolite recovered in the different organs. Indeed, T-OCA was the predominant form in liver and small intestine content. Other minor metabolites were also formed, including the glycine conjugate (limited to the liver), the 3-glucuronide (only in the liver and small intestine), and the 3-oxo metabolite (limited to the colon content and faeces). The possible mechanism for increased glycine conjugation in the liver is uncommon for the rat and is particularly interesting. Taurine conjugation depends on the balance of amino acids and the free taurine content in the liver. When OCA concentration exceeds taurine bioavailability, glycine conjugation occurs. After administration, the large amount of OCA reaching the liver is conjugated, firstly with taurine and then with glycine, in order to be secreted into bile.

In the intestine, T-OCA and G-OCA are deconjugated by intestinal bacteria and OCA is passively reabsorbed. There is then less recycling of OCA to the liver, with taurine synthesis supporting its concentration in the liver. This affords a more efficient taurine conjugation over time.

OCA is almost completely recovered (85% after 24 h, and 98% after 48 h), showing that it is not extensively converted to any uncommon or toxic metabolite and it does not remain in non-target tissues, with potential undesirable effects. Indeed, OCA reaches the hepatocytes via the portal vein by intestinal passive absorption, sharing hepatic uptake systems with BAs. This accounts for the similar pharmacokinetics, without any difference in metabolic pathways (except for the lack of 7α-dehydroxylation), leading to higher conservation of the OCA pool.

2.4.6 Hepatic metabolism and biliary secretion of OCA in the bile fistula rat model

OCA was administered by intravenous infusion to cirrhotic rats (after 8, 10, and 13 weeks of CCl_4 inhalation). Using this model, the hepatic uptake, transport, and secretion of OCA into bile, independently of portosystemic shunt, have been evaluated.

After 13 weeks of CCl_4-induced liver damage, as reported in Figure 22, bile flow had significantly and progressively decreased from 60 ± 6 μL/min/kg (in healthy animals) to less than 20 ± 2 μL/min/kg ($p < 0.01$).

Figure 22. Bile flow during femoral infusion of OCA at a dose of 1 μmol/min/kg for 1 hour in rats after 0 (control, Ctrl), 8, 10, and 13 weeks of CCl4 inhalation. Bile was collected every 15 min for 3 h. The bile flow is expressed as μL/min/kg (mean ± SD). The gray area represents the normal range of bile flow variation

Similarly, between week 8 and week 13 of CCl$_4$ exposure, biliary secretion of OCA (entirely as T-OCA) progressively decreased. As reported in Figure 23, the maximum secretion rate of OCA in control rats decreased from 0.80 ± 0.10 µmol/min/kg, to 0.40 ± 0.05, 0.20 ± 0.03, and then to less than 0.05 ± 0.01 µmol/min/kg as cirrhosis progressed (p<0.01). Similarly, endogenous BA secretion decreased as cirrhosis progressed, as outlined in Figure 23, which reports the data for TCA and TmuCA, the most representative endogenous BAs of the bile composition. The hepatic clearance of OCA and endogenous BAs thus decreases as cirrhosis progresses.
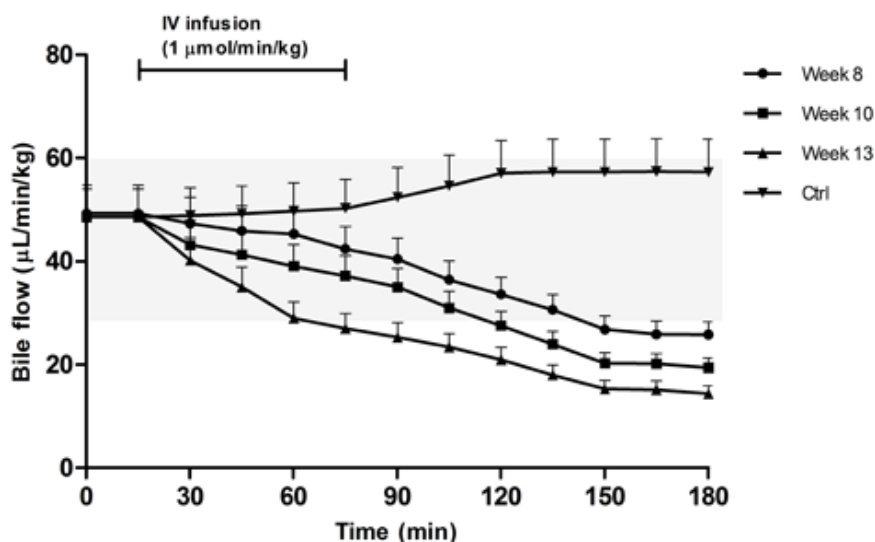

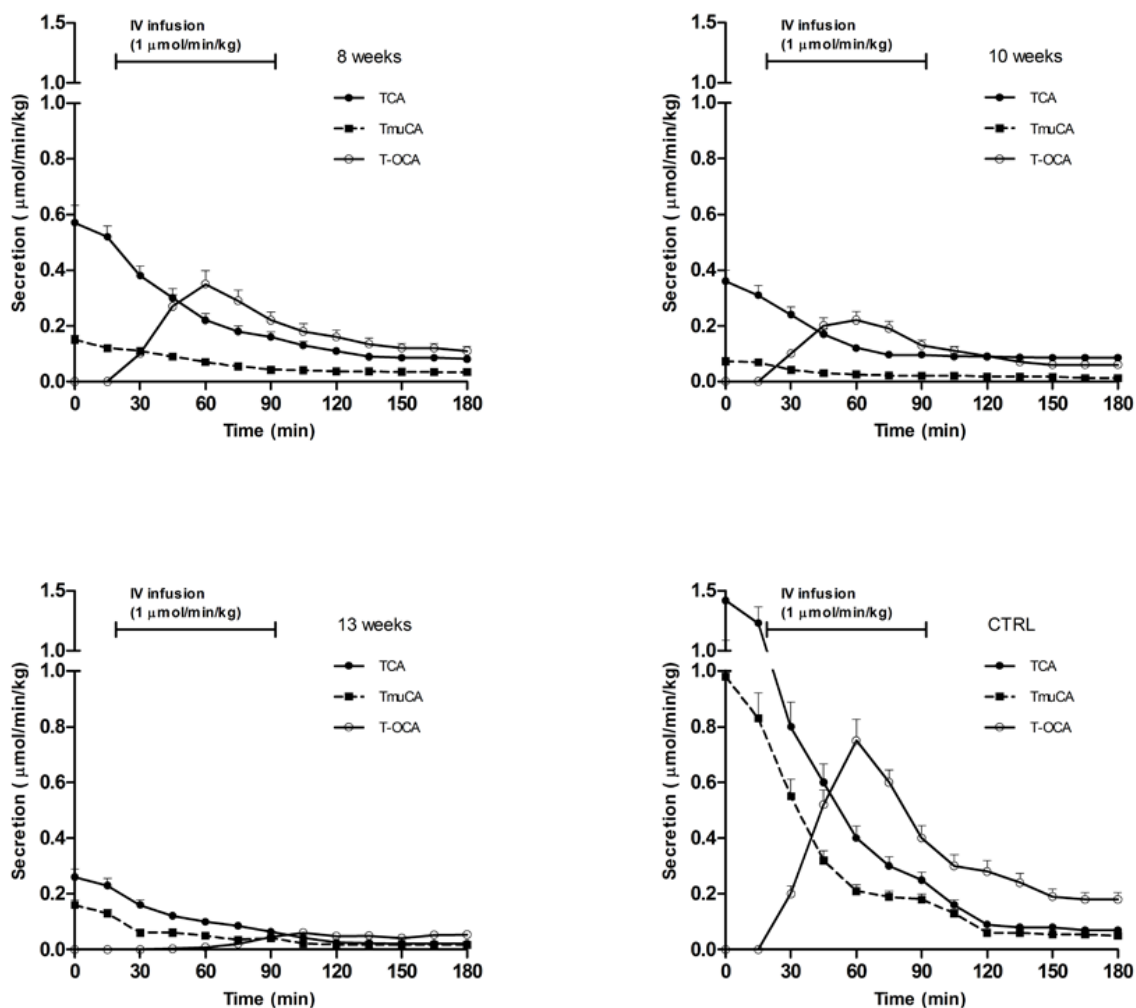**Figure 23.** Secretion rates during femoral infusion of OCA at a dose of 1 µmol/min/kg for 1 h after 0 (control, CTRL), 8, 10, and 13 weeks of CCl$_4$ inhalation. Bile was collected every 15 min for 3 h. The secretion rate is expressed as µmol/min/kg (mean ± SD)

2.5   Conclusions

Bile acids and their semisynthetic analogues are gaining much attention due to their potential therapeutic role in the treatment of cholestatic diseases. In this scenario, OCA covers an important role, being the first and only BA analogue currently approved for the treatment of PBC by virtue of its FXR activity. Unfortunately, its metabolism and biodistribution in conditions of severe liver disease have not been properly addressed, leading to several concerns about its safety profile. In this context, an HPLC–ESI-MS/MS method for the quantification of endogenous BAs, OCA and its main metabolites in rat plasma, liver, stools, small intestine content, colon content, urine and kidney samples. This method has been validated and successfully applied to an *in vivo* rat model of induced decompensated liver cirrhosis, in order to exclude the occurrence of any uncommon metabolism or bioaccumulation in specific organs.

The results showed that, in decompensated cirrhosis, OCA metabolism and biodistribution in liver, plasma, and intestine are similar to endogenous BAs. There was no formation of unexpected phase 1 or 2 hepatic metabolites of OCA, suggesting lack of hepatotoxicity, even when OCA is present at higher liver concentrations compared to controls. OCA is efficiently conjugated with taurine and glycine and promptly secreted into bile. Therefore, after a single oral administration of 30 mg/kg, OCA concentration in the liver reflects the altered biodistribution of BAs in decompensated cirrhosis, as recently reported [83]. OCA is always present at significantly lower concentrations than BAs, which are potentially much more cytotoxic. OCA is almost completely recovered (85% after 24 h, and 98% after 48 h), showing that it does not remain in non-target tissues, with potential undesirable effects. Two points have been clarified by results of the bile fistula rat experiments following intravenous infusion of OCA. Firstly, as liver damage increases, there is a progressive decrease in biliary flow and biliary secretion of OCA and BAs. This is independent of portal hypertension. This decrease can partially be explained by the altered hepatocellular and lobular localization of import and export proteins. Secondly, the biliary excretion for OCA and BAs becomes less effective with disease progression.

In conclusion, OCA and endogenous BAs share a similar metabolism and biodistribution in both normal and liver disease conditions, although a single-dose administration of OCA did not alter the qualitative or quantitative compositions of BAs or their biliary secretion. The biliary secretion of BAs and OCA progressively decrease as liver damage and loss of hepatic architecture progress. However, it is worth to point out that OCA presents a longer residence time in the cirrhotic liver

compared to healthy rats, suggesting that clinicians should carefully consider the potential accumulation of OCA.

CHAPTER 3

Target lipid determination in organic residue analysis

There is an increasing amount of evidence showing that organic residue analysis (ORA), performed on material residing within archaeological finds, is able to address many historical questions about past diets, ancient practices, early use of natural substances, but also vessel production and related use. Ceramic materials represent an ideal environment for the survival of residual organic matter, as its absorption into the microporous structure prevents from long-term degradation. In fact, some investigations have shown that possible contamination arising from migration of soil components, or compositional alterations through microbial activity, are minimal for compounds absorbed in potsherds. Unfortunately, poor data have been reported so far about ORA studies conducted on cooking hearths, as it is thought that it is unlikely that any useful analytes have been surviving over the millennia within this kind of environment. However, this assumption has never been experimentally confirmed, leaving some uncertainty on this scenario.

This chapter deals with the development of chromatographic/mass spectrometry based analytical methodologies to identify the organic pyrolysis products that reside within cooking hearths following the cooking of different foodstuffs. These protocols have been successfully applied for the analysis of residual organic materials present within archaeological finds, with the final aim to identify food/diet related chemicals whose qualitative and quantitative composition might represent biomarkers able to provide information related to past human activity.

3.1   Introduction

3.1.1 Organic residue analysis

The ability of our ancestors to fulfil their basic nutritional needs was a factor that shaped the evolution of modern man and the societies that followed. Therefore, the study of ancient dietary customs has been gaining much attention from historians and archaeologists. There is an increasing amount of evidence showing that organic residue analysis (ORA) is able to address many archaeological questions about past diets, ancient practices, early use of natural substances, but also vessel production and related use. Although many ORA applications target the identification of what food products were processed or stored in ancient vessels, it can also address wider questions regarding the ancient trade of goods and raw materials, ancient technologies, resource exploitation and acquisition, ritual practices, the domestication of plants and animals, and dietary reconstruction and subsistence practices. ORA has the potential to inform archaeological interpretations on scales ranging from a site context to local, national and global scale questions, together with the investigation of chronological change, again across small- to broad-scale contexts.

Most of the organic residue analysis have been performed on absorbed material recovered from archaeological finds, like pots and vessels [84, 85]. Ceramic materials represent an ideal environment for the survival of residual organic matter because its absorption into the microporous structure prevents from long-term degradation. In fact, some investigations have shown that possible contamination arising from migration of soil components, or compositional alterations through microbial activity, are minimal for compounds absorbed in potsherds [86]. Hence, these residues are a direct reflection of the original contents and usage of ceramic vessels.

It is always crucial to apply the analysis and subsequent interpretation of organic residues within the context of the archaeology and paleoecology of the settlement, region and period from which they derive. Organic residue information should be integrated with other lines of archaeological evidence, in order to provide the most meaningful answers to research questions. For example [87], in studies of animal product processing in prehistoric Britain, only a restricted range of ruminants need to be considered as likely sources of lipid extracted from vessels; these include cattle, sheep/goat and deer, with pig being the most common non-ruminant. In other regions or periods, the qualitative and quantitative composition of species might be different, guiding interpretations accordingly.

3.1.2 The *Archaeological Biomarker* concept

The development of powerful analytical techniques, such as mass spectrometry, has allowed the study organic residues within archaeological material at molecular level. ORA can be used to accomplish the effective recovery and identification of biomolecules and related degradation products in archaeological materials, achieved through the application of the so-called *Archaeological Biomarker* concept [88]. This concept surrounds all the analytical methodologies developed for the analysis of organic archaeological finds at biomolecular level, with the aim to provide information related to past human activity. For example, pottery used in brewery can be distinguished from that used in cookery as each one harbors characteristic biomarkers [89]. Although the archaeological biomarkers refer to a variety of organic compounds, most of the ORA applications have been focusing on lipid profiling, as they are considered to be the most durable and greatly occurring in the archaeological residues [90]. Obviously, the application of this concept bears some natural issues, especially for what concerns the accomplishment of ORA investigations. Indeed, considering that all the residues encountered at the archaeological sites have biological origin, very complex mixtures normally occur. This complexity is furtherly worsened by some human activities, such as food preparation, and by the natural compositional alteration due to chemical and microbial decay during burial.

The *Archaeological Biomarker* concept relies on matching the identified structures to molecules known to be present is organism or species likely exploited in the past [90] and sometimes the elucidation of a single component structure is sufficient to define the origin of an organic residue. For example [91], beeswax can be unequivocally identified by the highly specific aliphatic component pattern. Anyway, the assignment process of a biomarker to a specific organic source requires a high degree of rigor, as the consideration of other compounds in the residue might lead to the hypothesis of a putative source to be rejected. For example, a recent paper [92] reported the identification of beeswax in a residue on the basis of the presence of C_{23}, C_{25}, C_{27}, C_{29}, C_{31}, and C_{33} *n*-alkanes; however, this assignment has been successively questioned considering that the GC profile of the sample was very similar to a petroleum mixture. On these basis, in case of occurrence of such ambiguities, firm conclusions on the nature of an organic residue must be drawn only in presence of stronger supporting evidences.

Considering the complexity of the archaeological samples normally encountered in ORA studies and the often-occurring misleading interpretations, the correct identification of the biomarkers imperatively requires the use of advanced chromatographic and/or mass spectrometric

techniques. This is the reason for which the advances in this area have been greatly tied to analytical method improvements.

3.1.3 The occurrence of organic residues

Organic residues have the capacity to survive over considerable timescale within the archaeological site. They are often in association with several classes of artefacts, providing many insights on vessel use, site and regional economies/technologies. Organic residues can be recovered from ancient pottery as three main different forms:

- Original content preserved within the pot as vessel filling. This is the rarest case, as only few examples have been reported so far [93].

- Residual matter looking as surface residue on the internal or external side of the vessel. Among these, carbonized residues, assumed to be the result of cooking failures, are the most common cases. These kinds of samples have been largely used for dating purposes [94]. External residues, on the other hand, are often associated to the fuel used for fire, applied decorations or materials used for reparation [95].

- Residues absorbed in the walls of the pots, invisible to naked eye. This is the most common type of organic residue and it has revealed a wild series of biomarkers from an impressive range of commodities over several continents [96]. These include vegetable oils, terrestrial and marine animal fats, resins and plant waxes. These residues derive from the animal and plant products processing.

Although the residues associated to potteries have been the most analyzed samples, many other archaeological finds keep arising great interest. Indeed, several reports have documented analysis performed on human and animal remains (like skeletal or tissue remains) [97], natural and fossil resins (especially materials used in ancient practice of decoration and restauration) [98], soils and sediments [99], and miscellaneous organic remains (like the bog butter hoards that constitute the largest deposits of organic residues ever reported in archaeology) [100].

3.1.4 The stability of organic residues

The ability of organic residues to survive within a hostile environment is still field of debate. Indeed, all organic compounds are potentially subjected to degradation, both chemical and biological. Consequently, there must be some kind of protection that allow the survival of certain molecular species. However, it is obvious that the structural differences between compounds

account for different preservation. Normally, more polar the substances are, then more likely to degrade they will be, especially if any essential elements are present. Following this criterion, the stability toward degradation of the different classes of compounds follows the order: lipids > carbohydrates ≈ lignin > protein > nucleotides; however, there are several factors able to affect this order somehow, according for example to the environment or to the history of an artefact [101].

Lipids are the most targeted compounds in ORA studies, as they represent the vast majority of occurring biomarkers within archaeological finds. This is mainly due to their hydrophobicity, which allows them not to be easily lost by leakage from the site of original deposition because of the percolation of underground water. Besides, their absorption on the substrate prevents from microbial degradation. However, it is noteworthy that even within a class of compounds, substantial differences might exist in the degradation paths of different sub-classes. For example [102], the decay of plant epicuticular waxes and animal fats co-deposited onto replica ceramic showed different patterns of decay.

Mineral constituents of the pottery walls offer a protective environment in which organic molecules are partially shielded from microbiological degradation. It is presumed that this protective mechanism occurs through the enclosure of organic molecules within pore spaces inaccessible to exocellular enzymes produced by degrading microbes and protection through adsorption on substrate material surfaces [103]. Likewise, protection appears also to be conferred by entrapment within organic matrices, such as carbonized organic residues on pottery and aggregates of organic matter.

Several environmental factors have been recognized to play a role in the organic residue preservation, including temperature, light exposure, degree of waterlogging, redox conditions and so on [96]. Desiccation is a very important parameter in this context, as it hampers the microbial growth and the consequent biodegradation. However, it does not prevent the extensive chemical oxidation of residues normally occurring over millennia. Nutrient limitation, especially of essential elements, may also limit the progress of degradation: once the concentrations of these elements get limited, the microbe activities will inevitably be slowed or even stopped. Although extremes of waterlogging and desiccation are unquestionably conducive to the survival of organic residues, alternating wetting and drying in climate zones where seasons of high rainfall are followed by hot dry periods appears to be detrimental to residue survival [96].

3.2 Aim and rationale

Over the past three decades ORA studies have been performed on pottery from archaeological sites with great success. The detection of biomarkers indicative of specific foods has enabled researchers to develop an objective understanding of the diet consumed by ancient groups and cultures and allowed the possibility to trace the migration processes of ancient population across specific territories. Despite the achievements of potsherd analysis, the attempt of studying the dietary practices of individuals who lived prior to use of pottery has not been made with the same vigor. This lack of information about this kind of samples derives from a widespread and unverified assumption that biomarkers are highly unlikely to survive the destructive environment within a cooking hearth.

The project was developed with the aim of exploring what kind of lipids might have been survived within hearth samples excavated from different archaeological sites. The analyzed samples, dating back 20000-50000 BCE, corresponded to an era when Neanderthals habited Western Europe. With this aim, different instrumental approaches and protocols have been developed and optimized to determine the optimal chromatographic and/or mass spectrometric condition to study a range of expected compound families. These include FAs, FAMEs, TAGs, sterols and steryl glucosides (SGs). Indeed, considering the age and the complexity of the samples, the choice of a target approach toward the most stable lipid classes that are recognized to be indicative diet-related biomarkers was preferred. Considering the necessity to investigate several lipid families, the selective ionization processes offered by different atmospheric pressure ionization techniques have been tested. Besides, shotgun analysis using ultrahigh resolution mass spectrometry methods have been compared with modern LC-MS approaches (RP-UHPLC-MS and UHPSFC-MS).

The final aim of this project is to demonstrate that the study of hearth material in ORA has been critically undervalued and to provide the fundamentals for future investigations of new potential biomarkers in these kinds of samples.

3.3 Materials and methods

3.3.1 Chemicals

All the standards of FAs, FAMEs, TAGs, and sterols utilized in this study were of analytical grade. Capric acid (C10:0), valeric acid (C12:0), myristic acid (C14:0), palmitic acid (C16:0), stearic acid (C18:0) and arachidic acid (C20:0) standards were purchased from Sigma-Aldrich (Saint-Louis, US). Methyl decanoate (C10:0), methyl valerate (C12:0), methyl myristate (C14:0), methyl palmitate (C16:0), methyl stearate (C18:0), methyl oleate (C18:1), methyl linoleate (C18:2) and methyl linolenate (C18:3) were purchased from Sigma-Aldrich. β-sitosterol, stigmasterol, ergosterol and cholesterol were purchased from Sigma-Aldrich. Cholesteryl glucoside was purchased from Sigma-Aldrich, while a mixture of SGs (β-sitosteryl glucoside, campesteryl glucoside, stigmasteryl glucoside, Δ^5-avenasteryl and Δ^7-avenasteryl glucoside) was purchased from Matreya Inc. Mixture of three purified triglycerides (16:0/14:0/14:0, 14:0/14:0/14:0 and 12:0/14:0/14:0) was kindly donated by Dr. Simon Gerrard (University of Southampton, UK). Methanol, EtOH, iPrOH, ACN, dichloromethane (DCM) and hexane (Hex), all of MS grade, were purchased from Fischer Scientific (Pittsburgh, US). Carbon dioxide (CO_2) was >99% purity. Formic acid, ammonium acetate, ammonium hydroxide, sodium formate and other additives used were of analytical grade.

Sterol and SG stock standard solutions were prepared, respectively, in iPrOH and DCM:MeOH (3:1) at a concentration of 1 mg/ml, while FA, FAME and TAG stock standard solutions, also at concentration of 1 mg/ml, were prepared in Hex. All the stock solutions were aliquoted and stored at -20 °C. Individual stock solutions were properly diluted in hexane to prepare standard calibration solutions containing different compounds in a concentration range of 0.01-10 μg/mL. These solutions were stored at 4 °C in order to avoid any potential variation in the nominal concentration.

3.3.2 Instrumentation

The UHPSFC-MS apparatus consisted of an ACQUITY UPC^2 System with 96 positions autosampler and thermostat coupled with a single quadrupole mass spectrometer and API interface (Xevo XS-SQ; Waters, US). The column utilized in this study were: HSS C18 1.8 μm particle size (3×100 mm), BEH 1.7 μm particle size (3×100 mm), BEH 2-EP 1.7 μm particle size (3×100 mm) and Torus 1-AA 1.7 μm particle size (3×100 mm).

The UHPLC-MS apparatus consisted of an Ultimate 3000 System with 90 positions autosampler and thermostat coupled with a quadrupole-time of flight mass spectrometer and electrospray interface (Maxis; Bruker, US). The column utilized in this study was a HSS C18 1.8 μm particle size (3×50 mm).

The FT-ICR MS system consisted of a solariX XR high-resolution mass spectrometer (Bruker, US).

3.3.3 UHPSFC-MS analysis

Different chromatographic columns and conditions have been tested in order to achieve the optimal separation of the different compounds.

Final simultaneous separation of FAs, FAMEs and TAGs was achieved using a BEH 2-EP column. The selected mobile phase was CO_2 (A component) and MeOH with 25 mM ammonium acetate (B component). The best separation was obtained at flow rate of 1.5 mL/min with the following gradient of the B component: 0 to 1 min at 0%, then linear increase to 1% in 1 minute and maintained for 1.5 minutes, then linear increase to 5% in 1 minute, then to 30% in another minute and maintained for 2.5 minutes (total run time 8 minutes). The column reconditioning time between each chromatographic run was 2 minutes.

Final separation of sterols was achieved using a Torus 1-AA column. The selected mobile phase was CO_2 (A component) and MeOH with 25 mM ammonium acetate (B component). The best separation was obtained at flow rate of 1.5 mL/min with the following gradient of the B component: 0 to 1.5 min at 0%, then linear increase to 5% in 0.5 minute and maintained for 1 minute, then linear increase to 15% in 1.5 minute and maintained for 1 minute, then to 30% in 0.5 minute and maintained for 2 minutes (total run time 8 minutes). The column reconditioning time between each chromatographic run was 2 minutes.

In both separations, the column was maintained at 45 °C and the injected sample volume was 2 μL. The total ion current chromatogram (TICC) reporting the complete separation of all the tested compounds is reported in Figure 24.
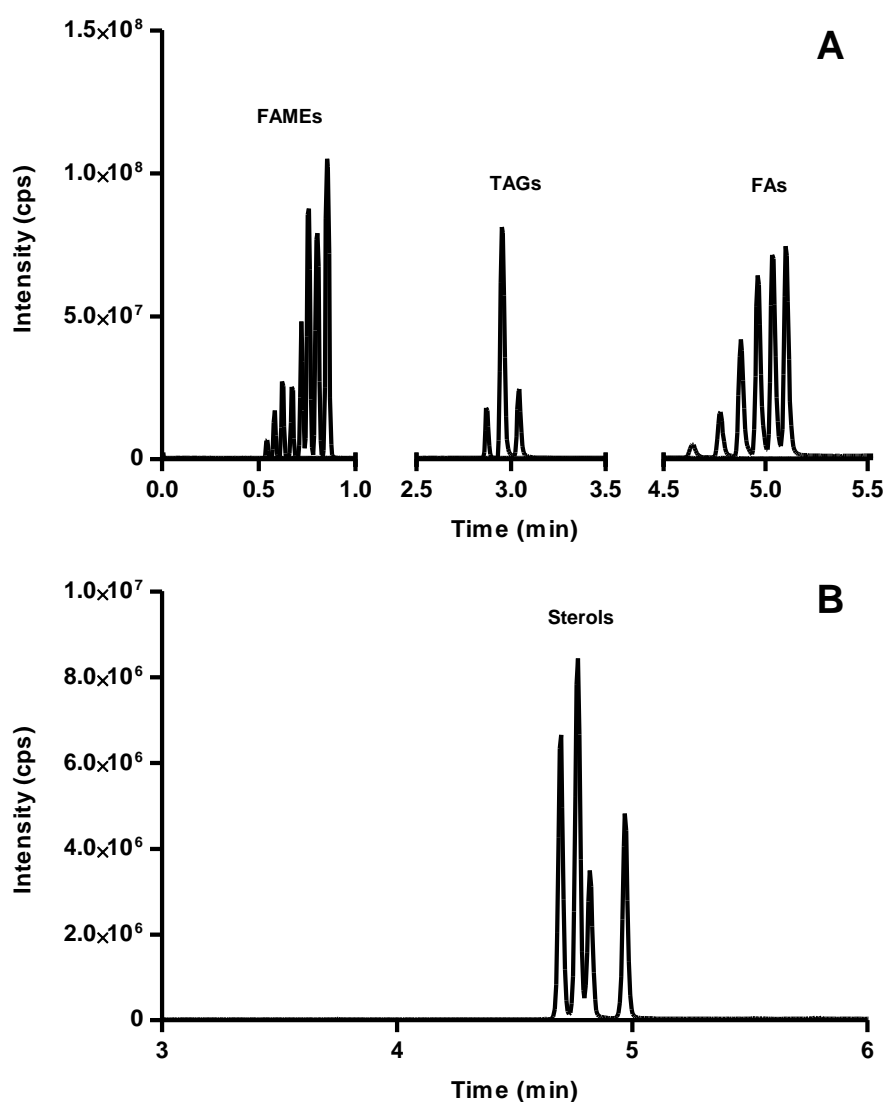
Figure 24. TICC reporting the separation of the tested FAs, FAMEs, TAGs using a BEH 2-EP column (A panel) and sterols (B panel) using a Torus 1-AA by UHPSFC-MS. The elution order for FAMEs is from C10:0 to C18:3; the elution order for TAGs is from 12:0/14:0/14:0 to 16:0/14:0/14:0; the elution order for FAs is from C10:0 to C20:0; the elution order for sterols is: cholesterol, β-sitosterol, stigmasterol and ergosterol

The column effluent was mixed with a make-up solvent, delivered by a secondary pump at a flow rate of 0.45 mL/min, and introduced into the API source, operating in negative or positive ion mode, connected to a single quadruple mass spectrometer operating in Full Scan mode or Single Ion Recording (SIM). ESI was selected as ionization interface for all the investigated lipid classes, except sterols, which were analyzed using an APCI interface. The use of a make-up solvent (sodium formate 20 μM in methanol for FAs, FAMEs, TAGs, and formic acid 1% in methanol for sterol analysis) was necessary in order to obtain a stable and reproducible spray and an ionization efficiency improvement. Table 9 reports the details regarding the detection of each compound.

In Table 10, the MS experimental conditions are reported, which were properly set up by single standard infusion.

Table 9. Retention times, unique *m/z* and ion types obtained from the analysis of the different lipids by UHPSFC-MS

Family	Compound	Retention time (min)	Ion mass (*m/z*)	Ion type
FA	Decanoic acid	4.64 ± 0.01	171.1	$[M - H]^-$
	Valeric acid	4.78 ± 0.01	199.2	$[M - H]^-$
	Myristic acid	4.88 ± 0.01	227.2	$[M - H]^-$
	Palmitic acid	4.96 ± 0.01	255.3	$[M - H]^-$
	Stearic acid	5.03 ± 0.01	283.3	$[M - H]^-$
	Arachidic acid	5.10 ± 0.01	311.4	$[M - H]^-$
FAME	Methyl decanoate	0.54 ± 0.01	209.3	$[M + Na]^+$
	Methyl valerate	0.58 ± 0.01	237.3	$[M + Na]^+$
	Methyl myristate	0.62 ± 0.01	265.4	$[M + Na]^+$
	Methyl palmitate	0.67 ± 0.01	293.4	$[M + Na]^+$
	Methyl stearate	0.72 ± 0.01	321.5	$[M + Na]^+$
	Methyl oleate	0.76 ± 0.01	319.5	$[M + Na]^+$
	Methyl linoleate	0.80 ± 0.01	317.5	$[M + Na]^+$
	Methyl linolenate	0.85 ± 0.01	315.5	$[M + Na]^+$
TAG	16:0/14:0/14:0	2.87 ± 0.01	773.8	$[M + Na]^+$
	14:0/14:0/14:0	2.95 ± 0.01	745.7	$[M + Na]^+$
	12:0/14:0/14:0	3.05 ± 0.01	717.6	$[M + Na]^+$
Sterol	Cholesterol	4.70 ± 0.01	369.5	$[M + H - H_2O]^+$
	β-sitosterol	4.77 ± 0.01	397.5	$[M + H - H_2O]^+$
	Stigmasterol	4.82 ± 0.01	395.5	$[M + H - H_2O]^+$
	Ergosterol	4.97 ± 0.01	379.5	$[M + H - H_2O]^+$

Table 10. Mass spectrometry conditions for the different API techniques utilised during analysis by UHPSFC-MS

Ionization mode	ES-	ES+	Ionization mode	APCI+
Capillary voltage (KV)	-2.7	+4.0	Corona voltage (KV)	+3.0
Cone voltage (V)	+40	-25	Cone voltage (V)	-30
Source temperature (°C)	150	150	Source temperature (°C)	150
Desolvation temperature (°C)	500	500	Probe temperature (°C)	400
Desolvation gas flow (L/h)	650	650	Desolvation gas flow (L/h)	550

3.3.4 UHPLC-QTOF analysis

Separation of FAs, FAMEs and TAGs was achieved using a C18 column. The selected mobile phase was water (A component) and MeOH (B component), both acidified with 0.2% of formic acid.

The best separation was obtained at a flow rate of 0.5 mL/min with the following gradient of the B component: linear increase from 60 to 90% in 3.5 minutes, then 90% until 6.5 minutes, then linear increase to 100% in 0.5 minute and maintained for 6 minutes (total run time 13 min). The column reconditioning time between each chromatographic run was 2 minutes.

The column was maintained at 40 °C and the injected sample volume was 2 µL. The TICC reporting the complete separation of all the tested compounds is reported in Figure 25.

The column effluent was introduced into the ESI source, operating in negative or positive ion mode, connected to a quadrupole-time of flight mass spectrometer operating in Full Scan mode. In Table 11 the MS experimental conditions were reported, properly set up firstly by single standard infusion.
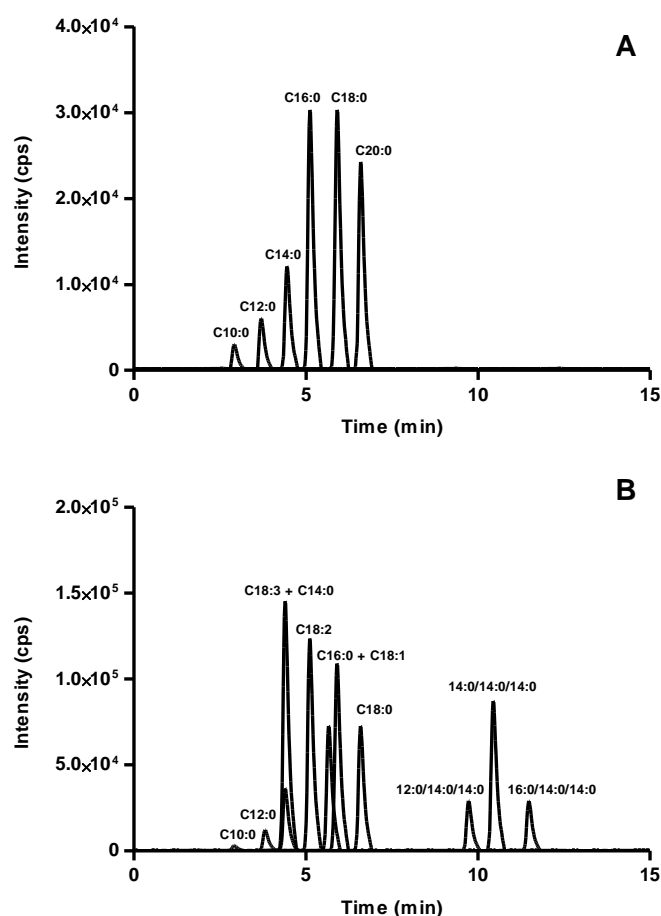

Figure 25. TICC reporting the UHPLC-ESI-QTOF separation of the tested FAs (A panel), FAMEs and TAGs (B panel), respectively in negative and positive ion scan, using a C18 column

Table 11. Mass spectrometry conditions for FAMEs, TAGs and FAs analysis by UHPLC-QTOF. The detection of FAMEs and TAGs was performed in positive ion mode, while FAs in negative

Ionization mode	ES-	ES+
End plate offset (V)	-500	+500
Capillary voltage (V)	+4000	-4000
Drying temperature (°C)	230	230
Nebuliser (Bar)	2.0	2.0
Drying gas (L/min)	6.0	6.0
m/z range	150-1500	150-1500

3.3.5 FT-ICR MS analysis

FT-ICR mass spectrometer was not coupled to any chromatographic system, as the high resolution and high accuracy of this instrument allows to discriminate ions with very close *m/z* values. The use of this instrumentation was limited to the confirmation of compounds suspected to be present in the samples but for which the relative standards were not available. The samples were directly infused onto the ESI source and mass spectra acquired according to the instrumental conditions reported in Table 12. Instrument was calibrated using a 10 ng/mL sodium formate solution. The instrumental conditions were optimized using standard solutions of the different compounds.

Table 12. FT-ICR MS ionization parameters. FAMEs and TAGs were detected in ES+, FAs in ES-

Ionization mode	ESI-	ESI+
End plate offset (V)	-500	+500
Capillary voltage (V)	+4000	-4000
Drying temperature (°C)	180	180
Nebuliser (Bar)	1.2	1.2
Drying gas (L/h)	4.0	4.0
m/z range	150-1500	150-1500

3.3.6 Sample preparation

Archaeological samples were extracted following a procedure developed and optimized by the research group of prof. George Attard (University of Southampton, UK). Briefly, the homogenized hearth-material was weighted into a cellulose thimble and then placed on the Soxhlet apparatus. The quantity of material extracted varied according to the mass of the archaeological sample. The still-pot was filled with the first extraction solvent (Hex, 150 mL) and brought to reflux (2 hours at 97.5 °C). Subsequently, the extract was dried under vacuum and then reconstituted in Hex. The extraction procedure was repeated using a secondary extraction solvent (Tol:MeOH, 1:2, 150 mL). Again, the extract was dried under vacuum prior resuspension in Hex. These samples were centrifuged, filtered and stored at -20 °C before analysis.

3.3.7 Method validation

Method validation was performed according to ICH guidelines. Selectivity, LOD, LOQ, calibration range, precision and accuracy were evaluated for each analyte according to the protocols reported in paragraph 1.3.4.

3.4 Results and Discussion

3.4.1 UHPSFC-MS method for the analysis of FAMEs, TAGs and FAs

One of the aims of this work was to develop a chromatographic method able to quantitatively analyze different lipid classes likely present within real archaeological samples. Considering that the amount of sample available for the analysis might be very low, it would be desirable that the method was able to target as many lipid classes as possible within a single chromatographic run. The targeted lipid classes selected for this kind of study were FAMEs, TAGs and FAs because they can be reasonably found in the real sample extracts and cover a large polarity range. Preliminary experiments using standard solutions of the analytes were performed in order to select the proper separation conditions, based on the choice of chromatographic column, mobile phase modifier, make-up solvent, column temperature, backpressure and mobile phase flow rate.

Considering the above issues, the column selection was of great importance for the acceptable separation of the studied compounds. In this study, four columns were screened, including Waters Acquity UPC2 BEH, BEH 2-EP, HSS C18 and Torus 1-AA. The column performances are reported in Figure 26, in which the separation is based mainly on the chain length and the unsaturation degree. The C18 column reveals to be the most suitable for separating compounds differing for the chain length, like saturated TAGs, FAs and FAMEs, but is ineffective for separation requiring selectivity towards unsaturation degree, like unsaturated FAME (and likely unsaturated FAs or TAGs). The Torus 1-AA column shows selectivity similar to C18 but is not able to separate TAG and FA classes. The BEH column exhibit chromatographic selectivity exactly opposite to C18, being very effective in the separation of FAMEs with different unsaturation but poorly suitable for the separation of the other compounds. The BEH 2-EP column, on the other hand, exhibit good selectivity in respect to both unsaturation degree and chain length, being the most effective for complete separation of all the tested compounds. In addition, BEH 2-EP column reveals to be very reliable in separating the different compounds within a specific lipid class but is also able to afford good separation between lipid classes through very mild variations in the mobile phase composition. For these reasons and considering the potential applicability and extendibility of the method to other lipid classes, the BEH 2-EP was the column of choice for our studies.

FAs are natural compounds characterized by the presence of the carboxylic group and therefore easily detectable in ES negative ion mode. FAMEs and TAGs, on the other hand, are detected only in positive ionization mode as sodium adducts. For this reason, a SIR program constituted of three

different detection windows, operating in negative or positive mode, was set making possible the simultaneous analysis of all these lipid classes within a single chromatographic run. In addition, the SIR detection mode ensures high sensitivity and specificity, reducing the interferences and increasing the signal to noise ratio.
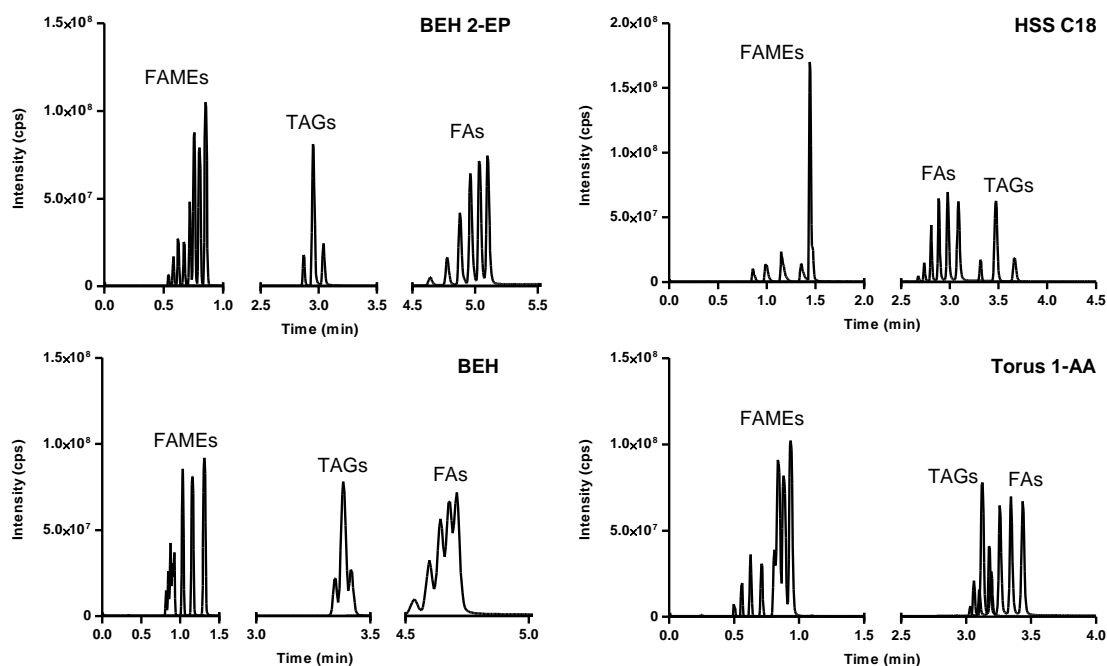

Figure 26. TICC reporting the UHPSFC separation of the tested FAs, FAMEs and TAGs using BEH 2-EP, BEH, BSS C18 and Torus 1-AA columns

The choice of a proper organic modifier was another important factor to evaluate in order to obtain a reliable chromatographic method. Organic modifiers are generally mixed with CO_2 to change the polarity of the mobile phase (allowing the elution of more polar compounds) and prevent interactions between non-functionalized active sites present on the stationary phase surface. This is particularly true for FAs, whose acid group exhibit strong interactions with the silanol groups at the surface of the packing materials, with consequent production of peak tailing. Different organic modifiers were screened, including MeOH, ACN, MeOH with 25 mM ammonium acetate and MeOH with 50 mM ammonium acetate and 2% of water. Acetonitrile, compared to MeOH, had poor eluting strength, while the addition of ammonium acetate to methanol at a concentration of 25 mM led to a significant reduction of peak tailing with improved peak resolution and shorter retention times. The increase in the ammonium acetate concentration and the addition of small water percentages did not improve either the separation and the peak shape; consequently, MeOH with 25 mM ammonium acetate was selected as mobile phase

modifier. The significant effect produced by the addition of ammonium acetate on the asymmetry factors may be explained by the ability to compete with the analyte for the proton accepting sites on the stationary phase.

In SFC analysis, the effluent coming off the column is mixed with a proper organic make-up solvent before entering the ES source. The use of a make-up solvent is crucial, as it is able to stabilize the spray formation and improving the ionization efficiency. Different make-up solvents were tested, including MeOH with different concentrations of formic acid, ammonium acetate and sodium formate. Among these, the most effective was a mixture of MeOH and sodium formate at a concentration of 20 µM at a delivery flow rate of 0.45 µL/min. This played a very important role, as it forced the formation of the sodium adduct during the detection of TAGs and FAMEs. The use of different make-up solvents led to an uncontrolled ionization of these compounds, with consequent formation of protonated molecules and adducts with sodium, ammonium and potassium.

Column temperature, backpressure and mobile phase flow rate also play an important role in retention behavior in SFC. The increase of the column temperature causes a decrease in the fluid density when working at constant back pressure and flow rate, nevertheless the effect on retention varies [104]. In this study, column temperature was changed between 40 and 60 °C. With the increase of the column temperature, all saturated compounds had longer retention times and broadening peaks. It might be due to the decreasing viscosity of the mobile phase and the increasing diffusion coefficients of analytes. However, changes of resolution for saturated and unsaturated FAMEs were different. The separation factor of unsaturated FAMEs decreased with the increase of temperature, and the opposite trend was observed for saturated FAMEs. Consequently, the best compromise in terms of resolution and shape of the peaks was reached at a column temperature of 45 °C. As regard the backpressure and flow rate, their decrease led to longer retention times and peak broadening. Considering that higher flow rate could be obtained under lower backpressure, a backpressure of 150 bar and a flow rate of 1.5 mL/min were chosen as the optimized separation conditions.

3.4.2 UHPSFC-MS method for sterol analysis

Analysis of sterols was performed separately from the other lipid classes. This was related to the fact that ES source is not suitable for free sterol ionization [105]. Consequently, in order to avoid derivatization of these compounds prior analysis, different approaches based on APCI [106] or

APPI [107] are available. In order to make a comparison between these different API techniques, single sterol standards and mixtures of them were analyzed by direct infusion using ESI, APCI and APPI. Results for ergosterol analysis, as example, are reported in Figure 27.
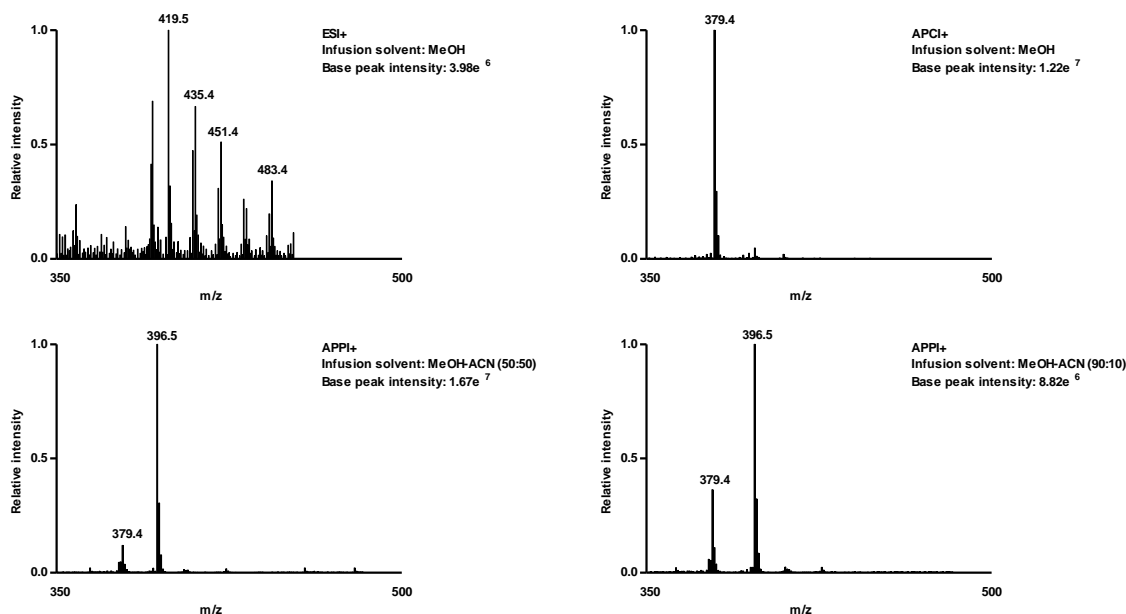

Figure 27. Mass spectra recorded after direct infusion of an ergosterol solution onto ESI, APCI and APPI ion sources

ESI analysis of ergosterol resulted in a relatively low sensitivity and formation of different ions, corresponding to the sodium (*m/z* 419.5) and potassium adducts (*m/z* 435.4), and cluster with solvent molecules (*m/z* 451.4 and 483.4).

APCI analysis, on the other hand, resulted in higher sensitivity and formation of only one ion, occurred from protonation and consequent loss of water (*m/z* 379.4) [108].

APPI analysis was performed infusing the ergosterol standard dissolved in mixtures MeOH-toluene 90:10 and 50:50. The use of toluene as dopant is necessary in APPI experiments in order to enhance the ionization through electron transfer mechanism [109]. Neat toluene was not used as it would have not represented the chromatographic conditions in which MeOH is always present in the mobile phase. APPI analysis raised two main points. First, two main ions are formed during the ionization process, corresponding to the $[M + H - H_2O]^+$ (*m/z* 379.4) and $[M]^{\cdot +}$ (*m/z* 396.5); second, the increase in toluene percentage resulted in a sensitivity increase and in a preferential formation of $[M]^{\cdot +}$ over $[M + H - H_2O]^+$ ion.

In analogy to the other lipid classes investigated, experiments using standard solutions of sterols were performed in order to select the proper separation conditions, based on the choice of chromatographic column, mobile phase modifier, make-up solvent, column temperature, backpressure and mobile phase flow rate. Figure 28 shows the separation profiles obtained by using four different columns; the best performances, in terms of baseline separation and peak shape, was obtained by using the Torus 1-AA column.
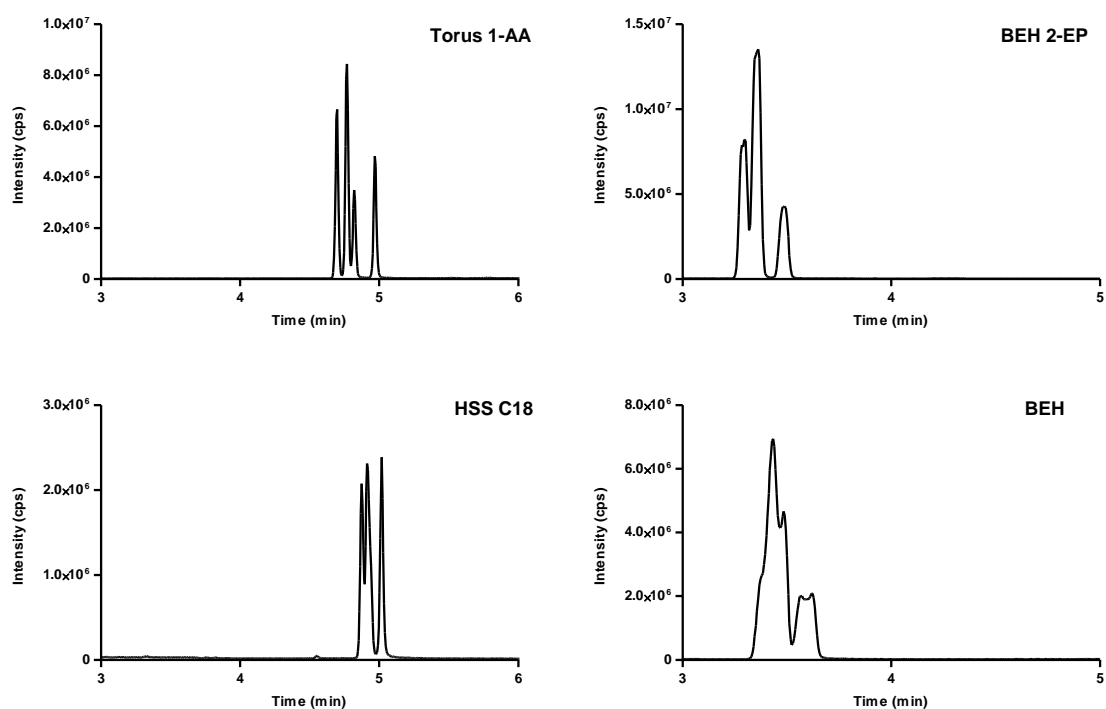

Figure 28. TICC reporting the UHPSFC separation of the tested sterols using BEH 2-EP, BEH, BSS C18 and Torus 1-AA columns. The elution order is cholesterol, β-sitosterol, stigmasterol and ergosterol

Furtherly, a comparison between APCI and APPI performances after chromatographic analysis was performed. Results showed that peak intensities in TICC is slightly higher for APPI ionization, but this is due to the fact that two ions are formed for each compound (Figure 29), while in APCI only one occurs. Consequently, as for quantitative analysis it is desirable that only one ion is formed, APCI was selected as ionization source for sterol analysis.
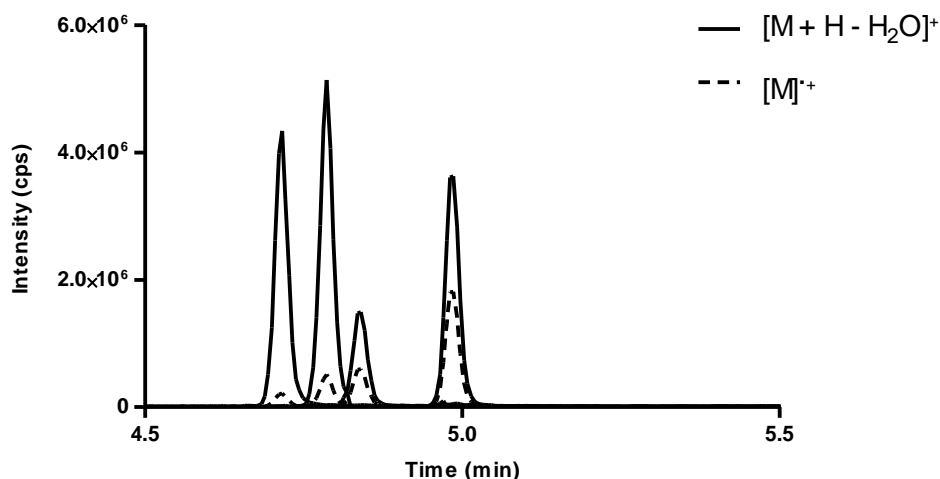
Figure 29. Separation of sterol mixture using a Torus 1-AA column and APPI as ion source. Two ions are formed for each compound, corresponding to $[M + H - H_2O]^+$ and $[M]^{\cdot+}$

3.4.3 UHPSFC-MS method validation

Under the optimal conditions, the developed UHPSFC-MS method was validated for the different tested lipid classes. Results are summarized in Table 13 and Table 14.

Selectivity was established by injection of single standards and of mixtures of them, in order to determinate their retention time. The comparison between standard solutions and samples fortified with known amounts of analyte, using SIR detection, showed absence of any interference in the matrices.

Seven-point calibration curves, affording correlation coefficients ≥0.995 for all the analytes, based on peak area and without internal standard, were used for the quantification. The calibration ranges specific to each tested compound are reported in Table 13, except for TAGs for which no calibration curve was established because of lack of single compound standards.

LOD and LOQ values were determined as the concentrations giving a signal to noise ratio of, respectively, 3 and 10. Experimentally determined LODs were in the range 5-50 ng/mL, while LOQs ranged from 10 to 100 ng/mL. The LOD and LOQ values for each tested compound are reported in Table 13.

Precision (SD%) and Accuracy (Bias%) values were less than 15% for all the studied compounds. These results indicate that the method fulfils the ICH guidelines, being sufficiently precise and accurate, and although its use is generally recommended, internal standard is not necessary. Precision and accuracy were not determined for TAGs because of lack of single compound standards.

Table 13. LODs, LOQs and calibration curves for all the studied compounds

Compound	LOD (ng/mL)	LOQ (ng/mL)	Calibration range (µg/mL)	r^2
Decanoic acid	50	100	0.10-10	>0.995
Valeric acid	20	50	0.10-10	>0.995
Myristic acid	10	40	0.10-10	>0.995
Palmitic acid	10	20	0.10-10	>0.995
Stearic acid	10	20	0.10-10	>0.995
Arachidic acid	10	20	0.10-10	>0.995
Methyl decanoate	50	100	0.10-10	>0.995
Methyl valerate	50	100	0.10-10	>0.995
Methyl myristate	50	100	0.10-10	>0.995
Methyl palmitate	50	100	0.10-10	>0.995
Methyl stearate	50	100	0.10-10	>0.995
Methyl oleate	5	10	0.01-1	>0.995
Methyl linoleate	5	10	0.01-1	>0.995
Methyl linolenate	5	10	0.01-1	>0.995
16:0/14:0/14:0	10	20	-	-
14:0/14:0/14:0	10	20	-	-
12:0/14:0/14:0	10	20	-	-
Cholesterol	10	30	0.10-10	>0.995
β-sitosterol	10	30	0.10-10	>0.995
Stigmasterol	10	30	0.10-10	>0.995
Ergosterol	10	30	0.10-10	>0.995

3.4.4 UHPLC-QTOF analysis

The developed and validated UHPSFC-MS method for the analysis of FAMEs, TAGs and FAs was compared to well established [110, 111] liquid chromatography methods. This was done in order to prove the reliability of the SFC for lipidomic analysis. The results (Figure 25) showed that UHPLC separation by means of C18 column and MeOH-Water based mobile phase is able to separate compounds within a lipid class. However, FAs (detected in negative ion mode) and FAMEs (detected in positive ion mode) have very similar retention times, and consequently they cannot be simultaneously analyzed within the same chromatographic run. On the contrary, SFC method is able to separate compounds within both a class and different classes of lipids, allowing the simultaneous analysis of analytes detected in different ionization modes simply by switching the polarity of the ion source within the same run. In addition, the three TAGs tested were eluted

after 12 minutes, suggesting that, in order to analyze all TAGs likely occurring in real samples, significantly longer chromatographic analysis, compared to UHPSFC, might be required.

On the other hand, the described UHPLC method revealed to be more suitable than SFC for the analysis of SGs. These molecules, differently from sterols, show better ionization using ESI source (where they are detected as $[M + Na]^+$) than APCI (where, similarly to their free analogues, the predominant positive ion corresponds to the loss of glucose and then water after protonation). This is due to the amphipathic nature of SGs, where the presence of the glucoside moiety increases the polarity and the response in ESI [112]. All the previously tested SFC columns were tried on SGs separation, giving poor results (Figure 30).
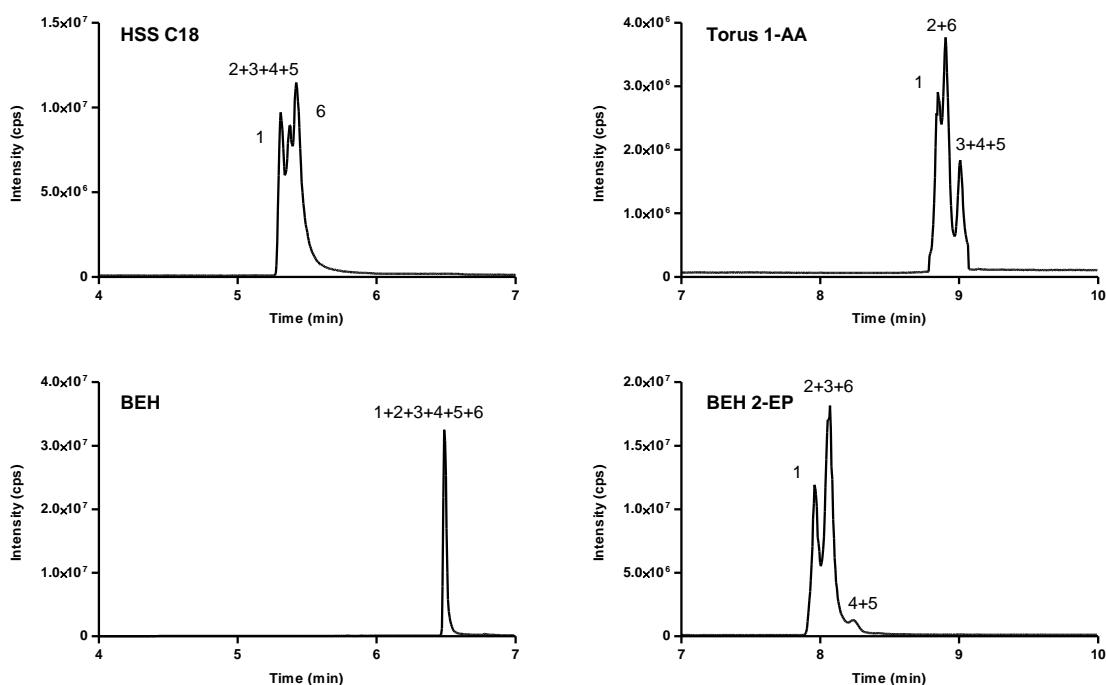

Figure 30. TICC reporting the UHPSFC separation of the tested SGs using BEH 2-EP, BEH, BSS C18 and Torus 1-AA columns. 1=cholesteryl glucoside, 2=campesteryl glucoside, 3=stigmasteryl glucoside, 4=Δ^7-avenasteryl glucoside, 5=Δ^5-avenasteryl glucoside, 6=β-sitosteryl glucoside

Satisfactory chromatographic separation, on the other hand, was achieved using reversed phase chromatography, as showed in Figure 31.

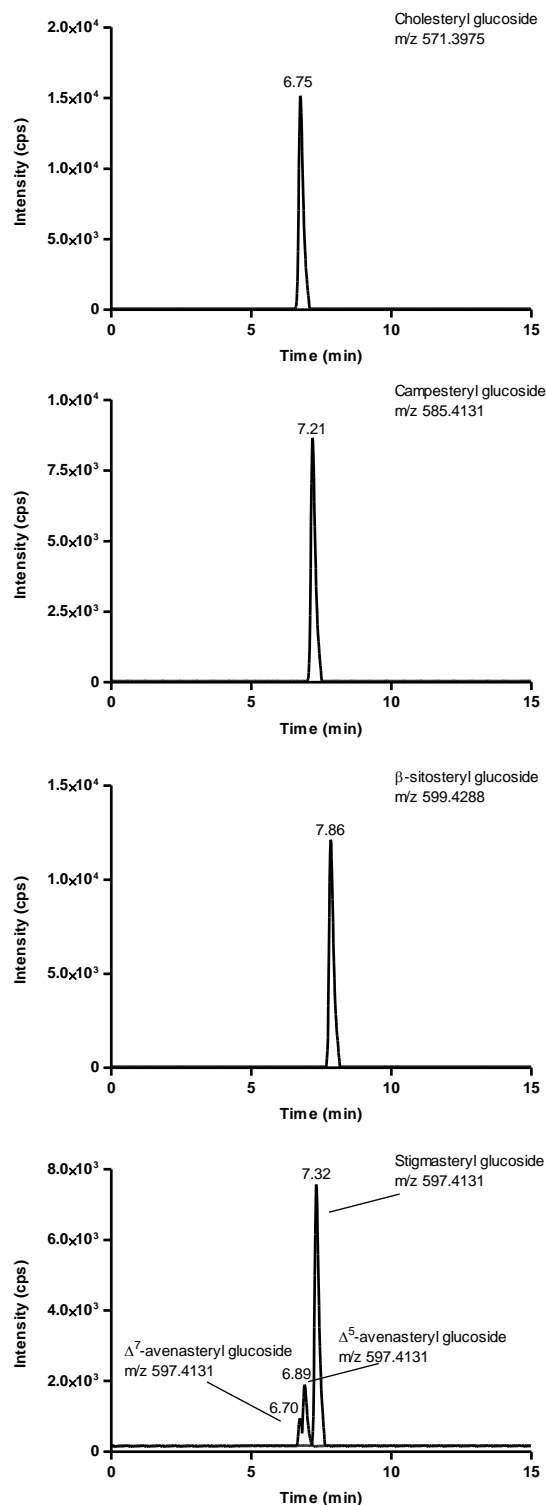**Figure 31.** EIC of the targeted SGs detected as [M + Na]⁺ ions by ESI-QTOF after UHPLC separation using a C18 column

The order of elution using a C18 column and a mobile phase made of MeOH and water (both acidified with 0.2% of formic acid) was Δ⁷-avenasteryl glucoside (6.70 min), cholesteryl glucoside (6.85 min), Δ⁵-avenasteryl glucoside (6.89 min), campesteryl glucoside (7.21 min), stigmasteryl

glucoside (7.32 min), and sitosteryl glucoside (7.86 min). All SGs were separated, except for stigmasteryl and campesteryl glucosides, Δ^5-avenasteryl, and cholesteryl glucosides, which coeluted, but which could still be distinguished by their *m/z* values. Due to the lack of pure standards for all the SGs, quantification of each compound was performed using the calibration curve of cholesterol glucoside. The determined LOD and LOQ were, respectively, 10 and 30 ng/mL. In conclusion, the use of the UHPLC-QTOF is a very valuable tool for targeted analysis of compounds not appropriate for SFC, and for untargeted lipid analysis [113], where chromatographic separation, tandem mass spectrometry and accurate mass measurements are required in order to confirm the identity of compounds for which the corresponding analytical standard is not available.

3.4.5 Analysis of archaeological samples

Different extracts from real archaeological samples and artificial cooking hearth were analyzed using the methods described above. These extracts were obtained from solid samples throughout Soxhlet extraction using Hex (type A sample) or MeOH/Tol (type B sample), according to the procedure reported in Paragraph 3.3.6. Over 80 samples were analyzed using the UHPSFC-ES/APCI-MS methods described above and FT-ICR MS analysis was carried out as well in order to confirm the identities of the compounds lacking the respective analytical standard. Figures 32 and Figure 33 show the results obtained, respectively, from the analysis of one type A and one type B archaeological samples.
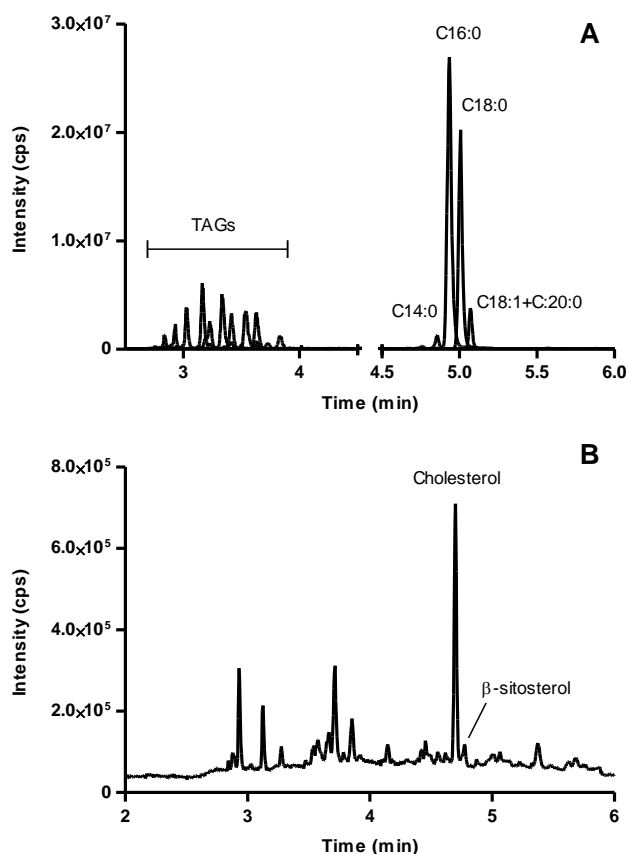
Figure 32. RIC obtained from the UHPSFC-MS analysis of a type A archaeological sample, showing its composition in terms of TAGs, FAs (A panel) and sterols (B panel).

The results obtained from the analysis of type A samples showed that the extraction procedure using hexane was able to recover detectable amounts of TAGs, FAs and sterols (mainly cholesterol and β-sitosterol). The detected TAGs, identified by the expected *m/z* value and chromatographic behavior, were both saturated and unsaturated and in a range of chain lengths and double bonds ranging from 44:0 to 54:6. The FA composition was very interesting as, according to the retention time and the *m/z* value of the standard references, it showed the presence of compounds ranging from C10:0 to C20:0, with also C18:1, C18:2 and C18:3. Among these, palmitic acid and stearic acid were the most abundant, followed by arachidic acid, oleic acid and myristic acid.
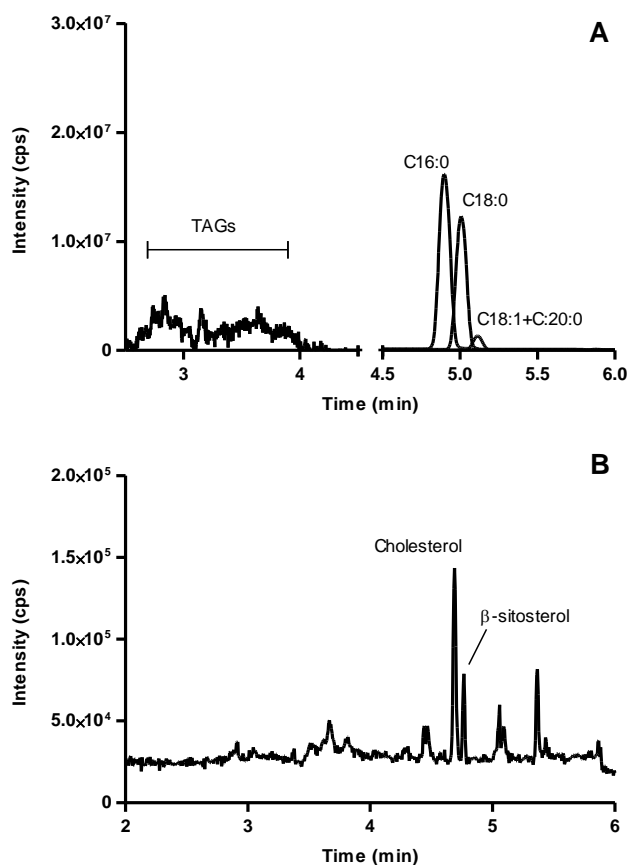
Figure 33. RIC obtained from the UHPSFC-MS analysis of a type B archaeological sample, showing its composition in terms of TAGs, FAs (A panel) and sterols (B panel)

The results obtained from the analysis of type B samples showed that the extraction procedure using Tol:MeOH was able to recover very low amounts of TAGs and sterols, but higher quantities of FAs, compared to the corresponding type A extract.

It is important to keep into account that the composition of these samples might be very variable, therefore is not possible to easily extent the above considerations to all the samples analyzed without a proper evaluation of the recorded data. Indeed, many of these samples belong to different geographic areas, archaeological sites and historical age. For this reason, in order to avoid any misleading assumptions, the data interpretations must be carefully carried out accordingly to these variables.

3.5 Conclusions

Organic residue analysis can address archaeological questions regarding diet and subsistence practices, as well as the ancient trade of goods and raw materials, technology (including vessel production, use and provenance), resource acquisition/exploitation, and the domestication of plants and animals, among other issues. The majority of organic residue analyses are carried out on absorbed organic residues from ceramic vessels. These residues generally come from the original contents either stored or processed in the vessels, either from use for a single product, or from an accumulation of individual uses in a vessel over its life history. Organic residues survive widely in association with ceramics and can endure over considerable timescales.

Conversely, the analysis performed on excavated hearth-material have been poorly explored, thus they represent an intriguing and comparable alternative. Indeed, to the best of knowledge, only two papers have been reported so far about this kind of material [114, 115]. Unfortunately, none of them had as primary goal the identification of foodstuff related the cooking practices, then it is still completely unknown whether complex dietary biomarkers, namely lipids, can survive and persist within the charcoal, ash or inorganic base of a hearth in detectable levels.

This project has been developed with the aim of identifying the organic pyrolysis products that reside within a hearth following the cooking of food. This would provide evidence to ascertain whether hearth-ash is undervalued in its potential role within archaeological ORA. With this aim, different analytical approaches have been developed for the target analysis of specific lipid classes, namely FAMEs, FAs, TAGs, sterols and SGs, in order to find the best instrumental conditions for their analysis. The choice to proceed with a target approach toward selected lipid classes was due to the necessity of improving the method performances, especially selectivity and sensitivity, in order to detect and identify with sufficient confidence low concentrations of the expected biomarkers.

The developed methods, based on the combination of chromatography, low resolution and high-resolution mass spectrometry, have been applied to the analysis of several archaeological sample extracts and proved to be effective for the detection and identification of biomarkers belonging to the expected lipid families. With great surprise, more compounds than expected have been found, especially for what concerns (poli)unsaturated FAs/TAGs that are known for being less stable than their saturated analogues. These results have great importance in the area of the archaeological sciences, as they open the lead for the investigation of a field that has been completely ignored so

far. Although more accurate insights and data interpretation are needed for confirming these preliminary results, hearth-material has shown to hold great promise for future ORA applications. Future work might involve the extension of these methods to other classes of biomarkers so that it could be possible to distinguish between the food types cooked on hearths, providing new insights in the diet habits of Neanderthal men or, more generally, addressing other issues not yet fully elucidated.

REFERENCES

1. Fahey, J. W., Zalcmann, A. T., & Talalay, P. (2001). The chemical diversity and distribution of glucosinolates and isothiocyanates among plants. *Phytochemistry*, *56*(1), 5-51.

2. Bennett, R. N., Carvalho, R., Mellon, F. A., Eagles, J., & Rosa, E. A. (2007). Identification and quantification of glucosinolates in sprouts derived from seeds of wild Eruca sativa L. (salad rocket) and Diplotaxis tenuifolia L. (wild rocket) from diverse geographical locations. *Journal of agricultural and food chemistry*, *55*(1), 67-74.

3. Halkier, B. A., & Du, L. (1997). The biosynthesis of glucosinolates. *Trends in plant science*, *2*(11), 425-431.

4. Xue, J., Lenman, M., Falk, A., & Rask, L. (1992). The glucosinolate-degrading enzyme myrosinase in Brassicaceae is encoded by a gene family. *Plant molecular biology*, *18*(2), 387-398.

5. Bones, A. M., & Rossiter, J. T. (2006). The enzymic and chemically induced decomposition of glucosinolates. *Phytochemistry*, *67*(11), 1053-1067.

6. Bones, A. M., & Rossiter, J. T. (1996). The myrosinase-glucosinolate system, its organisation and biochemistry. *Physiologia Plantarum*, *97*(1), 194-208.

7. Lin, C. M., Kim, J., Du, W. X., & Wei, C. I. (2000). Bactericidal activity of isothiocyanate against pathogens on fresh produce. *Journal of food protection*, *63*(1), 25-30.

8. Hashem, F. A., & Saleh, M. M. (1999). Antimicrobial components of some cruciferae plants (Diplotaxis harra Forsk. and Erucaria microcarpa Boiss.). *Phytotherapy Research*, *13*(4), 329-332.

9. Nastruzzi, C., Cortesi, R., Esposito, E., Menegatti, E., Leoni, O., Iori, R., & Palmieri, S. (1996). In vitro cytotoxic activity of some glucosinolate-derived products generated by myrosinase hydrolysis. *Journal of Agricultural and Food Chemistry*, *44*(4), 1014-1021.

10. Barillari, J., Canistro, D., Paolini, M., Ferroni, F., Pedulli, G. F., Iori, R., & Valgimigli, L. (2005). Direct antioxidant activity of purified glucoerucin, the dietary secondary metabolite contained in rocket (Eruca sativa Mill.) seeds and sprouts. *Journal of Agricultural and food chemistry*, *53*(7), 2475-2482.

11. Papi, A., Orlandi, M., Bartolini, G., Barillari, J., Iori, R., Paolini, M., Ferroni, F., Fumo, M., Pedulli, G., & Valgimigli, L. (2008). Cytotoxic and antioxidant activity of 4-methylthio-3-butenyl isothiocyanate from Raphanus sativus L.(Kaiware Daikon) sprouts. *Journal of agricultural and food chemistry*, *56*(3), 875-883.

12. Talalay, P., Fahey, J. W., Holtzclaw, W. D., Prestera, T., & Zhang, Y. (1995). Chemoprotection against cancer by phase 2 enzyme induction. *Toxicology letters*, *82*, 173-179.

13. Hayes, J. D., Kelleher, M. O., & Eggleston, I. M. (2008). The cancer chemopreventive actions of phytochemicals derived from glucosinolates. *European journal of nutrition*, *47*(2), 73-88.

14. Skupinska, K., Misiewicz-Krzeminska, I., Stypulkowski, R., Lubelska, K., & Kasprzycka-Guttman, T. (2009). Sulforaphane and its analogues inhibit CYP1A1 and CYP1A2 activity induced by benzo [a] pyrene. *Journal of biochemical and molecular toxicology*, *23*(1), 18-28.

15. Heiss, E., Herhaus, C., Klimo, K., Bartsch, H., & Gerhäuser, C. (2001). Nuclear factor κB is a molecular target for sulforaphane-mediated anti-inflammatory mechanisms. *Journal of Biological Chemistry*, *276*(34), 32008-32015.

16. Myzak, M. C., Karplus, P. A., Chung, F. L., & Dashwood, R. H. (2004). A novel mechanism of chemoprotection by sulforaphane. *Cancer research*, *64*(16), 5767-5774.

17. Bonnesen, C., Eggleston, I. M., & Hayes, J. D. (2001). Dietary indoles and isothiocyanates that are generated from cruciferous vegetables can both stimulate apoptosis and confer protection against DNA damage in human colon cell lines. *Cancer research*, *61*(16), 6120-6130.

18. Haack, M., Löwinger, M., Lippmann, D., Kipp, A., Pagnotta, E., Iori, R., Bonien, B.H., Glatt, H., Brauer, M.N., Wessjohann, L.A., & Brigelius-Flohé, R. (2010). Breakdown products of neoglucobrassicin inhibit activation of Nrf2 target genes mediated by myrosinase-derived glucoraphanin hydrolysis products. *Biological chemistry*, *391*(11), 1281-1293.

19. Dominguez-Perles, R., Moreno, D. A., Carvajal, M., & Garcia-Viguera, C. (2011). Composition and antioxidant capacity of a novel beverage produced with green tea and minimally-processed byproducts of broccoli. Innovative Food Science & Emerging Technologies, 12(3), 361-368.

20. Deng, Q., Zinoviadou, K. G., Galanakis, C. M., Orlien, V., Grimi, N., Vorobiev, E., ... & Barba, F. J. (2015). The effects of conventional and non-conventional processing on glucosinolates and its derived forms, isothiocyanates: extraction, degradation, and applications. Food Engineering Reviews, 7(3), 357-381.

21. Egner, P. A., Chen, J. G., Wang, J. B., Wu, Y., Sun, Y., Lu, J. H., ... & Jacobson, L. P. (2011). Bioavailability of sulforaphane from two broccoli sprout beverages: results of a short-term, cross-over clinical trial in Qidong, China. Cancer prevention research, 4(3), 384-395.

22. Li, F., Hullar, M. A., Beresford, S. A., & Lampe, J. W. (2011). Variation of glucoraphanin metabolism in vivo and ex vivo by human gut bacteria. British journal of nutrition, 106(3), 408-416.

23. Mithen, R. F., Dekker, M., Verkerk, R., Rabot, S., & Johnson, I. T. (2000). The nutritional significance, biosynthesis and bioavailability of glucosinolates in human foods. Journal of the Science of Food and Agriculture, 80(7), 967-984.

24. Schnug, E. (1987). Eine Methode zur schnellen und einfachen Bestimmung des Gesamtglucosinolatgehaltes in Grünmasse und Samen von Kruziferen durch die quantitative Analyse enzymatisch freisetzbaren Sulfates. European Journal of Lipid Science and Technology, 89(11), 438-442.

25. Thies, W. (1976). Quantitative gas liquid chromatography of glucosinolates on a microliter scale. European Journal of Lipid Science and Technology, 78(6), 231-234.

26. ISO 9167-1 (1992). Graines de colza – Dosage des glucosinolates – Partie 1: Methode par chromatographie liquide à haute performance

27. Cataldi, T. R., Rubino, A., Lelario, F., & Bufo, S. A. (2007). Naturally occurring glucosinolates in plant extracts of rocket salad (Eruca sativa L.) identified by liquid chromatography coupled with negative ion electrospray ionization and quadrupole ion-trap mass spectrometry. Rapid Communications in Mass Spectrometry, 21(14), 2374-2388.

28. Kim, S. J., Ishida, M., Matsuo, T., Watanabe, M., & Watanabe, Y. (2001). Separation and identification of glucosinolates of vegetable turnip rape by LC/APCI-MS and comparison of their contents in ten cultivars of vegetable turnip rape (Brassica rapa L.). Soil science and plant nutrition, 47(1), 167-177.

29. Ares, A. M., Nozal, M. J., Bernal, J. L., & Bernal, J. (2014). Optimized extraction, separation and quantification of twelve intact glucosinolates in broccoli leaves. Food chemistry, 152, 66-74.

30. Tian, Q., Rosselot, R. A., & Schwartz, S. J. (2005). Quantitative determination of intact glucosinolates in broccoli, broccoli sprouts, Brussels sprouts, and cauliflower by high-performance liquid chromatography–electrospray ionization–tandem mass spectrometry. Analytical biochemistry, 343(1), 93-99.

31. Franco, P., Spinozzi, S., Pagnotta, E., Lazzeri, L., Ugolini, L., Camborata, C., & Roda, A. (2016). Development of a liquid chromatography–electrospray ionization–tandem mass spectrometry method for the simultaneous analysis of intact glucosinolates and isothiocyanates in Brassicaceae seeds and functional foods. Journal of Chromatography A, 1428, 154-161.

32. Fenwick, G. R., Eagles, J., & Self, R. (1982). The fast atom bombardment mass spectra of glucosinolates and glucosinolate mixtures. Journal of Mass Spectrometry, 17(11), 544-546.

33. Zhang, Y., Wade, K. L., Prestera, T., & Talalay, P. (1996). Quantitative determination of isothiocyanates, dithiocarbamates, carbon disulfide, and related thiocarbonyl compounds by cyclocondensation with 1, 2-benzenedithiol. Analytical biochemistry, 239(2), 160-167.

34. Guideline, I. H. T. (2005). Validation of analytical procedures: text and methodology. Q2 (R1), 1.

35. Haack, M., Löwinger, M., Lippmann, D., Kipp, A., Pagnotta, E., Iori, R., ... & Brigelius-Flohé, R. (2010). Breakdown products of neoglucobrassicin inhibit activation of Nrf2 target genes mediated by myrosinase-derived glucoraphanin hydrolysis products. Biological chemistry, 391(11), 1281-1293.

36. Barillari, J., Canistro, D., Paolini, M., Ferroni, F., Pedulli, G. F., Iori, R., & Valgimigli, L. (2005). Direct antioxidant activity of purified glucoerucin, the dietary secondary metabolite contained in rocket (Eruca sativa Mill.) seeds and sprouts. Journal of Agricultural and food chemistry, 53(7), 2475-2482.

37. Dinkova-Kostova, A. T., & Kostov, R. V. (2012). Glucosinolates and isothiocyanates in health and disease. Trends in molecular medicine, 18(6), 337-347.

38. Lazzeri, L., Leoni, O., Manici, L. M., Palmieri, S., & Patalano, G. (2008). European Patent EP1530421B1, Use of seed flour as soil pesticide. Register of European patents.

39. Bradstreet, R. B. (1954). Kjeldahl method for organic nitrogen. Analytical Chemistry, 26(1), 185-187.

40. UNI EN ISO 5508:1998, Animal and vegetable fats and oils – analysis by gaschromatography of methyl esters of fatty acids. Oli E Grassi Animali E Vege-tali – Analisi Gascromatografica Degli Esteri Metilici Degli Acidi Grassi, Ente Nazionale Italiano di Unificazione, 1998 (in Italian).

41. Finiguerra, M. G., Iori, R., & Palmieri, S. (2001). Soluble and total myrosinase activity in defatted Crambe abyssinica meal. Journal of agricultural and food chemistry, 49(2), 840-845.

42. De Nicola, G. R., Bagatta, M., Pagnotta, E., Angelino, D., Gennari, L., Ninfali, P., ... & Iori, R. (2013). Comparison of bioactive phytochemical content and release of isothiocyanates in selected brassica sprouts. Food chemistry, 141(1), 297-303.

43. U.S. Dept. of Health and Human Services, CFR – Code of Federal RegulationsTitle 21, 1 April 2010.

44. Commission Directive 80/891/EEC of 25 July 1980 relating to the Communitymethod of analysis for determining the erucic acid content in oils and fatsintended to be used as such for human consumption and foodstuffs containingadded oils or fats. EurLex Official Journal 254.

45. Clarke, J. D., Hsu, A., Riedl, K., Bella, D., Schwartz, S. J., Stevens, J. F., & Ho, E. (2011). Bioavailability and inter-conversion of sulforaphane and erucin in human subjects consuming broccoli sprouts or broccoli supplement in a cross-over study design. Pharmacological Research, 64(5), 456-463.

46. Omirou, M., Papastylianou, I., Iori, R., Papastephanou, C., Papadopoulou, K. K., Ehaliotis, C., & Karpouzas, D. G. (2009). Microwave-assisted extraction of glucosinolates from Eruca sativa seeds and soil: comparison with existing methods. Phytochemical analysis, 20(3), 214-220.

47. Agerbirk, N., & Olsen, C. E. (2012). Glucosinolate structures in evolution. Phytochemistry, 77, 16-45.

48. Hofmann, A. F., & Borgström, B. (1964). The intraluminal phase of fat digestion in man: the lipid content of the micellar and oil phases of intestinal content obtained during fat digestion and absorption. Journal of Clinical Investigation, 43(2), 247.

49. Hofmann, A. F., Hagey, L. R., & Krasowski, M. D. (2010). Bile salts of vertebrates: structural variation and possible evolutionary significance. Journal of lipid research, 51(2), 226-246.

50. Chiang, J. Y. (2009). Bile acids: regulation of synthesis. Journal of lipid research, 50(10), 1955-1966.

51. Meier, P. J. (1995). Molecular mechanisms of hepatic bile salt transport from sinusoidal blood into bile. American Journal of Physiology-Gastrointestinal and Liver Physiology, 269(6), G801-G812.

52. Wong, M. H., Oelkers, P., & Dawson, P. A. (1995). Identification of a mutation in the ileal sodium-dependent bile acid transporter gene that abolishes transport activity. Journal of Biological Chemistry, 270(45), 27228-27234.

53. Rao, A., Haywood, J., Craddock, A. L., Belinsky, M. G., Kruh, G. D., & Dawson, P. A. (2008). The organic solute transporter α-β, Ostα-Ostβ, is essential for intestinal bile acid transport and homeostasis. Proceedings of the National Academy of Sciences, 105(10), 3891-3896.

54. Alrefai, W. A., & Gill, R. K. (2007). Bile acid transporters: structure, function, regulation and pathophysiological implications. Pharmaceutical research, 24(10), 1803-1823.

55. Vessey, D. A. (1978). The biochemical basis for the conjugation of bile acids with either glycine or taurine. Biochemical Journal, 174(2), 621-626.

56. Hylemon, P. B. (1985). Metabolism of bile acids in intestinal microflora. New comprehensive biochemistry, 12, 331-343.

57. Parks, D. J., Blanchard, S. G., Bledsoe, R. K., Chandra, G., Consler, T. G., Kliewer, S. A., ... & Lehmann, J. M. (1999). Bile acids: natural ligands for an orphan nuclear receptor. Science, 284(5418), 1365-1368.

58. Kawamata, Y., Fujii, R., Hosoya, M., Harada, M., Yoshida, H., Miwa, M., ... & Hinuma, S. (2003). AG protein-coupled receptor responsive to bile acids. Journal of Biological Chemistry, 278(11), 9435-9440.

59. Gadaleta, R. M., van Mil, S. W., Oldenburg, B., Siersema, P. D., Klomp, L. W., & van Erpecum, K. J. (2010). Bile acids and their nuclear receptor FXR: Relevance for hepatobiliary and gastrointestinal disease. Biochimica et Biophysica Acta (BBA)-Molecular and Cell Biology of Lipids, 1801(7), 683-692.

60. Duboc, H., Taché, Y., & Hofmann, A. F. (2014). The bile acid TGR5 membrane receptor: from basic research to clinical application. Digestive and Liver Disease, 46(4), 302-312.

61. Rizzo, G., Passeri, D., De Franco, F., Ciaccioli, G., Donadio, L., Rizzo, G., ... & Levi, M. (2010). Functional characterization of the semisynthetic bile acid derivative INT-767, a dual farnesoid X receptor and TGR5 agonist. Molecular pharmacology, 78(4), 617-630.

62. Pellicciari, R., Costantino, G., Camaioni, E., Sadeghpour, B. M., Entrena, A., Willson, T. M., ... & Gioiello, A. (2004). Bile acid derivatives as ligands of the farnesoid X receptor. Synthesis, evaluation, and structure–activity relationship of a series of body and side chain modified analogues of chenodeoxycholic acid. Journal of medicinal chemistry, 47(18), 4559-4569.

63. Gioiello, A., Cerra, B., Mostarda, S., Guercini, C., Pellicciari, R., & Macchiarulo, A. (2014). Bile acid derivatives as ligands of the Farnesoid x receptor: molecular determinants for bile acid binding and receptor modulation. Current topics in medicinal chemistry, 14(19), 2159-2174.

64. Sato, H., Macchiarulo, A., Thomas, C., Gioiello, A., Une, M., Hofmann, A. F., ... & Auwerx, J. (2008). Novel potent and selective bile acid derivatives as TGR5 agonists: biological screening, structure– activity relationships, and molecular modeling studies. Journal of medicinal chemistry, 51(6), 1831-1841.

65. Beuers, U., Trauner, M., Jansen, P., & Poupon, R. (2015). New paradigms in the treatment of hepatic cholestasis: from UDCA to FXR, PXR and beyond. Journal of hepatology, 62(1), S25-S37.

66. Gershwin, M. E., Selmi, C., Worman, H. J., Gold, E. B., Watnik, M., Utts, J., ... & Vierling, J. M. (2005). Risk factors and comorbidities in primary biliary cirrhosis: A controlled interview-based study of 1032 patients. Hepatology, 42(5), 1194-1202.

67. Chazouillères, O., Wendum, D., Serfaty, L., Montembault, S., Rosmorduc, O., & Poupon, R. (1998). Primary biliary cirrhosis–autoimmune hepatitis overlap syndrome: clinical features and response to therapy. Hepatology, 28(2), 296-301.

68. Parés, A., Caballería, L., & Rodés, J. (2006). Excellent long-term survival in patients with primary biliary cirrhosis and biochemical response to ursodeoxycholic acid. Gastroenterology, 130(3), 715-720.

69. Gong, Y., & Gluud, C. (2004). Colchicine for primary biliary cirrhosis. The Cochrane Library.

70. Rudic, J. S., Poropat, G., Krstic, M. N., Bjelakovic, G., & Gluud, C. (2012). Bezafibrate for primary biliary cirrhosis. Cochrane Database Syst Rev, 1.

71. Giljaca, V., Poropat, G., Stimac, D., & Gluud, C. (2010). Methotrexate for primary biliary cirrhosis. The Cochrane Library.

72. Crosignani, A., Setchell, K. D., Invernizzi, P., Larghi, A., Rodrigues, C. M., & Podda, M. (1996). Clinical pharmacokinetics of therapeutic bile acids. Clinical pharmacokinetics, 30(5), 333-358.

73. Ali, A. H., Carey, E. J., & Lindor, K. D. (2015). Recent advances in the development of Farnesoid X receptor agonists. Annals of translational medicine, 3(1).

74. Nevens, F., Andreone, P., Mazzella, G., Strasser, S. I., Bowlus, C., Invernizzi, P., ... & Trauner, M. (2016). A placebo-controlled trial of obeticholic acid in primary biliary cholangitis. New England Journal of Medicine, 375(7), 631-643.

75. Mudaliar, S., Henry, R. R., Sanyal, A. J., Morrow, L., Marschall, H. U., Kipnes, M., ... & Dillon, P. (2013). Efficacy and safety of the farnesoid X receptor agonist obeticholic acid in patients with type 2 diabetes and nonalcoholic fatty liver disease. Gastroenterology, 145(3), 574-582.

76. Neuschwander-Tetri, B. A., Loomba, R., Sanyal, A. J., Lavine, J. E., Van Natta, M. L., Abdelmalek, M. F., ... & Kowdley, K. V. (2015). Farnesoid X nuclear receptor ligand obeticholic acid for non-cirrhotic, non-alcoholic steatohepatitis (FLINT): a multicentre, randomised, placebo-controlled trial. The Lancet, 385(9972), 956-965.

77. Boonstra, K., Beuers, U., & Ponsioen, C. Y. (2012). Epidemiology of primary sclerosing cholangitis and primary biliary cirrhosis: a systematic review. Journal of hepatology, 56(5), 1181-1188.

78. Kilkenny, C., Browne, W., Cuthill, I. C., Emerson, M., & Altman, D. G. (2010). Animal research: reporting in vivo experiments: the ARRIVE guidelines. British journal of pharmacology, 160(7), 1577-1579.

79. Jiménez, W., Clària, J., Arrojo, V., & Rodés, J. (1992). Carbon tetrachloride induced cirrhosis in rats: a useful tool for investigating the pathogenesis of ascites in chronic liver disease. Journal of gastroenterology and hepatology, 7(1), 90-97.

80. Roda, A., Pellicciari, R., Gioiello, A., Neri, F., Camborata, C., Passeri, D., ... & Montagnani, M. (2014). Semisynthetic bile acid FXR and TGR5 agonists: physicochemical properties, pharmacokinetics, and metabolism in the rat. Journal of Pharmacology and Experimental Therapeutics, 350(1), 56-68.

81. Carrott, P. J. M., & Carrott, M. R. (2007). Lignin–from natural adsorbent to activated carbon: a review. Bioresource technology, 98(12), 2301-2312.

82. Fischer, S., Beuers, U., Spengler, U., Zwiebel, F. M., & Koebe, H. G. (1996). Hepatic levels of bile acids in end-stage chronic cholestatic liver disease. Clinica chimica acta, 251(2), 173-186.

83. Edwards, J. E., LaCerte, C., Peyret, T., Gosselin, N. H., Marier, J. F., Hofmann, A. F., & Shapiro, D. (2016). Modeling and experimental studies of obeticholic acid exposure and the impact of cirrhosis stage. Clinical and translational science, 9(6), 328-336.

84. Shillito, L. M., Almond, M. J., Wicks, K., Marshall, L. J. R., & Matthews, W. (2009). The use of FT-IR as a screening technique for organic residue analysis of archaeological samples. Spectrochimica Acta Part A: Molecular and Biomolecular Spectroscopy, 72(1), 120-125.

85. Copley, M. S., Bland, H. A., Rose, P., Horton, M., & Evershed, R. P. (2005). Gas chromatographic, mass spectrometric and stable carbon isotopic investigations of organic residues of plant oils and animal fats employed as illuminants in archaeological lamps from Egypt. Analyst, 130(6), 860-871.

86. Evershed, R. P., Heron, C., & Goad, L. J. (1990). Analysis of organic residues of archaeological origin by high-temperature gas chromatography and gas chromatography-mass spectrometry. Analyst, 115(10), 1339-1342.

87. Stevens, R. E., Lightfoot, E., Allen, T., & Hedges, R. E. (2012). Palaeodiet at Eton College Rowing Course, Buckinghamshire: isotopic changes in human diet in the Neolithic, Bronze Age, Iron Age and Roman periods throughout the British Isles. Archaeological and Anthropological Sciences, 4(3), 167-184.

88. Isaksson, S., Karlsson, C., & Eriksson, T. (2010). Ergosterol (5, 7, 22-ergostatrien-3β-ol) as a potential biomarker for alcohol fermentation in lipid residues from prehistoric pottery. Journal of Archaeological Science, 37(12), 3263-3268.

89. Charters, S., Evershed, R. P., Goad, L. J., Leyden, A., Blinkhorn, P. W., & Denham, V. (1993). Quantification and distribution of lipid in archaeological ceramics: implications for sampling potsherds for organic residue analysis and the classification of vessel use. Archaeometry, 35(2), 211-223.

90. Evershed, R. P. (1993). Biomolecular archaeology and lipids. World Archaeology, 25(1), 74-93.

91. Heron, C., Nemcek, N., Bonfield, K. M., Dixon, D., & Ottaway, B. S. (1994). The chemistry of Neolithic beeswax. Naturwissenschaften, 81(6), 266-269.

92. McGovern, P. E., Zhang, J., Tang, J., Zhang, Z., Hall, G. R., Moreau, R. A., ... & Cheng, G. (2004). Fermented beverages of pre-and proto-historic China. Proceedings of the National Academy of Sciences of the United States of America, 101(51), 17593-17598.

93. Charrié-Duhaut, A., Connan, J., Rouquette, N., Adam, P., Barbotin, C., de Rozieres, M. F., ... & Albrecht, P. (2007). The canopic jars of Rameses II: real use revealed by molecular study of organic residues. Journal of Archaeological Science, 34(6), 957-967.

94. Oudemans, T. F. M., Boon, J. J., & Botto, R. E. (2007). FTIR and solid-state ^{13}C CP/MAS NMR spectroscopy of charred and non-charred solid organic residues preserved in roman iron age vessels from the netherlands. Archaeometry, 49(3), 571-294.

95. Connan, J., Nieuwenhuyse, O. P., Van As, A., & Jacobs, L. (2004). Bitumen in Early Ceramic Art: Bitumen-Painted Ceramics from Late Neolithic Tell Sabi Abyad (Syria). Archaeometry, 46(1), 115-124.

96. Evershed, R. P. (2008). Organic residue analysis in archaeology: the archaeological biomarker revolution. Archaeometry, 50(6), 895-924.

97. Corr, L. T., Richards, M. P., Grier, C., Mackie, A., Beattie, O., & Evershed, R. P. (2009). Probing dietary change of the Kwäday Dän Ts' ìnchi individual, an ancient glacier body from British Columbia: II. Deconvoluting whole skin and bone collagen δ 13 C values via carbon isotope analysis of individual amino acids. Journal of Archaeological Science, 36(1), 12-18.

98. van Bergen, P. F., Peakman, T. M., Leigh-Firbank, E. C., & Evershed, R. P. (1997). Chemical evidence for archaeological frankincense: boswellic acids and their derivatives in solvent soluble and insoluble fractions of resin-like materials. Tetrahedron Letters, 38(48), 8409-8412.

99. Bull, I. D., Simpson, I. A., Dockrill, S. J., & Evershed, R. P. (1999). Organic geochemical evidence for the origin of ancient anthropogenic soil deposits at Tofts Ness, Sanday, Orkney. Organic Geochemistry, 30(7), 535-556.

100. Thornton, M. D., Morgan, E. D., & Celoria, F. (1970). The composition of bog butter. Science and archaeology, 1(2 3), 20-25.

101. Olsson, M., & Isaksson, S. (2008). Molecular and isotopic traces of cooking and consumption of fish at an Early Medieval manor site in eastern middle Sweden. Journal of Archaeological Science, 35(3), 773-780.

102. Evershed, R. P., Payne, S., Sherratt, A. G., Copley, M. S., Coolidge, J., Urem-Kotsu, D., ... & Akkermans, P. M. (2008). Earliest date for milk use in the Near East and southeastern Europe linked to cattle herding. Nature, 455(7212), 528-531.

103. Regert, M., Bland, H. A., Dudd, S. N., Bergen, P. V., & Evershed, R. P. (1998). Free and bound fatty acid oxidation products in archaeological ceramic vessels. Proceedings of the Royal Society of London B: Biological Sciences, 265(1409), 2027-2032.

104.   Bernal, J. L., Martín, M. T., & Toribio, L. (2013). Supercritical fluid chromatography in food analysis. Journal of Chromatography A, 1313, 24-36.

105.   Sun, J., Zhao, X. E., Dang, J., Sun, X., Zheng, L., You, J., & Wang, X. (2016). Rapid and sensitive determination of phytosterols in functional foods and medicinal herbs by using UHPLC–MS/MS with microwave-assisted derivatization combined with dual ultrasound-assisted dispersive liquid–liquid microextraction. Journal of Separation Science.

106.   Bedner, M., Schantz, M. M., Sander, L. C., & Sharpless, K. E. (2008). Development of liquid chromatographic methods for the determination of phytosterols in Standard Reference Materials containing saw palmetto. Journal of Chromatography A, 1192(1), 74-80.

107.   Lembcke, J., Ceglarek, U., Fiedler, G. M., Baumann, S., Leichtle, A., & Thiery, J. (2005). Rapid quantification of free and esterified phytosterols in human serum using APPI-LC-MS/MS. Journal of lipid research, 46(1), 21-26.

108.   Careri, M., Elviri, L., & Mangia, A. (2001). Liquid chromatography–UV determination and liquid chromatography–atmospheric pressure chemical ionization mass spectrometric characterization of sitosterol and stigmasterol in soybean oil. Journal of chromatography A, 935(1), 249-257.

109.   Robb, D. B., Covey, T. R., & Bruins, A. P. (2000). Atmospheric pressure photoionization: an ionization method for liquid chromatography– mass spectrometry. Analytical Chemistry, 72(15), 3653-3659.

110.   Mottram, H. R., Woodbury, S. E., & Evershed, R. P. (1997). Identification of triacylglycerol positional isomers present in vegetable oils by high performance liquid chromatography/atmospheric pressure chemical ionization mass spectrometry. Rapid Communications in Mass Spectrometry, 11(12), 1240-1252.

111.   Hellmuth, C., Weber, M., Koletzko, B., & Peissner, W. (2012). Nonesterified fatty acid determination for functional lipidomics: comprehensive ultrahigh performance liquid chromatography–tandem mass spectrometry quantitation, qualification, and parameter prediction. Analytical chemistry, 84(3), 1483-1490.

112.   Oppliger, S. R., Münger, L. H., & Nyström, L. (2014). Rapid and Highly Accurate Detection of Steryl Glycosides by Ultraperformance Liquid Chromatography–Quadrupole Time-of-Flight Mass Spectrometry (UPLC-Q-TOF-MS). Journal of agricultural and food chemistry, 62(39), 9410-9419.

113.   Hyötyläinen, T., Bondia-Pons, I., & Orešič, M. (2013). Lipidomics in nutrition and food research. Molecular nutrition & food research, 57(8), 1306-1318.

114.   Kedrowski, B. L., Crass, B. A., Behm, J. A., Luetke, J. C., Nichols, A. L., Moreck, A. M., & Holmes, C. E. (2009). GC/MS analysis of fatty acids from ancient hearth residues at the Swan Point archaeological site. Archaeometry, 51(1), 110-122.

115.   Pierce, C., Adams, K. R., & Stewart, J. D. (1998). Determining the fuel constituents of ancient hearth ash via ICP-AES analysis. Journal of Archaeological Science, 25(6), 493-503.